

School of Electrical, Electronic & Computer
Engineering



Design and Measurement of Synchronizers

by

Jun Zhou

Technical Report Series

NCL-EECE-MSD-TR-2008-138

November 2008

Contact:

jun.zhou@ncl.ac.uk

EPSRC supports this work via EP/C007298/1 (SYRINGE)

NCL-EECE-MSD-TR-2008-138

Copyright © 2008 Newcastle University

School of Electrical, Electronic & Computer Engineering,

Merz Court,

Newcastle University,

Newcastle upon Tyne, NE1 7RU, UK

<http://async.org.uk/>

University of Newcastle upon Tyne
School of Electrical, Electronic and Computer Engineering

Design and Measurement of Synchronizers

by

Jun Zhou

A thesis submitted for the degree of Doctor of Philosophy (Ph.D) at

Newcastle University

November 2008

Content

List of Publications	ix
List of Figures	x
List of Tables	xiii
Acknowledgements	xiv
Glossary of Abbreviations	xv
Abstract	xvi
1. Introduction	1
1.1 Background	1
1.2 Synchronizer Issues.....	4
1.3 Contributions.....	7
1.4 Thesis Structure.....	9
2. Literature Review	11
2.1 Synchronizer	11
2.1.1 Why are synchronizers needed.....	11
2.1.2 How are synchronizers used?.....	14
2.2 Synchronizer modelling	16
2.2.1 Metastability.....	16

2.2.2 Resolution of Metastability in Synchronizers	21
2.2.3 Synchronizer Failure Rates	24
2.3 Synchronizer Circuits.....	29
2.3.1 Latches	29
2.3.2 Jamb Latch	30
2.3.3 Other proposed synchronizers.....	32
2.4 Synchronizer Simulation and Measurement	37
2.4.1 Synchronizer Simulation.....	37
2.4.2 Synchronizer Measurement.....	39
2.5 Effects of On-chip Variability on Synchronizers.....	46
3. Robust Synchronizer	48
3.1 Jamb Latch	49
3.2 Modified Jamb Latch	55
3.3 Improved Synchronizer (Robust Synchronizer).....	58
3.4 Summary	62
4. On-chip Measurement of Deep Metastability in Synchronizers	64
4.1 Measurement of Metastability in Synchronizers.....	65
4.1.1 Traditional Measurement Methods	66

4.1.2 On-chip Deep Metastability Measurement	68
4.2 Implementation of On-chip Deep Metastability Measurement.....	69
4.2.1 Variable Delay Lines.....	70
4.2.2 Devices Under Test (synchronizers)	73
4.2.3 Control Logic	74
4.2.4 Layout of On-chip Measurement Circuit	78
4.3 Measurement Results	79
4.3.1 Input Histogram	79
4.3.2 Output Histogram.....	79
4.3.3 Corrected Input Histogram.....	81
4.3.4 Input Time vs Output Time.....	84
4.3.5 Tau vs Vdd	87
4.4 Summary	88
5. Adapting Synchronizers to the Effects of On-chip Variability	90
5.1 On-chip Measurement of Failure Rates	93
5.2 Calculation of τ and MTBF.....	94
5.2.1 Calculate τ from Measured Failure Rates	94
5.2.2 Calculate MTBF from Measured Failure Rates	95
5.3. Two Proposed Adaptation Schemes.....	96

5.3.1 Synchronizer Selection Scheme.....	96
5.3.2 Synchronization Time Adjustment Scheme.....	98
5.4 Implementation	100
5.4.1 Architecture of Synchronizer Selection Scheme.....	100
5.4.2 Architecture of Synchronization Time Adjustment Scheme	102
5.4.3 Failure Detector.....	104
5.4.4. Failure Counters.....	104
5.4.5 Synchronizer Selection Circuit	105
5.4.6 Variable Delay Line	106
5.4.7 Implementation of τ and MTBF Calculation	107
5.4.8 Hardware Saving.....	110
5.5 Applications of Two Schemes	111
5.6 Test Results	112
5.7 Summary	114
6. Conclusions and Future Work	116
6.1 Conclusions.....	116
6.2 Future Work	123

Appendix A. TSMC 0.18μm SPICE Parameters from MOSIS	125
Appendix B. UMC 0.18μm/90nm SPICE Parameters from Europractice	127
Bibliography	129

List of Publications

1. **J. Zhou**, D. J. Kinniment, G. Russell, and A. Yakovlev, “Adapting Synchronizers to the Effects of On Chip Variability”, 14th IEEE International Symposium on Asynchronous Circuits and Systems, pp. 39-47, 2008.
2. **J. Zhou**, D. J. Kinniment, G. Russell, and A. Yakovlev, “On-Chip Measurement of Deep Metastability in Synchronizers”, IEEE Journal of Solid-State Circuits, Vol. 43, No. 2, pp. 550-557, 2008.
3. **J. Zhou**, D. J. Kinniment, G. Russell, and A. Yakovlev, “A Robust Synchronizer Circuit”, IEEE Computer Society Annual Symposium on VLSI, pp. 442-443, 2006.
4. **J. Zhou**, D. J. Kinniment, G. Russell, and A. Yakovlev, “On-chip Measurement of MTBF for A Robust Synchronizer”, 19th UK Asynchronous Forum, 2007.
5. H. Ramakrishnan, S. Shedabale, **J. Zhou**, G. Russell, and A. Yakovlev, “Variability analysis of a high performance strained silicon Jamb latch synchronizer”, 19th UK Asynchronous Forum, 2007.

List of Figures

Figure 2.1 Metastability in flip-flop.....	12
Figure 2.2 Two flip-flops synchronizer	13
Figure 2.3 GALS system.....	15
Figure 2.4 Synchronizers in system	16
Figure 2.5 D Latch	17
Figure 2.6 Metastable state	18
Figure 2.7 Metastable equilibrium	19
Figure 2.8 Metastable outputs [20]	20
Figure 2.9 Metastable events and output histogram.....	20
Figure 2.10 Small signal models of gate and flip-flop.....	22
Figure 2.11 Occurrence and resolution of metastability	25
Figure 2.12 Input time and output time relationship.....	27
Figure 2.13 Latches based synchronizer	29
Figure 2.14 Latch with filter	30
Figure 2.15 Structure of Jamb latch	31
Figure 2.16 Metastability blocker [31].....	34
Figure 2.17 Metastability shaker.....	35
Figure 2.18 Low input coupling latch [27]	36
Figure 2.19 Switch method	38
Figure 2.20 Two-oscillator measurement method	40
Figure 2.21 Deep metastability measurement.....	41
Figure 2.22 Input and output histograms	42
Figure 2.23 Input time to output time	43

Figure 2.24 Analog implementation of deep metastability measurement [38].....	45
Figure 3.1 Jamb latch	49
Figure 3.2 Simulating Jamb latch.....	51
Figure 3.3 Diverging nodes.....	52
Figure 3.4 Semilog plot of the voltage difference of the two nodes	52
Figure 3.5 Plot of τ vs V_{dd} for Jamb latch	53
Figure 3.6 Energy consumption	54
Figure 3.7 Synchronization time constant τ	55
Figure 3.8 Modified Jamb latch	56
Figure 3.9 Plot of τ vs V_{dd} for modified Jamb latch.....	57
Figure 3.10 Improved synchronizer (robust synchronizer).....	58
Figure 3.11 Plot of τ vs V_{dd} for improved synchronizer	60
Figure 3.12 Improved synchronizer, input vs output time at 1.8v	61
Figure 3.13 Improved synchronizer, input time vs output time at 0.9V	62
Figure 4.1 Traditional measurement method using two oscillators	66
Figure 4.2 Typical event histogram [38].....	67
Figure 4.3 Deep metastability measurement.....	68
Figure 4.4 Traditional VDL	70
Figure 4.5 Improved VDL.....	72
Figure 4.6 Multiplexer circuit for DUTs.....	74
Figure 4.7 Controlling counters	75
Figure 4.8 Loading circuit for controlling counters	76
Figure 4.9 Generation of RESET signal	77
Figure 4.10 Layout of on-chip measurement circuit.....	78
Figure 4.11 Input histogram.....	79

Figure 4.12 Output histogram	80
Figure 4.13 High output events vs low output events.....	81
Figure 4.14 Measurement of actual input time distribution.....	82
Figure 4.15 Corrected input histogram	83
Figure 4.16 Measured Input time (s) vs output time (ns).....	85
Figure 4.17 Simulated input time (s) vs output time (ns)	86
Figure 5.1 On-chip measurement of failure rates.....	94
Figure 5.2 Architecture of Synchronizer Selection Scheme	101
Figure 5.3 Architecture of Synchronization Time Adjustment Scheme	102
Figure 5.4 Failure counters	105
Figure 5.5 Synchronizer Selection Circuit.....	106
Figure 5.6 Variable delay line.....	107
Figure 5.7 Calculation flow.....	108
Figure 5.8 Divider	109
Figure 5.9 Log calculation circuit.....	110
Figure 5.10 Calculated MTBF vs Data Rate (Synchronization Time=3.5ns, Clock Frequency=10MHz).....	112
Figure 5.11 Calculated MTBF vs Synchronization Time (Data Rate=5MHz, Clock Frequency=10MHz).....	113
Figure 5.12 Tau vs Vdd.....	113

List of Tables

Table 4.1 Tau vs V_{dd} for Jamb B and Robust Synchronizer.....	87
Table 5.1 Jamb latch τ vs V_{dd} at 90nm.....	98

Acknowledgements

I would like to express my gratitude to my supervisors, Dr Gordon Russell and Professor Alex Yakovlev for their patient guidance, kind encouragement and constant support in all the time of my PhD research and writing of this thesis.

I am deeply indebted to Professor David Kinniment for his tremendous help and valuable suggestions during my research. His deep knowledge of synchronizer and logical way of thinking have been of great value to me. Without his help this work could not have been done.

I would like to acknowledge the support from EPSRC grant EP/C007298/1 and Intel Corporation. Special thanks to Charles Dike from Intel for his valuable suggestions in my research work.

I am grateful to my colleagues who have helped me in last three years. I want to thank Julian Murphy for his introduction of the usage of EDA tools. I have furthermore to thank Nikolaos Minas and Hiran K Ramakrishnan with whom I had a many valuable discussions on my research work and writing of thesis. My special thanks go to Yuan Chen, Yu Zhou, Ping Wang and Jincheng Zhu who have offered me a lot of help and made my life in UK interesting.

Especially, I would like to give my special thanks to my parents whose constant love and support enabled me to complete this work.

Glossary of Abbreviations

DLL	Delay Locked Loop
DPE	Data Processing Engine
DUT	Device Under Test
DVFS	Dynamic Voltage & Frequency Scaling
GALS	Global Asynchronous and Local Synchronous
MTBF	Mean Time Between Failure
SoC	System on Chip
VDL	Variable Delay Line

Abstract

Future Systems on Chip (SoCs) are likely to consist of many independent or semi-independent clock regions with the need to synchronize the data passing between them. Consequently, there will be many synchronizers together with interconnecting and routing elements forming an on-chip communication network. Due to the rapidly increasing size of SoCs in terms of the number of IP cores on a single chip, the on-chip communication is likely to impact on the system performance more than processing. As an important part of on-chip communication network, the performance of synchronizers on chip is critical to the performance of the entire system.

To address the issues of the effects on performance resulting from the inclusion of synchronizers in SoCs, several aspects related to synchronizer design and measurement need to be investigated; to date these aspects have either not been considered or inadequately addressed. A common problem with synchronizers is that their performance degrades rapidly with decreasing V_{dd} and is sensitive to V_{dd} , V_{th} and temperature variations. Another problem is that the existing synchronizer simulation and measurement techniques are not sufficiently accurate for estimating synchronizer performance to predict long term mean time between failures (MTBF). In addition, synchronizer performance is heavily affected by the on-chip variability, which needs to be addressed as the on-chip variability issue becomes more and more significant in deep submicron process technologies.

This thesis investigates the above issues and proposes solutions to each of them. Based on the commonly used Jamb latch synchronizer, a novel synchronizer circuit, which is able to work at low V_{dd} and is robust to V_{dd} , V_{th} and temperature variations, has been proposed. The simulation and measurement results show that the robust synchronizer only consumes slightly higher power than the Jamb latch, but it is much faster when working at low V_{dd} and much less sensitive than the Jamb latch to V_{dd} , V_{th} and temperature variations. An on-chip measurement circuit, which can measure deep metastability in synchronizers, has been designed and fabricated with a $0.18\mu\text{m}$ process. The measurement results show that the measurement method works stably and provides reliable results into the deep metastability region for predicting long term MTBF. Two adaption schemes have also been proposed to greatly mitigate the effects of on-chip variability on synchronizer performance. Their feasibility has been demonstrated using FPGA, showing that they work as expected.

Chapter 1

Introduction

1.1 Background

The System on Chip (SoC) emerged as a design concept as early as 2002 and was considered as the ideal replacement for multichip solutions. In general SoCs include multiple CPU cores, on-chip memory, and interconnections between them, along with built-in I/O interfaces as shown in Figure 1.1.

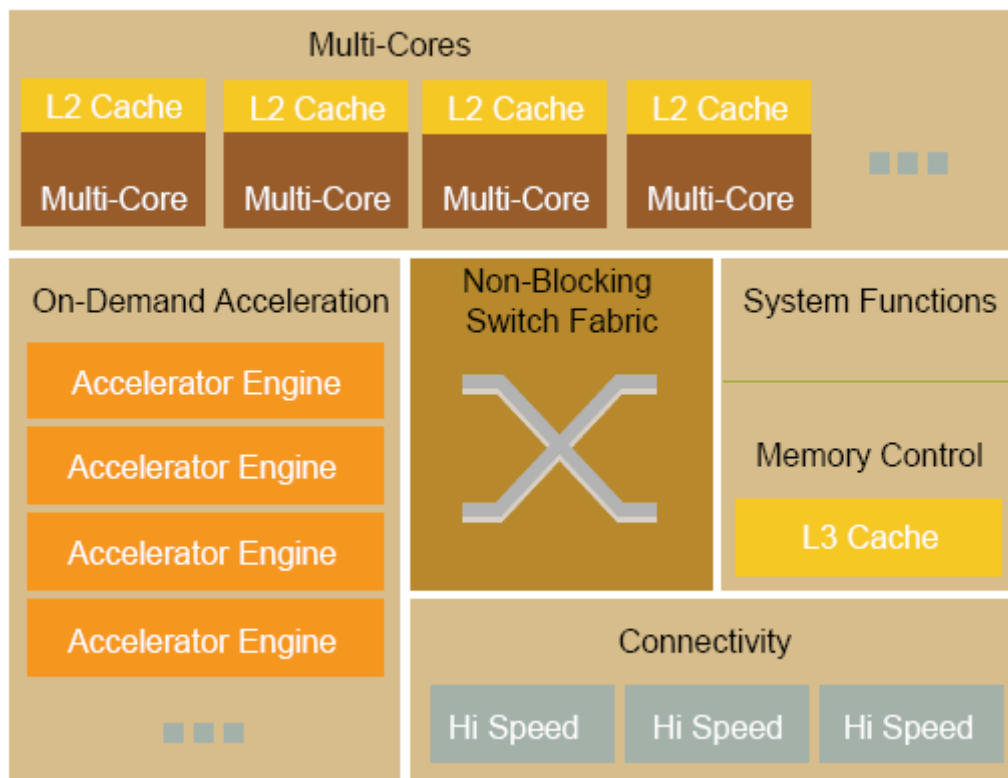


Figure 1.1 Achitecture of SoC [1]

Compared to multichip solutions, the SoC has the following advantages:

1. Better system performance
2. Lower power consumption
3. Greater functionality
4. Smaller system size
5. Lower part counts

Using SoCs can shorten development cycle while increasing product functionality, performance and quality. Due to the above advantages, SoCs have been applied in many areas such as consumer electronics, medical electronics, networking and communication, automotive and defence.

The goal of SoC design is to maximize reuse of existing functional blocks or IP cores by increasing levels of the integration. Figure 1.2 shows the trend of SoC design complexity predicted in ITRS 2007 [1]. Here, a Data Processing Engine (DPE) is a processor dedicated to data processing which achieves high throughput by eliminating general purpose features. A main processor is a general purpose processor which allocates the schedules jobs to DPEs.

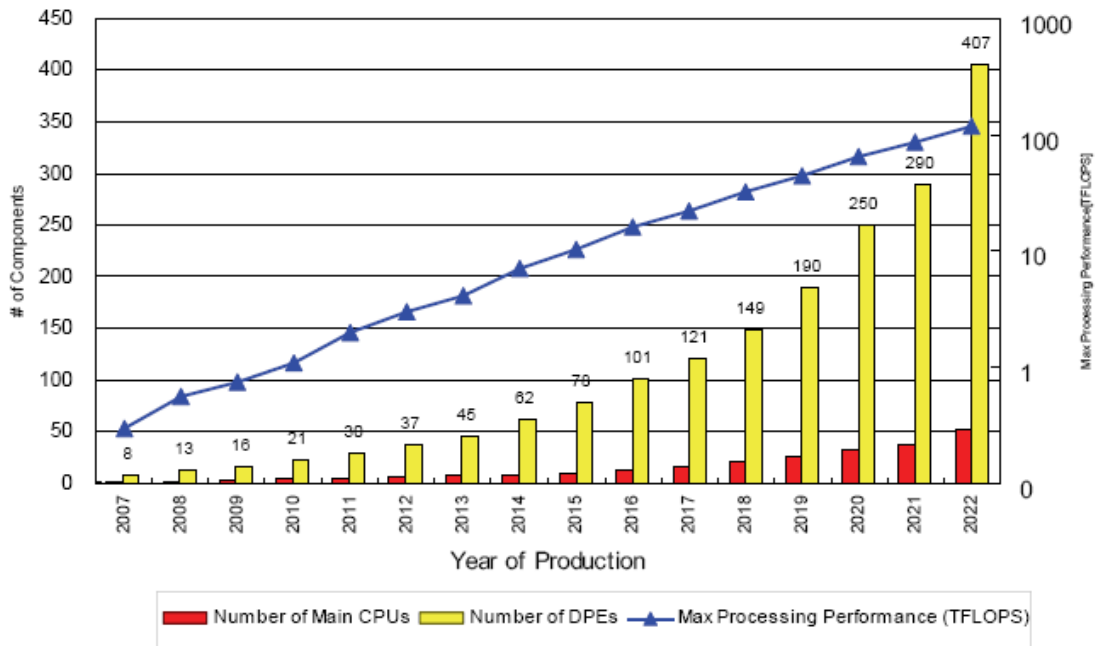


Figure 1.2 Trend of SoC design complexity [1]

Due to the ever growing size of SoCs, plus increasing clock frequency and shrinking device dimensions, it has become difficult or impossible to accurately distribute a single global clock across the entire chip [2][3][16]. In addition, as power saving techniques such as dynamic voltage and frequency scaling (DVFS) are widely used, different parts of the SoC are required to run at different frequencies to reduce the power consumption [4]. Future SoCs are likely to consist of many independently or semi-independently clocked regions, which are known as global asynchronous and local synchronous (GALS) systems [5][6][7][8][9]. Synchronization is needed for data passing between different clock regions in GALS systems, otherwise metastability will occur which may lead to severe system failures. Using synchronizers in interfacing different clock regions is a simple and economical solution to the synchronization issue in GALS systems. Instead of avoiding metastability, this solution is to leave some time for metastability to resolve itself in the synchronizer before it is sampled by subsequent circuits, so as to

reduce the probability of metastability being transferred to the next circuit. Consequently the mean time between failures (MTBF) is increased [27].

1.2 Synchronizer Issues

Future SoCs are likely to consist of many synchronizers on a single chip as the number of IP cores incorporated increases. For example, in a 64-core processor system, at least 128 synchronizers are needed by considering that one core needs at least two synchronizers for its input and output. In future SoCs, the on-chip communication including synchronization, routing and buffering is likely to affect the system performance more than processing [18]. As a critical part of on-chip communication network, the performance of the synchronizers on chip is crucial to the performance of the entire system.

The simplest synchronizer comprises two flip-flops. Metastability may occur at the first flip-flop. Then a full clock cycle is used for the metastability to settle. MTBF can be increased by increasing the clock period which is the synchronization time. However, the resolution of metastability in a two flip-flop synchronizer is relatively slow, which makes it unsuitable for high speed applications where clock frequencies are high. In the past, many different synchronizers with improved performance have been proposed [24][27][28][31][32][33][34]. However, they have a common problem, that is the synchronizer performance degrades rapidly with V_{dd} decreasing or V_{th} increasing because the synchronization time constant, τ , which determines the synchronizer performance depends on the small signal behaviour of the bistable element in the synchronizers. This situation is aggravated by lowering the temperature which results in a higher threshold voltage. Consequently, the

synchronizer performance is sensitive to V_{dd} , V_{th} and temperature variations. With the wider use of power saving techniques such as DVFS and the advances in process technology, V_{dd} will become lower and lower where synchronizers may fail to work. In addition, increasing on-chip variability could significantly degrade the synchronizer performance. Therefore, it is necessary to design synchronizers which are able to work at low V_{dd} and are robust to the V_{dd} , V_{th} and temperature variations.

The synchronizer performance can be estimated either by simulation or measurement. The simulation methods [24][37] are not sufficiently accurate for estimating synchronizer performance in the deep metastability region, which is the region for long metastability and is used to predict long term MTBF, because the resolution of simulators is limited and some devices exhibit variations in τ in the deep metastability region. Another disadvantage of the simulation methods is that noise may be important for the nondeterministic part of the synchronizer response, and so the result of a deterministic simulation may or may not be a true representation of the results in practice. The traditional measurement methods [24][28][29][30] using two oscillators are not accurate either for measuring synchronizer performance in the deep metastability region because different overlap times are generated at equal probabilities and thus deep metastability events that correspond to very short overlap times have a very small probability of occurrence. Even when they occur, it is not necessary that they can be recorded because the response speed of the oscilloscope used to record the metastability events is limited, which makes it more difficult to measure synchronizer performance in the deep metastability region. To cope with the above problems, a new measurement method has been proposed recently [36]. It greatly increases the probability of occurrence of deep metastability events by forcing the data to come close to the balance point by

using a delay locked loop (DLL). However, the method was implemented using off-chip analogue circuits, which makes it difficult to control the operation of variable delay lines or to characterise the actual input time distribution due to the instability of the off-chip analog components. It is also difficult to achieve an incremental delay of pico-second levels with an off-chip analogue delay line. These problems can be overcome by implementing the deep metastability measurement method on chip using digital variable delay lines and digital counters.

On-chip variability such as process, voltage and temperature variations is becoming an important issue on the performance of systems on silicon as the size of SoCs increases and the process technology advances [1]. Components such as logic circuits, memories on chip are all affected, but the performance of synchronizers which are used to synchronize data passing between different clock regions in future SoCs may affect the system performance to a greater extent than other components because the synchronizer performance depends on small signal rather than large signal behaviours and synchronization is a critical part of the on-chip communication which is likely to affect the system performance more than processing as the size of SoCs increases and the device dimensions shrink. Developing transistor level design techniques for more robust synchronizers [23] can be a way to improve the performance of the synchronizer as well as reducing its sensitivity to process, voltage and temperature variations, but all synchronizers exhibit variability. The synchronizer performance can be further enhanced using system level design techniques. Recently adaptation schemes have been used to mitigate the effect of process variation in microprocessor designs [43]. Similar ideas can be applied to synchronizer circuits to reduce the effects of on-chip variability on synchronizer performance.

1.3 Contributions

To address the above issues, research has been conducted in synchronizer design, measurement and performance variability, and the following contributions have been made through the research.

- 1) Based on the commonly used Jamb latch synchronizer, modifications have been made and an improved synchronizer which is able to work at very low V_{dd} and is robust to the V_{dd} , V_{th} and temperature variations has been proposed. The Jamb latch was first modified to be much less sensitive to V_{dd} variations. However, this led to a significant increase in the power consumption. Thereafter in an improved synchronizer a technique was used to reduce the power consumption while maintaining its robustness. The simulation and measurement results show that, for the improved synchronizer, the switching energy required is only a little higher than the Jamb latch, but it is much faster when working at low V_{dd} and much more robust than the Jamb latch to the V_{dd} , V_{th} and temperature variations. This work has been published in the 2006 IEEE Computer Society Annual Symposium on VLSI [23] and is presented in Chapter 3.
- 2) An on-chip measurement circuit using deep metastability measurement method for measuring synchronizer performance has been designed and fabricated using UMC 0.18 μm technology along with the devices under test (the Jamb latch synchronizer and the proposed robust synchronizer). A delay locked loop comprising digital variable delay lines and digital counters is used to force the data for the synchronizer to come close to the clock so as to increase the probability of occurrence of deep metastability events.

Compared with the previous off-chip implementation using analog circuits, the on-chip implementation using digital circuits allows integration of both the synchronizer circuits and the measurement method, and eliminates high speed off-chip paths which are a source of inaccuracy. It also makes control at the picosecond level easier because of the inherent stability of digital integrating counters and digital delay lines. The measurement results show that the on-chip deep metastability measurement method is stable and reliable, the data for the synchronizer is closely locked to the clock and τ can be measured in the deep metastability region. The measurement results also show that the tested devices are slower in the deep metastability region than they are in the deterministic region. For this reason the simulation which is only reliable for estimating the early part of synchronizer response cannot be relied upon to predict MTBF at realistic synchronization times, and it is necessary to check the value of τ in deep metastability with accurate measurement. In addition, a comparison was made between the Jamb latch and the robust synchronizer at different V_{dd} . The measurement results validated the previous simulation results, showing that the robust synchronizer circuit is much faster than the Jamb latch at low V_{dd} and is robust to V_{dd} variation. This work has been published in the IEEE Journal of Solid-State Circuits [39] and is presented in Chapter 4.

- 3) Two adaptation schemes used to mitigate the effects of on-chip variability on synchronizer performance have been proposed. Their feasibility has been demonstrated using an FPGA. The first scheme, namely **Synchronizer Selection Scheme**, is used to improve the synchronizer performance subject to process variation by selecting the best synchronizer to use out of a number

of synchronizers. Compared to simply increasing the transistor size in the synchronizer, this scheme can further reduce the effects of process variation and significantly reduce the power consumption. The second scheme, namely **Synchronization Time Adjustment Scheme**, is targeted at oversized synchronization times due to synchronizer performance variability caused by on-chip variability. It is used to improve the system performance by adjusting the synchronization time according to the actual process, voltage, temperature and data rate variations on the condition that the required MTBF is met. Assuming that the synchronization time constant τ which determines the resolution speed of metastability in synchronizers can increase by 25% due to process variation and a further 25% due to V_{dd} and temperature variations, this scheme can improve the performance of the system by 33%. This work has been published in the 14th IEEE International Symposium on Asynchronous Circuits and Systems [44] and presented in Chapter 5.

1.4 Thesis Structure

Having discussed the motivations and contributions of the research the roadmap for the remainder of the thesis is outlined below.

An overview of the main issues in current synchronizer research is outlined in Chapter 2. It first introduces why and how synchronizers are used. Then the theory of metastability and synchronization is reviewed. After that some of the existing synchronizer circuits are investigated and the common problems in synchronizer design are discussed. Next the existing simulation and measurement methods for

synchronizers are studied and their problems are discussed. Finally the effects of on-chip variability on synchronizer performance are studied and its impact on system performance is analyzed.

In Chapter 3 the commonly used Jamb latch synchronizer is investigated. A modified version of the Jamb latch is presented, which is much less sensitive to V_{dd} , V_{th} and temperature variations but consumes more power. Next a novel synchronizer circuit, which is both faster and much more robust than the Jamb latch while at the same time maintaining low power consumption, is presented. Finally the improvement resulting from the proposed synchronizer is summarized.

The on-chip measurement of deep metastability in synchronizers is described in Chapter 4. Initially the traditional measurement methods are reviewed and the principle of on-chip deep metastability measurement is described together with the implementation of the on-chip measurement circuit. Next, the measurement results are shown and a comparison is made with the simulation results, demonstrating that the on-chip measurement method is stable and reliable.

In Chapter 5 the two adaptation schemes proposed to reduce the effects of on-chip variability on synchronizer performance are described. Initially the on-chip measurement of failure rates is discussed, followed with an explanation of how τ and MTBF are calculated from the failure rates. Subsequently the synchronizer selection scheme and synchronization time adjustment scheme are described, followed by the implementation details of the two adaptation schemes. Next the applications of the two adaptation schemes are discussed and the test results are presented.

The conclusions resulting from the work undertaken in the thesis together with future work are presented in Chapter 6.

Chapter 2

Literature Review

2.1 Synchronizer

This section introduces why synchronizers are needed and how they are used.

2.1.1 Why are synchronizers needed

As the size of SoCs in terms of the number of modules incorporated increases and the process technology shrinks, it has become more and more difficult to accurately distribute a single global clock across the entire systems. Skew and jitter in both the clock and the data mean that the system may have to be divided into many subsystems, which are either independently clocked or at least semi-independent. In addition, in a multiple IP cores SoC, different IP cores are required to run at different frequencies in order to achieve low power and maximum performance. As a response to these challenges, GALS architectures which allow the reuse of synchronous IP cores in an asynchronous environment have been proposed and investigated [5][6][7][8][9].

In a GALS system, different cores are optimised to operate at different frequencies to achieve low power and maximum performance, and therefore form many different clock regions. Synchronization is needed for data passing between

different clock regions [10]. To understand this, let us look at a flip-flop. As shown in Figure 2.1, data from a different clock region is seen as an asynchronous signal by the flip-flop. It can arrive any time. When it arrives very close to the rising edge of the local clock and violates the setup condition, metastability may occur at the output of the flip-flop (which is explained in detail in Section 2.2.1). Metastability is often seen as an indeterminate level between logic 0 and logic 1 which may cause failures in subsequent circuit blocks which are designed only for defined logic levels. When metastability occurs, it will resolve to a logic 0 or 1 at a certain speed which is determined by the circuit parameters of the flip-flop. If the metastability cannot settle before the next rising edge of the read clock, the indeterminate logic level will be transferred to the subsequent circuits, which may lead to a system failure.

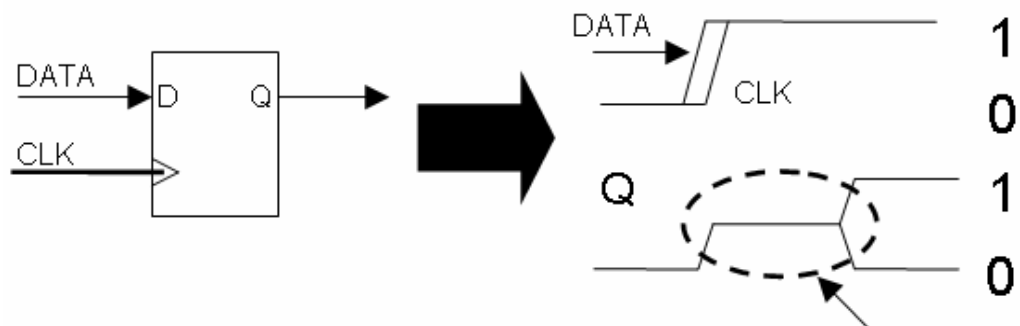


Figure 2.1 Metastability in flip-flop

Synchronizers are used to retime data passing between different clock regions, They are not used to avoid the metastability, but to leave some time for the metastability to resolve itself before the data is sampled by the following circuits, so as to reduce the probability of the indeterminate level passing to the subsequent circuits [11][12][13][14]. The simplest synchronizer comprises two flip-flops as shown in Figure 2.2. Here metastability may occur in the first flip-flop when data input arrives very close to the rising edge of the clock, and then a full clock cycle is

used for the metastability to resolve itself. If the metastability cannot settle before the next rising edge of the clock, the indeterminate level will be transferred to any subsequent circuit block, potentially resulting in system failures. For a particular synchronizer, the longer the synchronization time is, the smaller is the probability of the metastability being transferred to the following circuits.

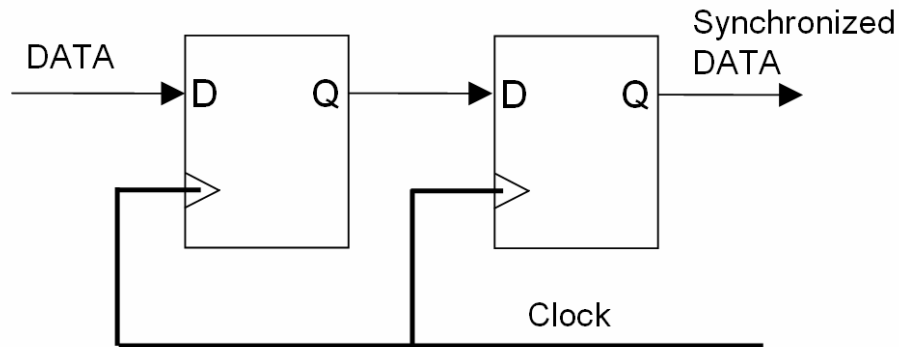


Figure 2.2 Two flip-flops synchronizer

Some may think that if the clocks in the GALS system are all phase locked, there is no need for synchronisation of data passing between different clock regions, since data originating in one clock region and passing to the next will always arrive at the same point in the receiving clock cycle. However, in practice it is difficult to achieve accurate and reliable locking between all the clock regions for a number of reasons.

- Clocks run at different frequencies.
- Jitter and noise may alter the phase relationships of two clock trees.
- Crosstalk between the data and the clock introduces noise into both, affecting the phase relationships of two clock trees.
- Input and output interfaces between the system and the outside world are not controllable and phase relationships cannot be predicted.
- Process variation may alter the phase relationship of two clock trees.

- Voltage variation which is either caused by purposely varying V_{dd} to reduce power consumption or by IR drop may alter the phase relationship of two clock trees.
- Temperature variation may alter the phase relationship of two clock trees.

These effects cause unpredictable variation in the time of arrival of a data item relative to the receiving clock, which becomes worse at smaller technology nodes and higher integration levels, and is particularly noticeable in high performance systems using IP cores with large clock trees [1]. Figures of 150ps noise [3], and 110ps clock skew [1] which is likely to increase as geometries shrink, have been reported in 0.18 μ m systems. Interfaces in high performance systems with fast clocks and large timing uncertainties then become more difficult to design as these uncertainties increase as a proportion of the receiving clock cycle. Due to the above reasons, it is simpler to assume that the timings of the two clock regions are independent and therefore synchronization is necessary.

2.1.2 How are synchronizers used?

Future systems on chip are likely to consist of many independent clock regions and thus many synchronizers will be required. These can be seen are part of on-chip communication. It is likely that, as the size of systems on chip increases, on-chip communication is going to affect the system performance more than processing, because the long wires needed for global interconnect become slower, causing unpredictable delays, propagation and synchronization error, high power consumption, etc [18]. Future systems on chip may incorporate hundreds of synchronizers on a single chip. For example, a 64-core system will incorporate at least 128 synchronizers considering that one core needs at least two synchronizers

for its input and output. As a critical part of on-chip communication network, the performance of the synchronizers is crucial to the performance of the whole system.

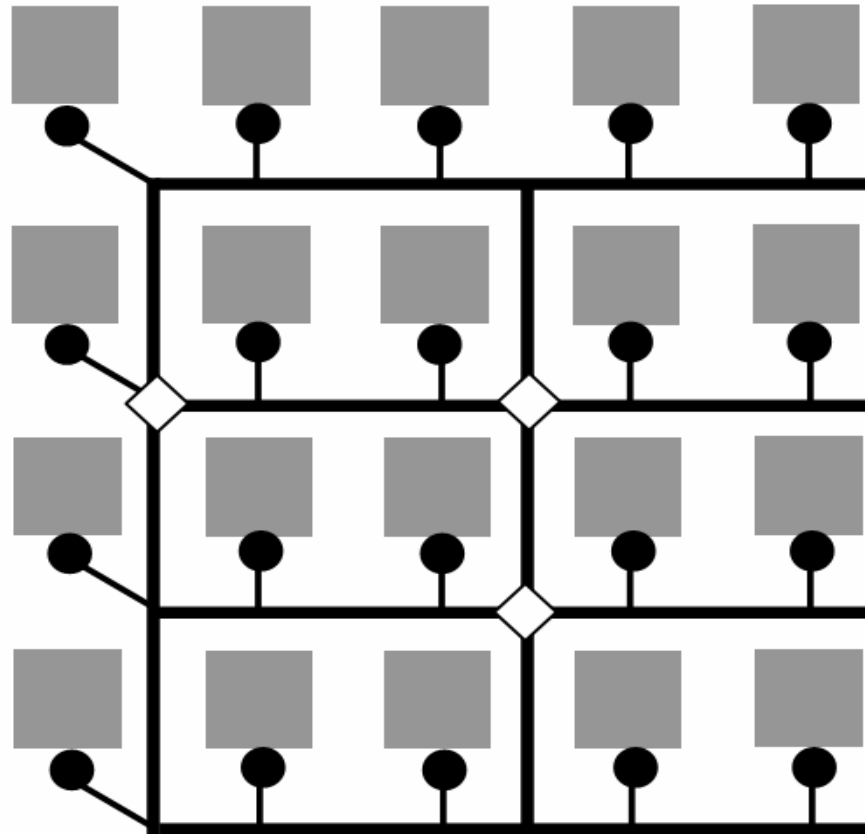


Figure 2.3 GALS system

Figure 2.3 shows an example of a multi-core GALS system. Here the grey squares represent IP cores, the white diamonds represent on-chip routers, the black lines represent on-chip buses and the black dots represent synchronizers. The routers, buses and synchronizers form an on-chip network. Synchronization is usually restricted to control signals rather than data signals in order to reduce the number of synchronizers required. Figure 2.4 shows a simple example of using synchronizers in system. Here Core A has some data to send to Core B. First the data is put onto the bus and the Req signal is sent to Core B through the on-chip network composed of the synchronizers and routers. When the Core B receives the Req signal it

samples the data on the bus and sends the Ack signal back to Core A. For this communication architecture each core needs at least two synchronizers for the Req and Ack signals.

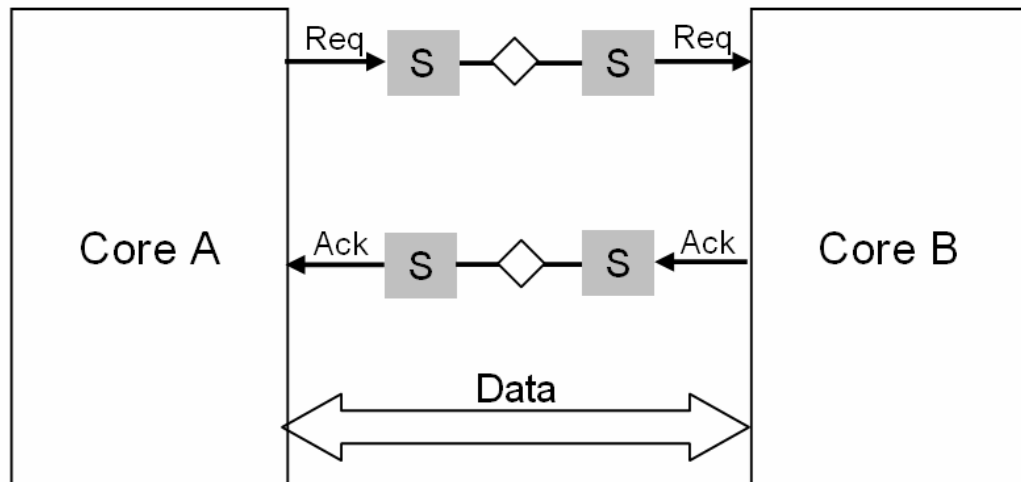


Figure 2.4 Synchronizers in system

2.2 Synchronizer modelling

In order to model a synchronizer circuit it is essential to understand several aspects related to the operation of a synchronizer, namely:

- Metastability
- Metastability resolution time
- Failure rates

2.2.1 Metastability

The setup and hold conditions of a flip-flop are always guaranteed by the design itself, so the output of the flip-flop always reaches one of the two stable states (logic 1 or logic 0) quickly. For flip-flops working as synchronizers in GALS architectures

the setup and hold conditions can be violated when the data changes at a time very close to the clock edge. The circuit outputs can then be left half way between a high and a low state, which is normally referred to as a metastable state, and the output time for this condition needs to be characterised. In Figure 2.5, initially the data is low and the clock is high. If the data goes high just before the clock goes low, M1 will go low first, causing the output Q to go high, and then go high when the clock goes low. If the overlap between the data and the clock is very small, at this time the output Q may not yet have reached a high state, but the inputs M1 and M2 are now high and only the cross-coupled gates can determine whether it ends up high or low.

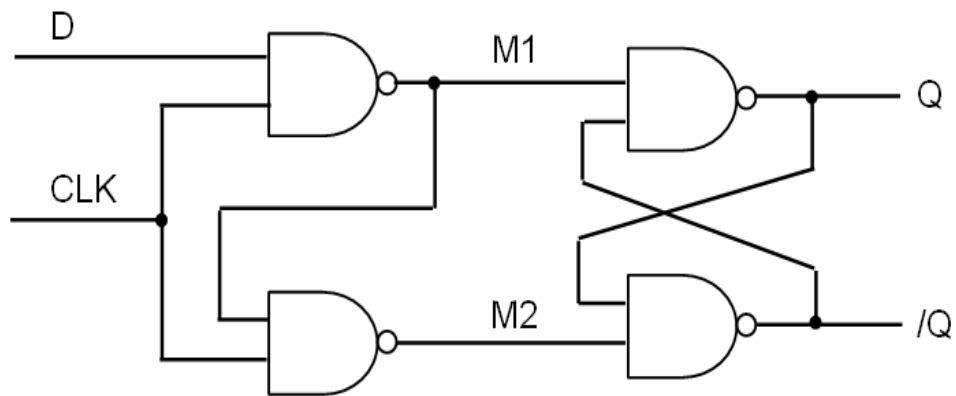


Figure 2.5 D Latch

Since M1 and M2 are now high, they take no further part in determining Q, so what happens is determined by the cross-coupled gates in the latch. This is similar to the cross-coupled inverters shown in Figure 2.6(a). Here the input to any of the two inverters is just the output of the other one. Figure 2.6(b) shows the DC transfer characteristics of the two inverters.

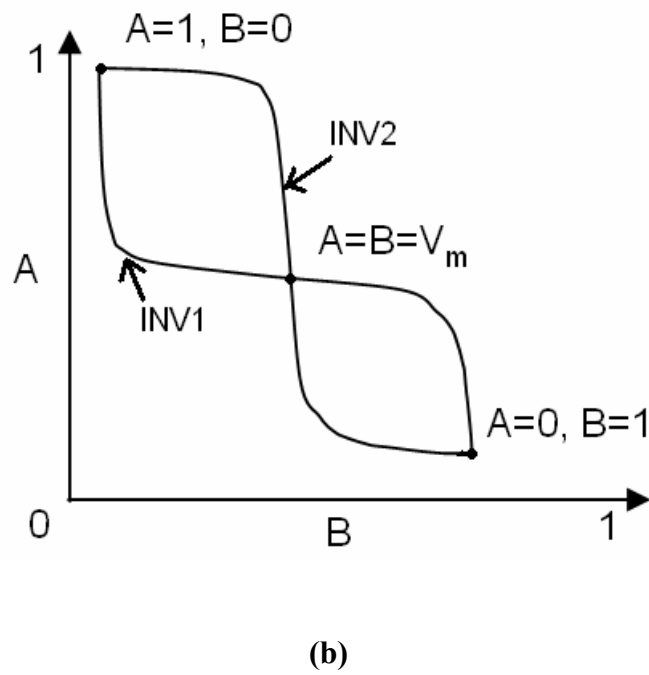
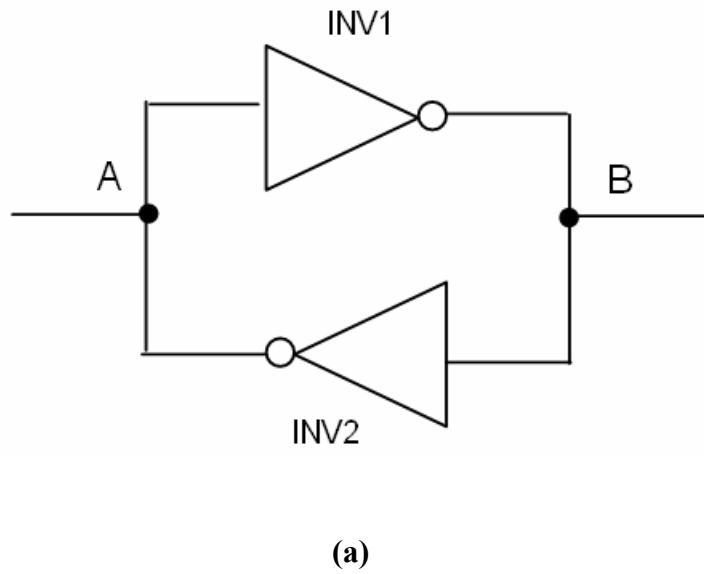


Figure 2.6 Metastable state

In Figure 2.6(b) there are three points where the curves of the two inverters intersect, that is $(A=1, B=0)$ and $(A=0, B=1)$ which are two stable states. There is a third point where the curves intersect, that is $A=B=V_m$, where V_m is not a legal logic level. This point is a metastable state because the voltage are self-consistent and can remain there indefinitely; however, any noise or other disturbance will cause it to

resolve to one of the two state states. Figure 2.7 shows an analogy of a ball on a hill. The top of the hill is a metastable state. Any disturbance will cause the ball to roll down to one of the two stable states on the left or right side of the hill. The problem of the metastable state is, with a net drive of zero, the ball may stay on the top of hill forever.

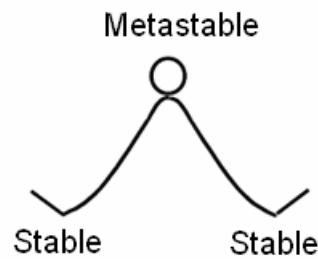


Figure 2.7 Metastable equilibrium

Metastability can be reached from either stable state if the overlap between data and clock is at a critical point, as shown in Figure 2.8. This particular photograph was taken by recording all the metastable events in a level triggered latch, which lasted longer than 10ns [20]. Several traces are superimposed, with outputs starting from both high and low levels, then reaching a metastable state about halfway between high and low, and finally going to a stable low level state. It can be seen that the traces become fainter to the right, showing that the number of events decreases as the metastability time increases.

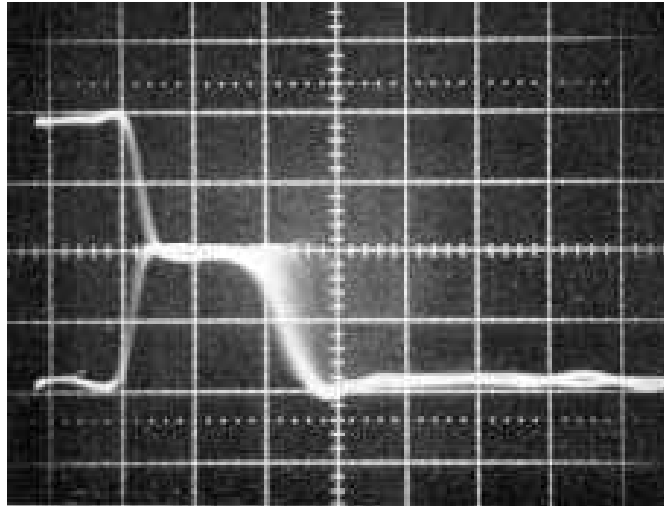


Figure 2.8 Metastable outputs [20]

When a flip-flop is used for synchronization, metastability may occur in the master latch and a long time may elapse before its output settles to a stable high or low level. A half level input, or a change of input close to the change of clock in the slave latch may then result in metastability at the output of the slave latch, which is first read by subsequent circuits as a low level, and then later as high level, or read by some circuits as low level, and the others as high.

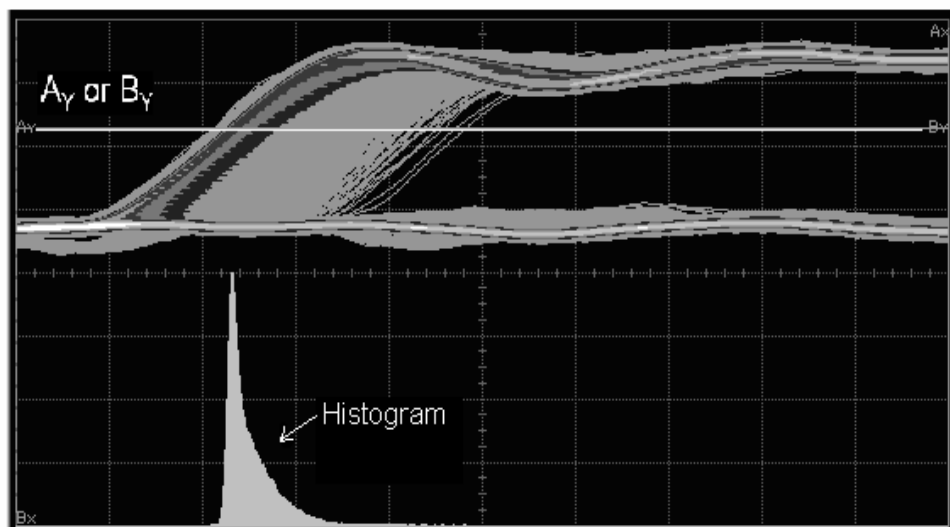


Figure 2.9 Metastable events and output histogram

Figure 2.9 shows the outputs of a flip flop used as a synchronizer. Many outputs have been captured using an advanced digital oscilloscope. As time increases from left to right, the density of the traces which is represented by the grey level reduces, because longer metastability events have lower probability (as explained in later sections). A histogram of the number of outputs with voltages higher than A_y or B_y line (these are two lines used in the setup of oscilloscope to define the threshold voltage for generating the histogram) at a particular time is also shown in this figure (the white area, in which the height at a particular time refers to the number of outputs hitting A_y or B_y line at that time). When metastability occurs it resolves at a certain speed which is determined by the synchronization time constant τ (defined in later sections). If the metastability cannot resolve itself before the next rising edge of the clock, a synchronization failure occurs and the metastability is passed as an input value to subsequent circuits. However, the longer the time allowed for synchronization, the less likely it is for the metastable value to be passed on. The slope of the output histogram is related to the synchronization time constant τ . The greater the slope, the smaller the τ and thus the shorter the metastability resolution time. The output histogram is used to evaluate the synchronizer performance qualitatively, but to assist the synchronizer design an accurate quantified model is needed.

2.2.2 Resolution of Metastability in Synchronizers

Most synchronizers designs are based on flip-flops. To understand the resolution of metastability it is necessary to analyze the analogue response of the bistable element in the flip-flop. The bistable elements in the flip-flop are normally made from cross-coupled gates or inverters. To simplify the model, the analysis will be

based on cross-coupled inverters rather than gates. In the metastable state the cross-coupled inverters are in a small signal mode, close to the metastable point. To make the analysis simpler by eliminating constants, it is assumed that the metastable point is at 0V, rather than $V_{dd}/2$. This means that a logic high is $+V_{dd}/2$, and a logic low is $-V_{dd}/2$. The inverters can now be modelled as two linear amplifiers [20][21][22][15][27]. Each inverter is represented by an amplifier of gain $-A$ and time constant CR , as shown in Figure 2.10. Differing time constants due to different loading conditions can also be taken into account.

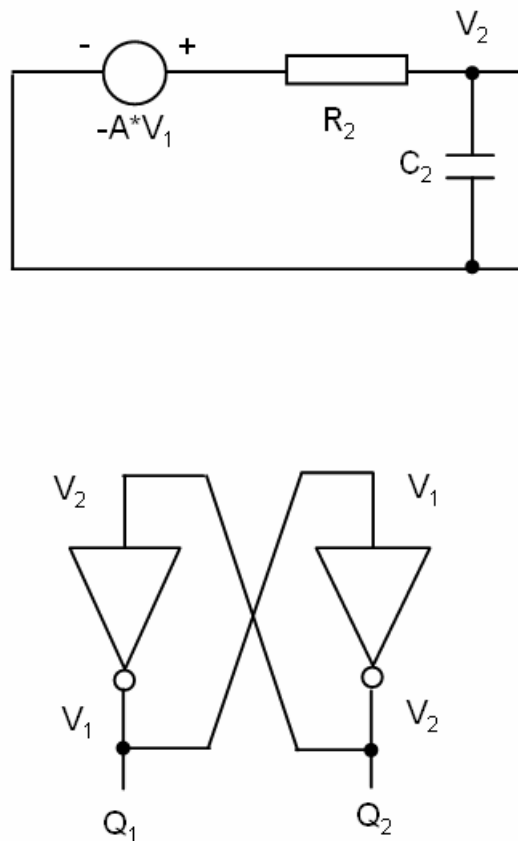


Figure 2.10 Small signal models of gate and flip-flop

The small signal model for each inverter has a gain $-A$ and its output time constant is determined by CR , where R is the inverter output resistance, and C is the

inverter output capacitance. In a synchronizer, both the data and clock timing may change within a very short time, but no further changes will occur for a full clock period, so it can also be assumed that the input is monotonic, and the response is unaffected by input changes.

For each inverter it can be written [27]:

$$-C_2 \frac{dV_2}{dt} = \frac{V_2}{R_2} + A \frac{V_2}{R_2} \quad (2.1)$$

$$-C_1 \frac{dV_1}{dt} = \frac{V_1}{R_1} + A \frac{V_2}{R_1}$$

The two time constants can be simplified to:

$$\tau_1 = \frac{R_1 C_1}{A}, \tau_2 = \frac{R_2 C_2}{A} \quad (2.2)$$

Eliminating V_1 this leads to:

$$0 = \tau_1 \cdot \tau_2 \cdot \frac{d^2 V_1}{dt^2} + \frac{(\tau_1 + \tau_2)}{A} \cdot \frac{dV_1}{dt} + \left(\frac{1}{A^2} - 1\right) \cdot V_1 \quad (2.3)$$

This is a second order differential equation, and has a solution of the form:

$$V_1 = K_a \cdot e^{\frac{-t}{\tau_a}} + K_b \cdot e^{\frac{t}{\tau_b}} \quad (2.4)$$

Normally the inverters have a high gain, and are identical, so

$$A \gg 1, \quad \tau_a = \tau_b = \sqrt{\tau_1 \tau_2}.$$

K_a and K_b are the initial conditions which are determined by the overlap time between data and clock. τ_a and τ_b are determined by τ_1 , τ_2 and A . Typical values of τ_1 , τ_2 and A for 0.18 μm process, are 35ps for τ_1 and τ_2 and 20 for A . Often the values of τ_1 and τ_2 track the FO4 inverter delay, since both times are determined by the load capacitance, conductance, and gain of the inverter.

This model is valid within the linear region of about 50mv either side of the metastable point. Outside this region the gain falls to less than 1 at few hundred millivolts; the output resistance of inverter and the load capacitance also drop significantly, R by a factor of more than 10, and C by a factor of about 2. Thus, even well away from the metastable point the values of τ_1 and τ_2 still have values similar to those at the metastable point.

2.2.3 Synchronizer Failure Rates

The synchronizer failure rates can be estimated by computing how long it will take for the metastability to resolve to logic high or low and comparing this with the given synchronization time. The metastable events of interest are only those that take a much longer time than the normal flip-flop response time, hence the first term in equation (2.4) can be neglected consequently:

$$V_1 = K_b \cdot e^{\frac{t}{\tau_b}} \quad (2.5)$$

The initial condition, K_b , depends on the overlap time between the clock and data. If the overlap time is very large, K_b will be positive, and the output voltage will reach a high output of $+V_{dd}/2$ quickly. If the overlap time is very small, K_b will be negative, and the output voltage will reach a low output of $-V_{dd}/2$ quickly. In

between, the value of K_b will vary according to the relative data clock timing, and at some critical point $K_b = 0$, so the output voltage is stuck at the metastable point of 0 V. The data clock timing that gives $K_b = 0$, is referred to the balance point, where the output time is theoretically infinite. The Figure 2.11 shows the occurrence and resolution of metastability. The *Input Time* is defined as the time between the rising edge of the data and the balance point and is defined by the symbol Δt_{in} to represent it. The *Output Time* is defined as the time of the output relative to the rising edge of the clock.

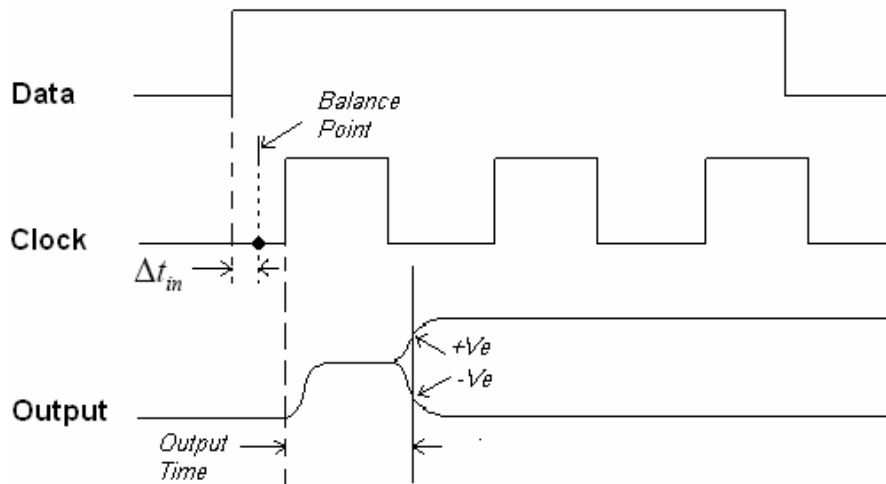


Figure 2.11 Occurrence and resolution of metastability

The value of K_b is given by:

$$K_b = \theta \cdot \Delta t_{in} \quad (2.6)$$

Where θ is a circuit constant which determines the rate at which the overlap time between data and clock converts into a voltage difference between the two nodes of the cross-coupled inverters.

In order to compute the time taken for the metastability to resolve, it is assumed that $+V_e$ and $-V_e$ are the borders of the metastability region, which means if the output voltage is within $[-V_e + V_e]$, the output is metastable, otherwise the output is out of metastability. Now what we need to do is to compute the time taken by the output to reach $|V_e|$, the exit voltage which can be regarded as a stable high or low state. Hence from equation (2.5) by substituting $V_1 = V_e$ and setting $K_b = \theta \cdot \Delta t_{in}$, the time taken for the metastability to resolve is given by:

$$t = \tau \cdot \ln \left[\frac{V_e}{\theta \cdot \Delta t_{in}} \right] \quad (2.7)$$

For a data from a different clock region, the input time Δt_{in} , which is the overlap time between the rising edge of the data and the balance point, is normally unknown, so all values of Δt_{in} are equally probable. In these circumstances, it is usual to assume that the probability of any input time smaller than a given Δt_{in} is proportional to the size of the Δt_{in} . This is usually true if the two clock regions are independently clocked. As mentioned before, the balance point ($\Delta t_{in} = 0$) is where the output will be stuck at the metastable point and the output time will be theoretically infinite. Before the balance point, the smaller the input time, the closer the initial voltage is to the metastable point, and thus the longer the output time, as shown in Figure 2.12. Given the clock period is T , the probability of any input time smaller than the given Δt_{in} is $\frac{\Delta t_{in}}{T}$, and given the data frequency is f_d , the frequency of any input time smaller than the given Δt_{in} is $f_d \cdot \frac{\Delta t_{in}}{T}$ or $f_d \cdot f_c \cdot \Delta t_{in}$, where f_c is the clock frequency.

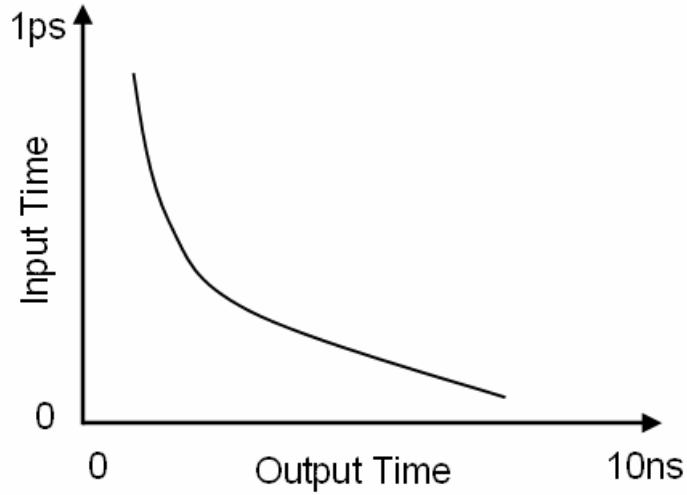


Figure 2.12 Input time and output time relationship

Assuming that any input time smaller than the given Δt_{in} will lead to an output time greater than the given synchronization time and thus produce a synchronizer failure, the synchronizer failure rate is $f_d \cdot f_c \cdot \Delta t_{in}$. The MTBF of the synchronizer is therefore given by:

$$MTBF = \frac{1}{f_d \cdot f_c \cdot \Delta t_{in}} \quad (2.8)$$

By substituting Δt_{in} with $\frac{V_e}{\theta} e^{-\frac{t}{\tau}}$ (from 2.7), another form of the equation for the

MTBF of the synchronizer is:

$$MTBF = \frac{e^{\frac{t}{\tau}} \theta}{f_d \cdot f_c \cdot V_e} \quad (2.9)$$

This is more usually written as:

$$MTBF = \frac{e^{\frac{t}{\tau}}}{f_d \cdot f_c \cdot T_w} \quad (2.10)$$

Where $T_w = \frac{V_e}{\theta}$, and T_w is known as the metastability window.

Equation (2.10) is usually used to estimate the MTBF from the circuit parameters τ and T_w in designing a synchronizer, while (2.8) is usually used to compute the MTBF from the input time and output time relationship in measuring synchronizer performance.

From equation (2.10) it can be seen that the synchronizer performance or MTBF is determined by the metastability window T_w and the synchronization time constant τ . T_w is determined by the time-voltage conversion rate θ and the voltage at which the flip-flop exits from metastability, V_e ; τ is determined by the feedback loop time constant. From equation (2.10) it can also be seen that τ is more important than T_w in determining the synchronizer performance because it directly affects the power of e .

It should be noted that the preceding failure rate analysis using the small signal gate model for an inverter is only applicable to the most simple synchronizers, but may not hold for more complex synchronizers made from gates with more than one time constant in the feedback loop, or with long interconnections, because in those cases the feedback interconnection may have additional time constants, and the differential equation that describes the small signal behavior will be correspondingly complex. An example of multiple time constants is shown in [19], where a latch has been built out of two FPGA cells. The measurement result shows an oscillation in the resolution speed of metastability due to multiple time constants.

It should also be noted that in most cases the first term $K_a \cdot e^{\frac{-t}{\tau_a}}$ in equation (2.4) can be neglected when estimating the synchronizer failure rates, because the metastable events that take a much longer time than the normal flip-flop response time are of interest. However, if the synchronization time allowed for metastability to resolve is very short, the first term must be taken into account in order to get accurate failure rates.

2.3 Synchronizer Circuits

2.3.1 Latches

Most synchronizers are made from latches using the master slave configuration as shown in Figure 2.13. Its reliability depends on the time allowed for metastability to resolve in the master and slave latches. The latches can be made up of cross-coupled gates with a metastability filter which prevents the metastable level being transferred to the subsequent circuits as shown in Figure 2.14. Here, metastability may occur when the data goes high just before the clock goes low. If both cross-coupled gate outputs go to a metastable level, the filter output will remain low. Only when there is a large enough voltage difference (say 1 V) between the gate outputs can the filter output go high.

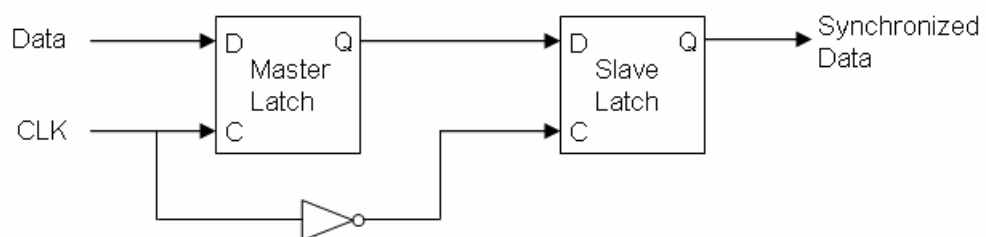


Figure 2.13 Latches based synchronizer

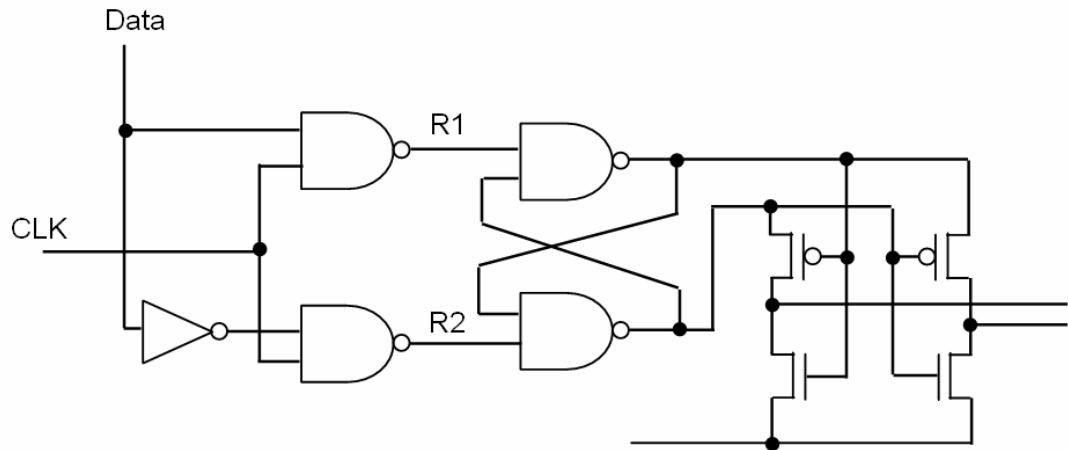


Figure 2.14 Latch with filter

2.3.2 Jamb Latch

As mentioned in Section 2.2.2, synchronizer performance depends on the circuit parameters T_w and τ . T_w is mainly determined by the input characteristics of the latch circuit and τ is determined by the transconductance and capacitance of the cross-coupled gates. τ is more important than T_w since it directly affects the power of e in determining the MTBF. In most applications it is important to increase the MTBF to a very high value, therefore the value of τ should be made as low as possible.

The Jamb latch is one of the most commonly used synchronizers because of its simple structure and relatively good performance [24]. It is based on cross-coupled inverters rather than gates, as inverters have a higher gain, and less capacitance than gates, which leads to a smaller τ . The structure of the Jamb latch is shown in Figure 2.15. The circuit is reset by pulling the node B to ground and set when data is high and clock is low by pulling the node A to ground. The output can either be taken from Out A or Out B. Metastability occurs when the data goes high just before the

clock goes low so that nodes A and B are pulled down and up to around $V_{dd}/2$. In a normal CMOS inverter, the p-type transistor has a width twice the n-type, in order to make the rise time the same as the fall time. However, the situation is different for synchronizers. For synchronizers τ is the most important parameter. The transconductance of the inverter depends on the transconductance of both p-type and n-type transistors, and the capacitance also depends on the capacitance of both devices. Previous simulation results show that the optimum value of τ is obtained when the ratio between p-type and n-type transistors is 1:1 [23][24][25][26]. For the correct set and reset operation, the data, clock and reset transistors must all be made wide enough, when compared to the transistors in the cross-coupled inverters, and the data and clock transistors must be made wider than the reset transistor because they are in series. A Jamb latch synchronizer can be made from two Jamb latches in a master-slave configuration as shown in Figure 2.13.

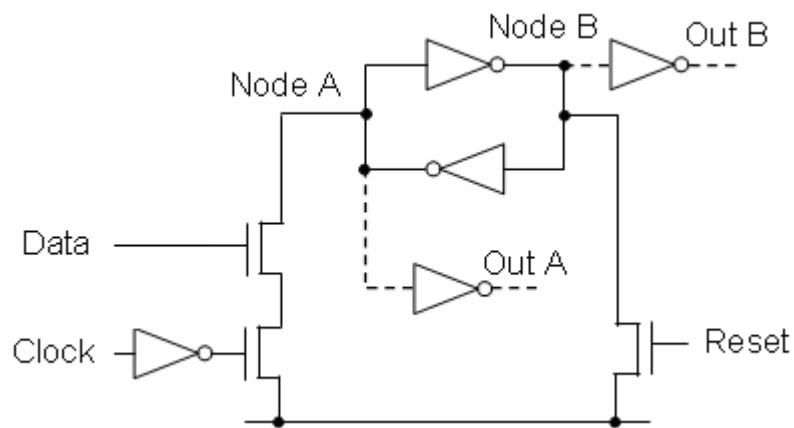


Figure 2.15 Structure of Jamb latch

The Jamb latch synchronizer is a commonly used synchronizer because of its simple structure and good performance. The problem with the Jamb latch is that its performance degrades rapidly with V_{dd} decreasing or V_{th} increasing, because the

synchronization time constant τ which is determined by the transconductance in the cross-coupled inverters, increases quickly with V_{dd} decreasing or V_{th} increasing. This situation is worsened by lowering the temperature because lower temperature gives higher threshold voltage. When V_{dd} is as low as the sum of threshold voltages of the p-type and n-type transistors in the cross-coupled inverters, both transistors are almost off, so τ becomes infinite.

2.3.3 Other proposed synchronizers

In the past several different synchronizer circuits have been proposed and these are discussed briefly below.

However before discussing the proposed synchronizer circuits, it is worthwhile asking the obvious question since, as described below, synchronizer circuits are problematic, so, what would be the MTBF if a synchronizer was not included?

This question can be easily answered by performing a simple calculation on how often a flip-flop, in a given situation, would go into metastability. Consider a flip-flop implemented in a $0.18\mu\text{m}$ CMOS technology, being driven by a 500 MHz clock, with a data rate of 50 MHz. Assuming T_w is 50 ps, the rate at which metastability occurs is $T_w \times f_c \times f_c = 50 \times 10^{-12} \times 500 \times 10^6 \times 50 \times 10^6 = 1.25 \times 10^6$. Hence the flip-flop goes into metastability every 800 ns – such a high MTBF cannot be tolerated, hence the exclusion of synchronizer is not a viable option.

The insertion of a synchronizer between two blocks in a circuit will obviously result in additional delay or latency in the signal path. Consequently, some of the proposed techniques were directed at reducing this delay or latency.

One of the common mistakes is to use only a single flip-flop, which equals, essentially, no synchronizer at all as there will be insufficient time for the synchronization process to take place resulting in a short MTBF.

Another technique is to synchronize the data bits instead of the control signals so that the handshake protocol is avoided and thus the communication latency is reduced. This scheme fails because each synchronizer may end up doing different things. Some may correctly sample the bit, some may lose the bit and retain the old one, and some may enter metastability and resolve to 1 or 0. Finally the data sampled by subsequent circuits is incorrect. Another disadvantage of this scheme is that it actually increases the failure rate since the number of the synchronizers used increases.

Other proposed synchronizer designs attempted to either block metastability from being passed to subsequent circuit blocks or to shorten metastability resolution time.

A metastability blocking circuit is shown in Figure 2.16. The RESET signal clears the SR latch and the synchronizing flip-flop. When the clock is high the asynchronous input will be selected by the multiplexer; if the input is high the SR latch is set. When the clock goes low, the output of the SR latch is selected by the multiplexer. When the clock goes high, the latched input is sampled by the synchronizing flip-flop without any metastability. The problem with this technique is that the metastability is not blocked, but transferred from the flip-flop to the latch. If the input goes high just before the clock goes low, a short pulse is created which may cause a metastability in the SR latch. The time allowed for the metastability to resolve is only half a cycle, which leads to even worse reliability.

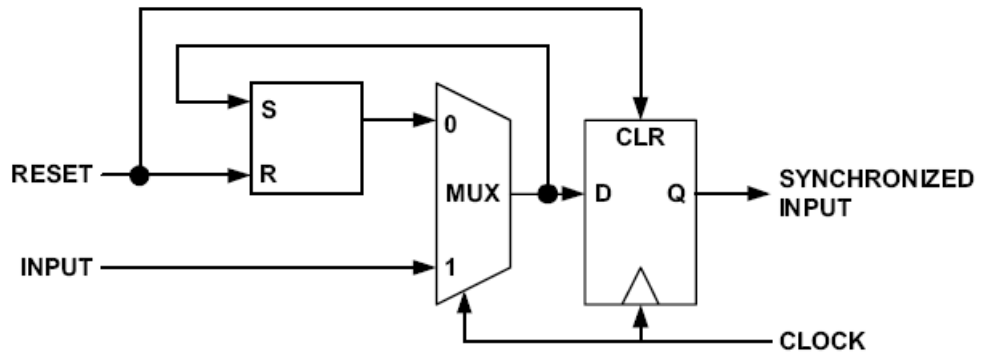


Figure 2.16 Metastability blocker [31]

A circuit which attempts to reduce the metastability resolution time is shown in Figure 2.17. The underlying principle of the Metastability Shaker [32][33] is that whenever a metastable state is detected a mechanism is activated which reduces the resolution time. The core element in this circuit is a Jamb latch. The detector circuit generates a pulse when a metastable state occurs, which is then applied to the gate input of a parallel clock transistor so that the evaluation time for the data input is extended. The principle of the ‘Shaker’ circuit relies on the sensitivity of the metastable state to external disturbance. So a small externally applied stimulus can shake the latch out of metastable state and so shorten the metastability resolution time. However, the problem with this approach is that if the pulse is applied when the metastability is about to resolve itself, it may pull the circuit back to metastability. The idea, in effect, just moves the balance point from one place to another. It does not accelerate the resolution of the metastability.

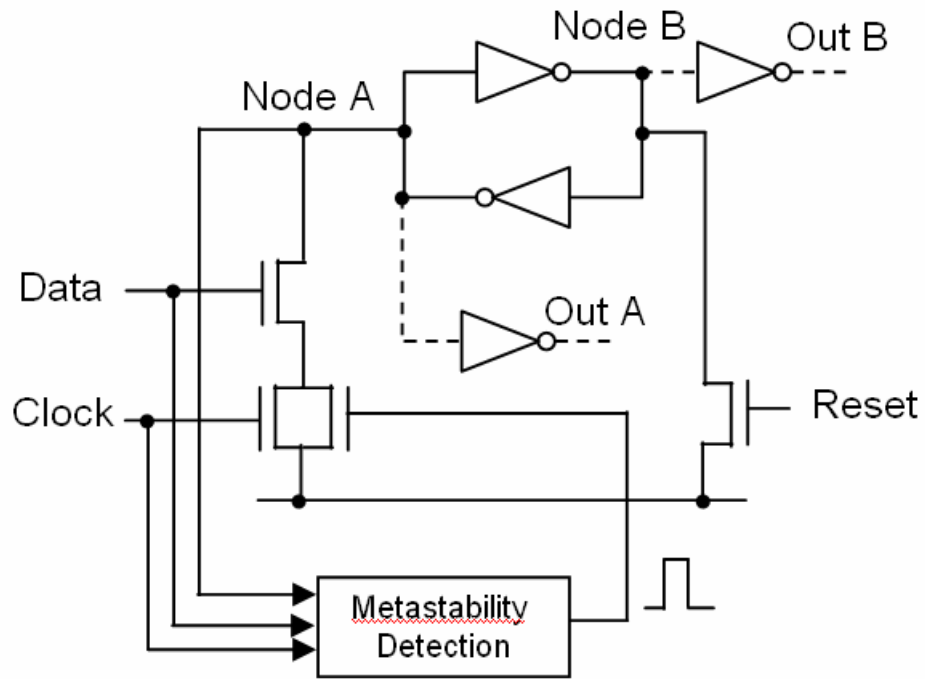


Figure 2.17 Metastability shaker

Most of the working synchronizers are based on the two flip-flop synchronizer and the Jamb latch described before. Improvement of synchronizer performance is usually done by increasing the transconductance or reducing the node capacitance in the cross-coupled gates. To reduce the capacitance, the size of all the transistors connected to the nodes should be minimized. In the Jamb latch, the size of the output inverters can be reduced, but the set and reset transistors can not be reduced below a certain size or the circuit will not function correctly. It is possible to overcome this problem by switching the latch between an inactive (no gain) and an active (high gain) state rather than two inactive states. In this way the drive needed to switch the latch is small, so the set transistors can be further reduced to minimize the node capacitance. A circuit based on this principle is shown in Figure 2.18 [27]. When clock is low the B0 and B1 nodes are connected and the circuit is in an active state. When clock goes high one of the B0 and B1 nodes goes low, giving a high at

the output if data is high before the clock. Since the drive needed to switch the latch between active state and inactive state is small compared to switching it between two inactive states, the p-type data transistors can be reduced to less than 1/4 the size of those in the Jamb latch, which is also necessary for maintaining the circuit in the fully active state. So the node capacitance is less and thus τ is smaller.

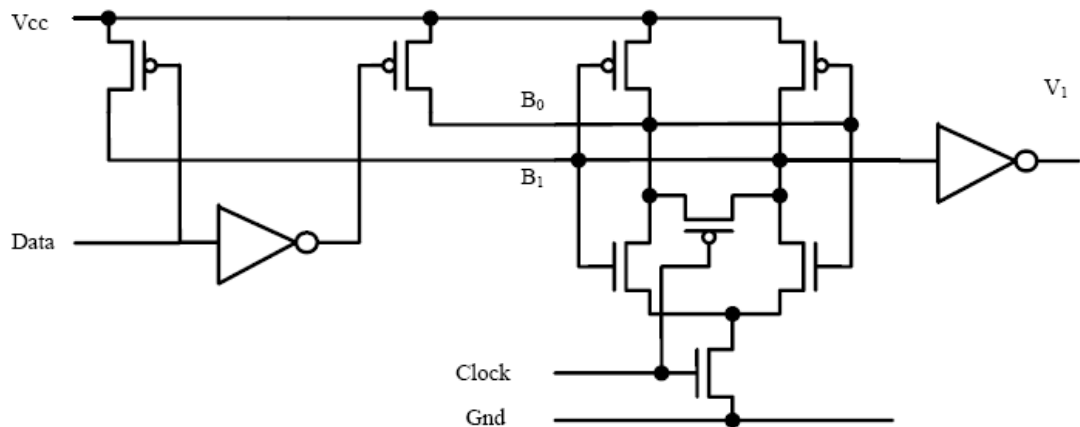


Figure 2.18 Low input coupling latch [27]

Synchronizers made up of many parallel flip-flops have also been proposed [34]. Some designs can give an advantage at the expense of complexity, others may not, but generally the advantage is small. The power and area required for a multiple flip-flop synchronizer might be better used in improving the synchronization time constant τ of the flip-flop itself.

All of the synchronizers discussed above have the same problem as the Jamb latch, which is that the synchronizer performance is sensitive to V_{dd} , V_{th} and temperature variations. As the process variations become a major issue for nanometer process technologies, and V_{dd} based power saving techniques such as DVFS are widely used, V_{dd} , V_{th} and temperature variations are going to affect the

synchronizer performance more than before. Future systems on chip could consist of hundreds of synchronizers on a single chip. Their performance is critical to the system performance since they are an important part of the on-chip communication network, and this problem has to be addressed.

2.4 Synchronizer Simulation and Measurement

2.4.1 Synchronizer Simulation

The performance of a synchronizer can be estimated either by simulation or measurement. There are two methods to simulate a synchronizer. The first is to feed the synchronizer model with different input times and record the output times. Then the input time and output time relationship can be plotted to calculate τ and MTBF; This approach is called the *input time and output time method*. The initial stage in this approach is the location of the balance point which is an iterative procedure. For example, at the start the data arrival time is set at 1.1ns and the clock arrival time at 2ns. If the output of the synchronizer is high which means the data arrives before the balance point, the data arrival time is increased slightly to 1.2ns. If the output is still high, the data arrival time is continually increased until the output becomes low which means the data arrives after the balance point. Assume that the data arrival time is now 1.6ns, the data arrival time must now be reduced back to a point between 1.5ns and 1.6ns, say 1.51ns where the output is high and then repeat the previous procedure until the output becomes low. This procedure of advancing and retarding the time delay between data and clock signals by ever decreasing increment continues until the balance point is located at some data arrival time of say, 1.52325284ns and a relatively long metastability time would be observed at the output of the synchronizer. This time is the balance point we have been looking for.

Thereafter the data arrival time is set at several points before the balance point and the corresponding output times are recorded. The relationship between the input time (the time between the data arrival time and the balance point) and the output time are then plotted as shown in Figure 2.12, from which τ and MTBF can be calculated by using the equations (2.7) and (2.8).

The second simulation method is to force the circuit to the metastable point first, and then remove the force to let the metastability resolve [24]. This method is used to estimate the synchronization time constant τ . This method is called the *switch method* because a switch is typically used in this method as shown in Figure 2.19 (a). In this technique the bistable element in the synchronizer is forced to the metastable point of 1mV by the switch at the outset. Subsequently the switch is opened to let the metastability resolve. Figure 2.19 (b) shows the diverging voltages on the nodes X and Y. From it, τ can be calculated by using the equation (2.5).

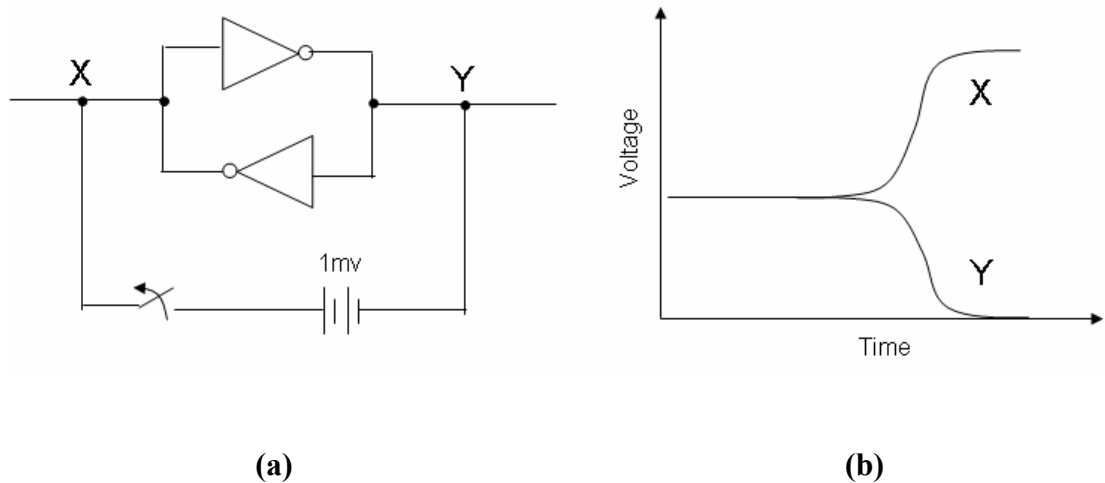


Figure 2.19 Switch method

The advantage of the simulation methods is that they are simple and economical. The disadvantage is that they are not sufficiently accurate especially for estimating

synchronizer performance in the deep metastability region, which is the region for long duration metastability corresponding to very small input times. The reason for this is that the timing resolution of simulators is limited and some devices exhibit variations in τ in the deep metastability region. Another disadvantage of simulation methods is that noise maybe important for the nondeterministic part of the synchronizer response, and so the result of a deterministic simulation may or may not be a true representation of the results in practice.

2.4.2 Synchronizer Measurement

Measurement is more accurate than simulation in estimating synchronizer performance, and it is valuable for validating simulation results. On the other hand, it is more costly requiring implementation of the circuits and expensive testing equipments.

2.4.2.1 Traditional measurement method

The traditional measurement method for synchronizers is to use two independent oscillators as data and clock for the synchronizer. An oscilloscope is used to record the outputs of the synchronizer. Figure 2.20 (a) shows the basic principle of this method, where oscillators A and B are independent and are set to similar frequencies (10 MHz and 10.1 MHz in this example). Hence different overlap times between the data and clock are generated with equal probabilities. The oscilloscope is used to record the outputs and generate a histogram of the results.

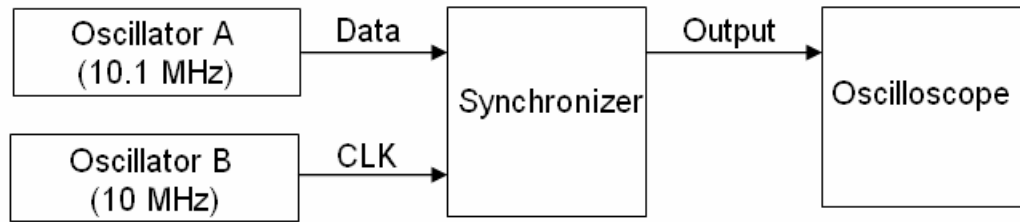


Figure 2.20 Two-oscillator measurement method

The drawback of this method is that because different input times are generated with equal probabilities, events which result in a much longer than normal propagation delay (deep metastability events) occur relatively rarely since they correspond to very small input times, say less than 1 ps. In the two-oscillator method with oscillator frequencies of 10MHz and 10.1MHz, input times less than 1 ps occur once every 10^5 clock cycles (or 10 ms). Even when they occur, it is not necessary that they can not always be recorded because the response speed of the oscilloscope is limited. For each event recorded, the oscilloscope has to store, process and display the histogram. There is a significant dead time between successive recorded events that limits the number of actual events recorded, often to less than 1 in 1000 of those generated. For example, equation (2.10) shows that with $f_c = f_d = 10^7$ Hz and $T_w = 100$ ps, a MTBF of around 5 minutes requires a synchronization time of 15τ , which means the events related to that MTBF occur every 5 minutes. If only 1 in 1000 of those events is recorded due to the limited response speed of the oscilloscope, it takes 1000×5 minutes or 83 hours to observe such an event. Increasing the data or clock frequencies can increase the number of events observed, but it is not practical to measure the MTBF to more than 13 minutes or beyond 16τ .

2.4.2.2 Deep metastability measurement method

Recently a new measurement method, which extends the measurement of synchronizer to deep metastability region, has been proposed [38]. The basic principle of this method is to use a DLL to make the data always arrive around the balance point so that many more deep metastability events occur. Figure 2.21 shows the arrangement for the deep metastability measurement method. Here only one oscillator and two variable delay lines (VDL) are used to generate data and clock signal for the synchronizer. A DLL is used to control the delay in the data path so that the data always arrives around the balance point. When there is a high output, which means that the data arrives before the balance point, the delay in the data path will be increased by a little. When there is a low output, which means that the data arrives after the balance point, the delay in the data path will be decreased by a little. In this way, the data is kept around the balance point so that many more deep metastability events occur.

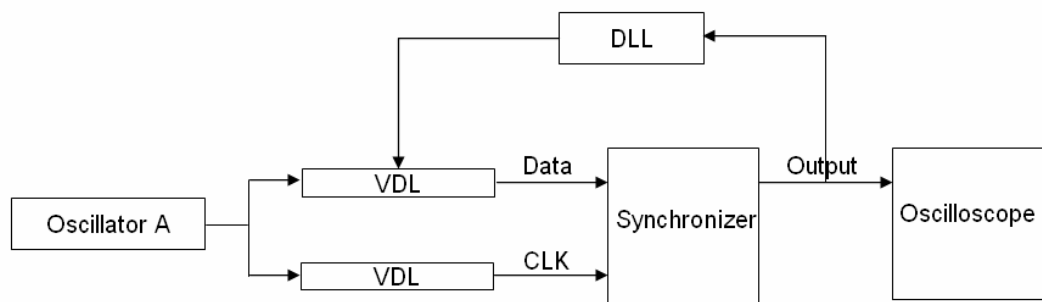
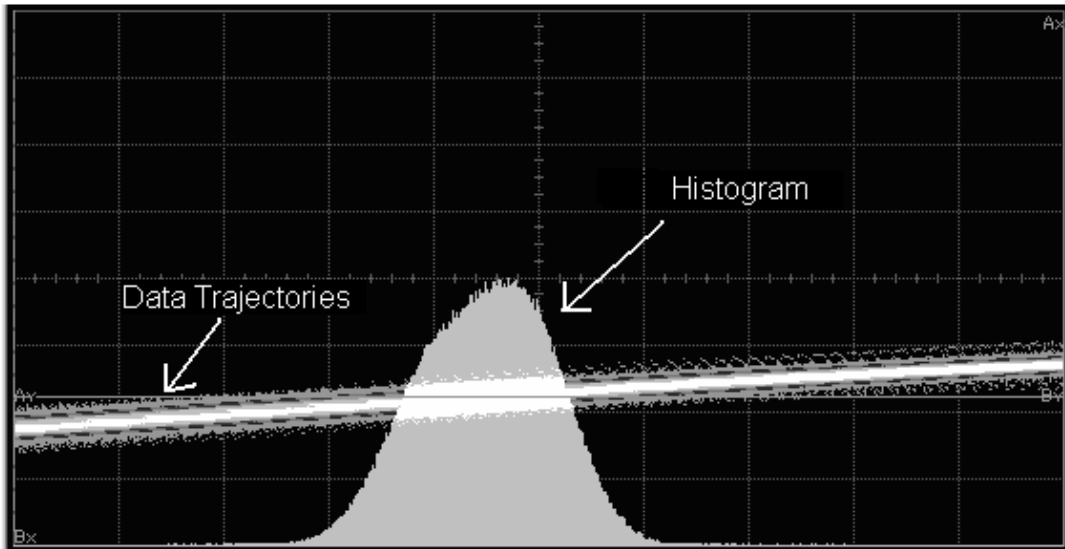


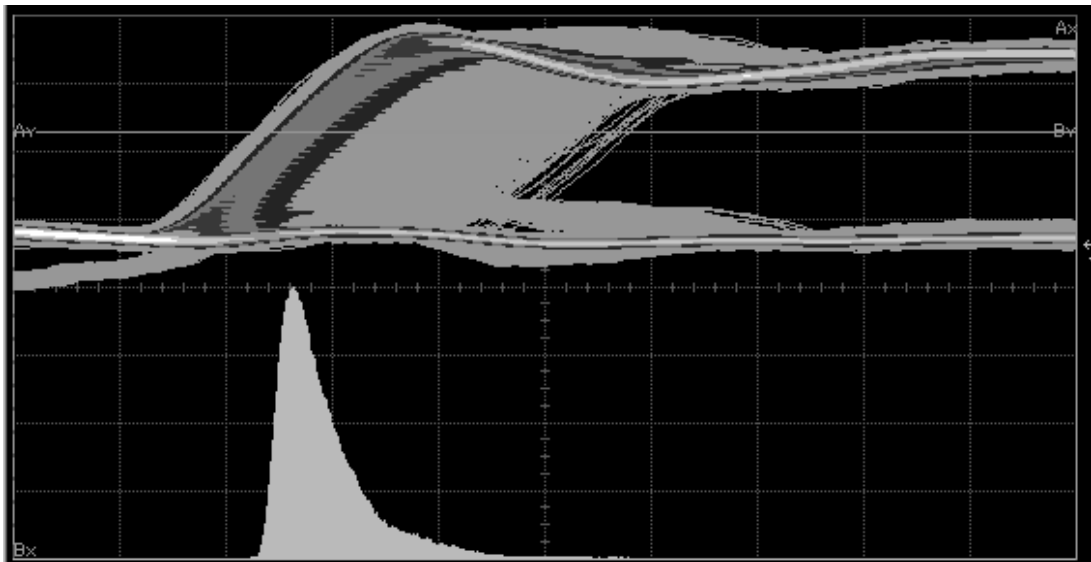
Figure 2.21 Deep metastability measurement

The oscilloscope is used to record the input and output histograms for plotting the input and output time relationship. Figure 2.22 shows an example of the input and output histograms which are recorded using an advanced digital oscilloscope. In

Figure 2.22 (a) the trajectories of data inputs are shown as well as its histogram, of which the height represents the number of data inputs at a particular time. The clock is used as trigger and is not shown in the figure. Figure 2.22 (b) shows the trajectories of outputs and the output histogram.



(a) Input histogram



(b) Output histogram

Figure 2.22 Input and output histograms

After the data collection is done, the input and output histograms can be exported from the oscilloscope and redrawn in EXCEL. Before plotting the input and output time relationship, it is necessary to plot the cumulative number of input events on the input histogram and normalize it to between -1 and +1. The same thing needs to be done to the output histogram. However, because only half of the input events cause an output event (only data inputs that arrive before the balance point will cause the output to go high), the cumulative number of events on the output histogram must be normalized to between 0 and 1. Figure 2.23 shows an example of the normalized cumulative number of input events and output events. Correspondence between input events and output events can now be found from the fact that, for a large enough number of events, the number of input events between the balance point and a particular input time must equal the number of output events recorded after a particular output time. In this way, a particular input time can be mapped to a particular output time and the relationship between the input times and output times can be plotted.

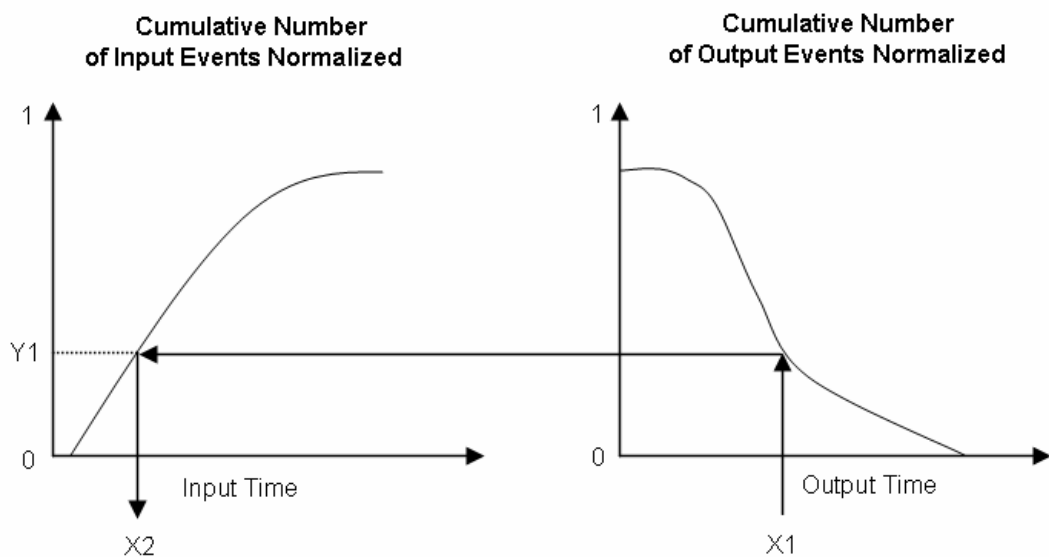


Figure 2.23 Input time to output time

For example, a horizontal line is drawn at the point Y1. The output time (X1) in the normalized cumulative output histogram and the input time (X2) in the normalized cumulative input histogram are obtained, which means the output time X1 corresponds to the input time X2. All the input events that occur between X2 and the balance point will have an output time greater than X1. In this way, the relationship between input time and output time can be built. Finally, a curve as shown in Figure 2.12 (Section 2.2.3) can be drawn.

However, the input histogram recorded by the oscilloscope is not sufficiently accurate, partly because the output of the synchronizer is, to some extent, determined by the internal thermal noise and partly because there is a significant measurement noise from the oscilloscope. This measurement noise can be estimated by producing a histogram of the clock waveform triggered by itself. Due to the relatively large measurement noise the input distribution recorded on the oscilloscope can not be reliably used to assign input times to output times. To overcome this problem it is necessary to find the real input time distribution from the noise mixed input time distribution. This can be done by varying the proportion of high and low outputs through some mechanism to shift the central point of the input time distribution and plotting a graph of the shifted time against a proportion of high outputs [38]. Assuming that the distribution of input events follows a normal distribution, this graph can be compared with the normal distributions having different values of standard deviation to find out the real input time distribution. This method is explained in detail in Section 4.3.3.

Figure 2.24 shows the implementation of the deep metastability measurement method using off-chip analog circuits. Here the DLL is implemented by using an

integrator and off-chip analog variable delay lines. The integrator consists of an operational amplifier with its reference input held at a voltage approximately half way between the logic high and logic low levels of the slave flip-flop. If the output of synchronizer is high, which means the data arrives before the balance point, the high output value of the slave flip-flop will cause the output voltage of the integrator to decrease a little to increase the delay in the data path. If the output of synchronizer is low, which means the data arrives after the balance point. The low output of the slave flip-flop will cause the output voltage of the integrator to increase a little to reduce the delay in the data path. In this way, the data is locked around the balance point.

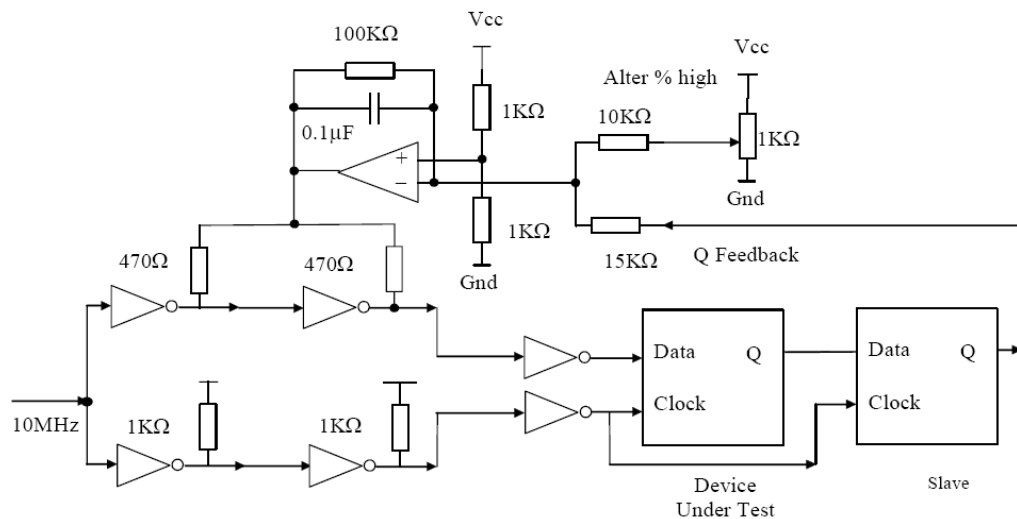


Figure 2.24 Analog implementation of deep metastability measurement [38]

The disadvantage of the off-chip analog implementation of the deep metastability measurement is that it is not easy to control the operation of the variable delay lines or to characterise the actual input time distribution due to the instability of the off-chip analog components. For example, it is difficult to get the incremental delay of the delay lines down to pico-second levels due to the instability

of the analog components and the significant off-chip delay. It is also difficult to accurately control the percentage of high outputs with the analog integrator. These problems can be overcome by implementing the deep metastability measurement method on chip using digital variable delay lines and digital counters. This is discussed in Chapter 4.

2.5 Effects of On-chip Variability on Synchronizers

On-chip variations normally refer to PVT variations, namely process, voltage and temperature variation. Process variation is caused by the deviations in the manufactured properties of the chip such as feature size, dopant density etc., which results in variations in threshold voltage, gate length and gate width. Voltage variation is caused by non-uniform power supply distribution, switching activity and IR drop. Temperature variation is caused by non-uniformities in heat flux of different functional units under different workloads and non-uniformities in the chip's interface to its package.

The PVT variations mainly affect the speed of circuits and can lead to failures such as timing failures and noise failures of the circuits. According to ITRS 2007 [1], at 45nm the circuit performance variability caused by the on-chip variations reaches to 50%. Components such as logic circuits, memories on chip are all affected, but the performance of synchronizers which are used to synchronize the data passing between different clock regions in future SoCs may affect the system performance to a greater extent than other components, because the synchronization time constant τ , which determines the synchronizer performance, depends on the small signal rather than large signal behaviour. They are more sensitive to the V_{dd} , V_{th} and temperature

variations than logic circuits. Another reason why the effects of on-chip variability on synchronizers are more important than that on other circuits is that in future systems on chip, the on-chip network communication is likely to affect the system performance more than processing, and synchronization is a critical part of on-chip communication. Therefore, the effects of on-chip variability on the synchronizers will have a great impact on the system performance. As the on-chip variations become increasingly significant and the size of systems on chip grows, this problem has to be addressed.

Chapter 3

Robust Synchronizer

As mentioned in Chapter 2, future systems are likely to consist of many independently, or semi-independently clocked regions, with a need for synchronization of the data passing between them. Consequently there will be many synchronizers whose reliability is crucial to the reliability of the system itself. An important effect of scaling is the increase in both dynamic and static power dissipation. Currently proposed solutions to this problem include dynamic lowering the voltage in selected sub-systems when high performance is not required. Unfortunately, reduced power supplies usually disproportionately affect the performance of synchronizers since the synchronization time constant τ depends on the small signal parameters in metastability rather than large signal switching times, and a 50% reduction in power supply voltage may result in over 100% increase in τ . This is because many synchronizer circuits have metastable levels that can cause both p and n type transistors to have low transconductance, particularly at low voltages and low temperature where V_{th} is high. Another important effect of scaling is the increase of on-chip variability including IR drop, process variation and temperature variation, which can cause further reduction of V_{dd} and increase of V_{th} . As the effects of on-chip variability become increasingly significant in submicron processes, the problem of increased τ and therefore greatly increased synchronization time becomes worse.

In this chapter the commonly used Jamb latch synchronizer is investigated in Section 3.1, a modified version of Jamb latch, which is less sensitive to V_{dd} , V_{th} and temperature variations but consumed more power, is presented in Section 3.2, a novel synchronizer circuit, which is both faster and much more robust than the Jamb latch while at the same time maintaining low power consumption, is presented in Section 3.3 [23]. The improvement resulting from the proposed synchronizer is summarized in Section 3.4.

3.1 Jamb Latch

The Jamb latch, shown in Figure 3.1, is a simple circuit commonly used as a synchronizer because of its relatively good performance [24].

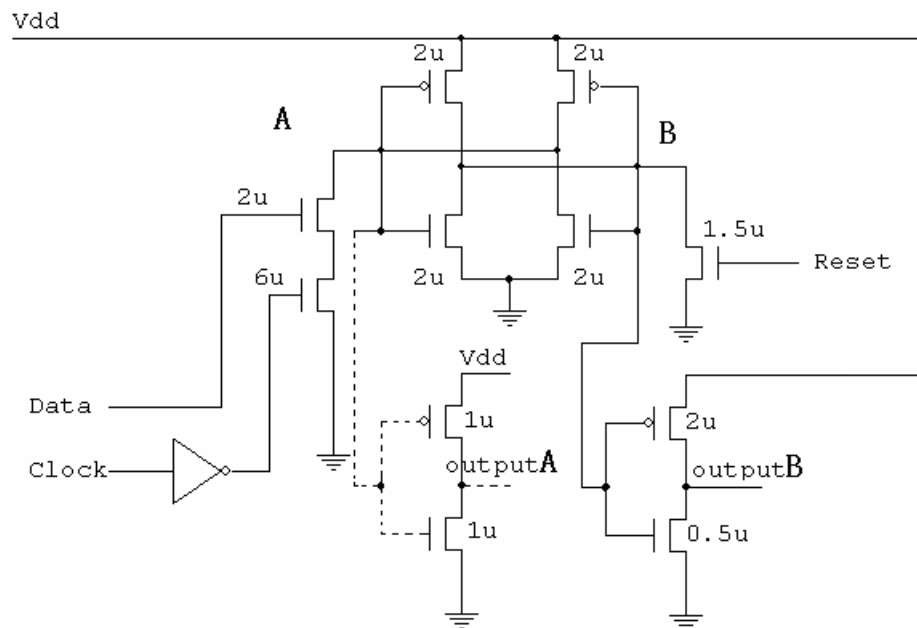


Figure 3.1 Jamb latch

In this circuit, the flip-flop is reset by pulling node B to ground, and then set if the data is high and clock is low, by pulling node A to ground. Metastability occurs

if the overlap of the data and clock signals is at a critical value which causes node A to be pulled down, and node B up to around the metastable level. For correct operation, reset, data, and clock transistors must all be made wide enough, when compared to the inverter devices, to ensure that the nodes are pulled down. Typically, this means that the reset transistor has a similar width to the p-type transistors in the bistable, and the data transistor is a little wider than the reset transistor. The output inverter shown connected to node B has a p-type device which is much wider than the n-type to ensure that its output is high during metastability, and only goes low when the node rises above the metastable level of around 700mV.

τ of the Jamb latch can be estimated by simulation using the switch method mentioned in Chapter 2. Figure 3.2 shows the configuration of the simulation circuit. A switch is placed in series with a voltage source of 1mV between nodes A and B so that both nodes are held at a voltage difference of 1mV initially. Then the switch is opened allowing the nodes to diverge exponentially [24]. One node will drive to V_{dd} ; the other node will drive to ground. The voltage source placed between the two nodes determines the starting point and the direction of divergence. A voltage of only 1mV ensures that the Jamb latch is in the metastability region.

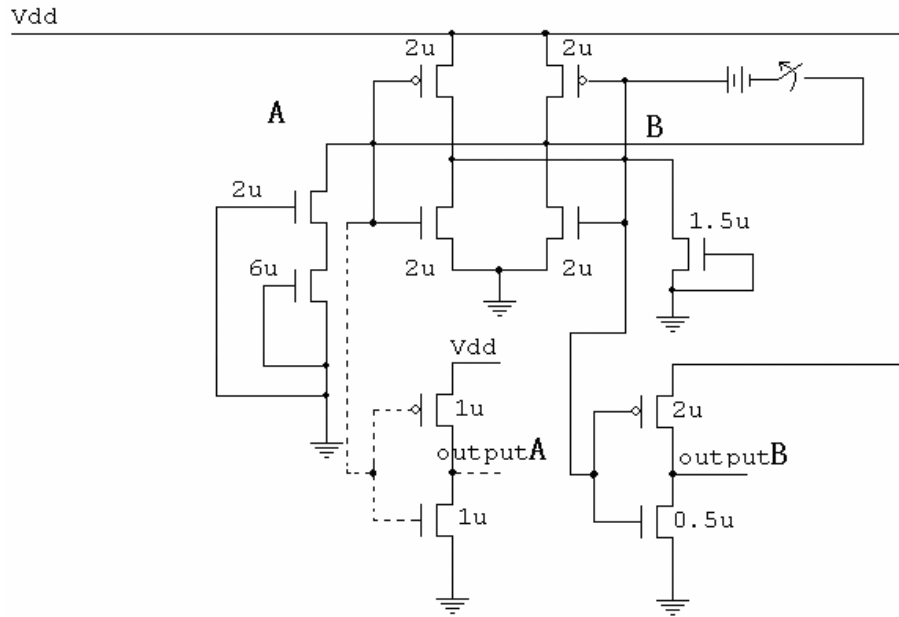


Figure 3.2 Simulating Jamb latch

The circuit simulation results from Figure 3.2 are shown in Figure 3.3 and Figure 3.4. Figure 3.3 shows the diverging nodes. Figure 3.4 is a semi-log plot of the voltage difference of the nodes A and B; the slope of the line defines τ . Equation (3.1) is used to determine τ , where t_x is time and V_x is voltage.

$$\tau = \frac{t_1 - t_2}{\ln(V_1 / V_2)} \quad (3.1)$$

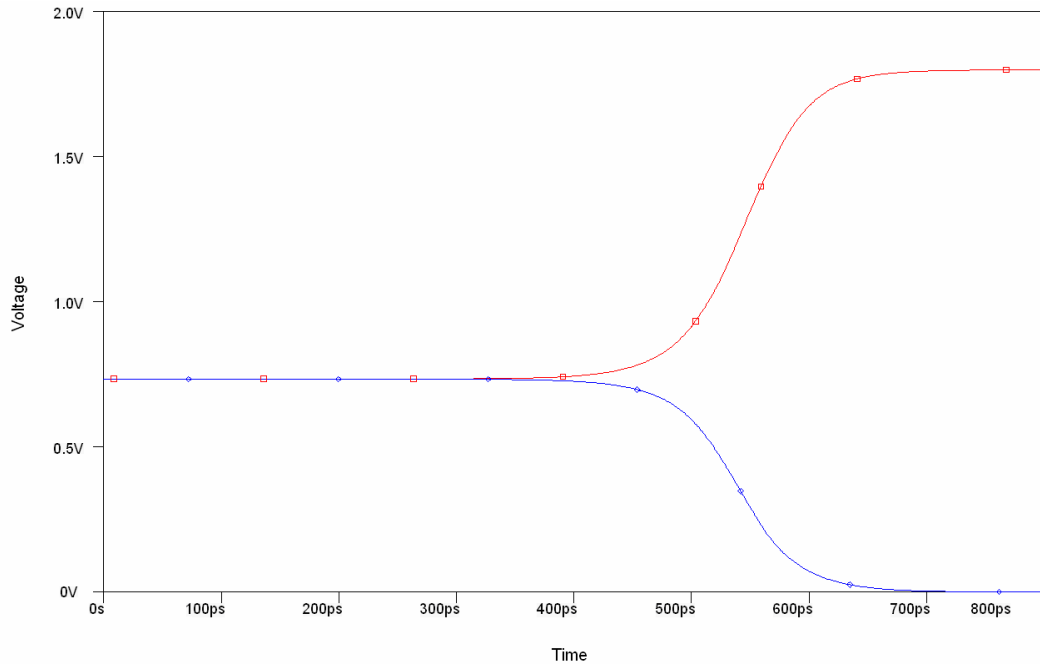


Figure 3.3 Diverging nodes

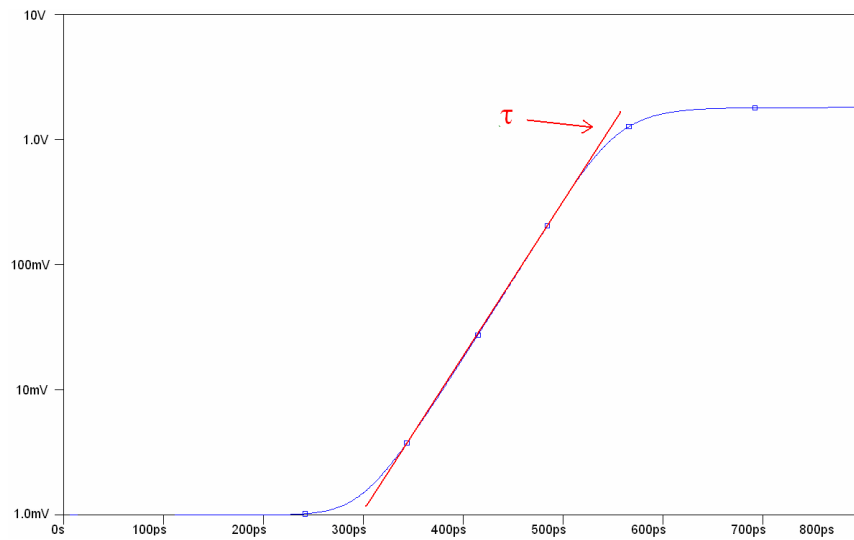


Figure 3.4 Semilog plot of the voltage difference of the two nodes

By extensive use of SPICE simulation using parameters for a 0.18 μm process, the transistor sizes for the Jamb latch were optimized to give a low value for τ and are shown in Figure 3.1. To ensure that the results are realistic, the output was

loaded with an inverter. The plot of simulated τ against V_{dd} and temperature is shown in Figure 3.5. At V_{dd} of 1.8v the value of τ is 35.6ps. The minimum value of τ is limited by the capacitance of the reset/set transistors, which cannot be further reduced in the Jamb latch, otherwise the circuit will not reliably set or reset. The actual value of τ is determined by the capacitance at the nodes A and B and the transconductance of the cross-coupled inverters when the circuit is in metastability [27]. The effective node capacitance and transconductance depends on both n and p type transistors. By extensive simulation, it was found that the best ratio between p-types and n-types is 1:1 [23], a result which is also reported by others [24][25][26].

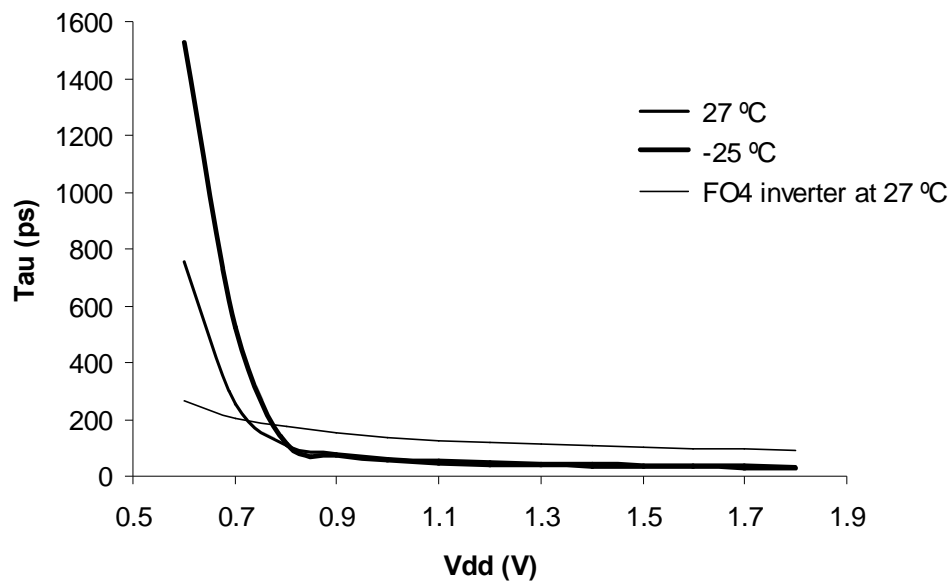


Figure 3.5 Plot of τ vs V_{dd} for Jamb latch

It can be observed from Figure 3.5 that τ increases with V_{dd} decreasing and this reduction in speed becomes quite rapid where V_{dd} approaches the sum of thresholds of p and n-type transistors so that the value of τ is more than doubled at a V_{dd} of 0.9V, and more than an order of magnitude higher at 0.7V and a temperature of -25

°C. This is because when V_{dd} is around the sum of the thresholds of the p and n-type transistors, both transistors are almost off and there is no current flowing through the inverters, so the transconductance is very low. The transconductance can be further reduced by lowering the temperature because low temperature gives high threshold voltage. In other words, variations in V_{dd} , V_{th} and temperature could make this circuit unviable, especially for deep submicron processes. For comparison the FO4 inverter delay in this technology is also shown in Figure 3.5, which demonstrates that τ is likely to track logic gates delay rather poorly.

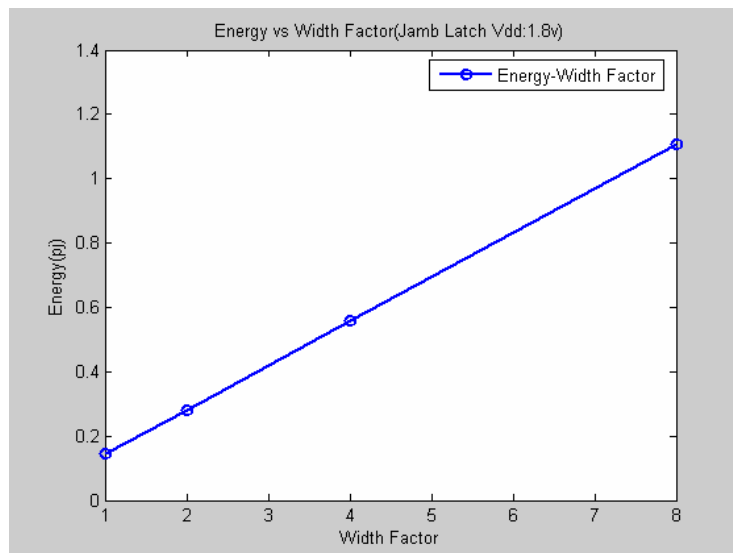


Figure 3.6 Energy consumption

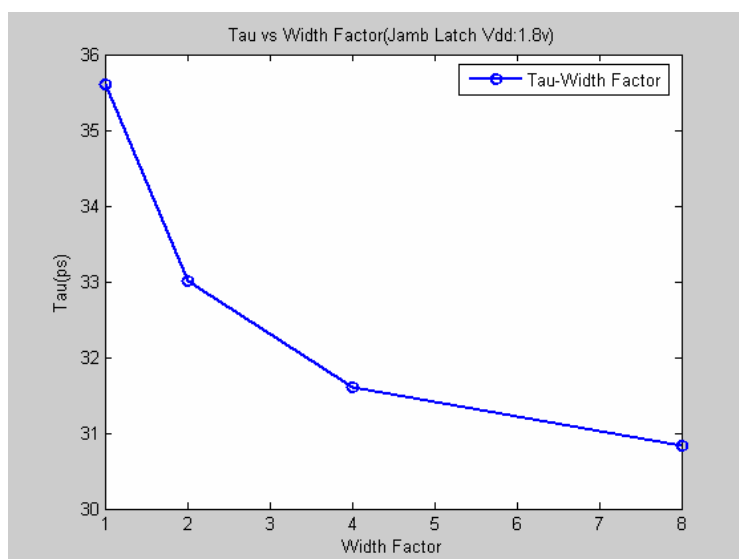


Figure 3.7 Synchronization time constant τ

The effect of increasing the width of all transistors by the same factor was also investigated. Figure 3.6 shows that the average energy (pj) required to switch from one state to the other increases as this width factor increases approximately in proportion to transistor sizes. Here a width factor of 1 implies the transistor sizes are all as in Figure 3.1 and a width factor of 2 would imply a doubling of all transistor widths. In order to estimate the average energy used during metastability, it is assumed that the average metastability time is τ . Figure 3.7 shows that τ (ps) only decreases slowly as transistor sizes increase, and reaches a limit at around 31ps.

3.2 Modified Jamb Latch

A modification aimed at reducing the sensitivity of Jamb latch to V_{dd} , V_{th} and temperature variations is shown in Figure 3.8. The optimum transistor size ratios for the modified Jamb latch, again found by extensive simulation, are also shown in Figure 3.8.

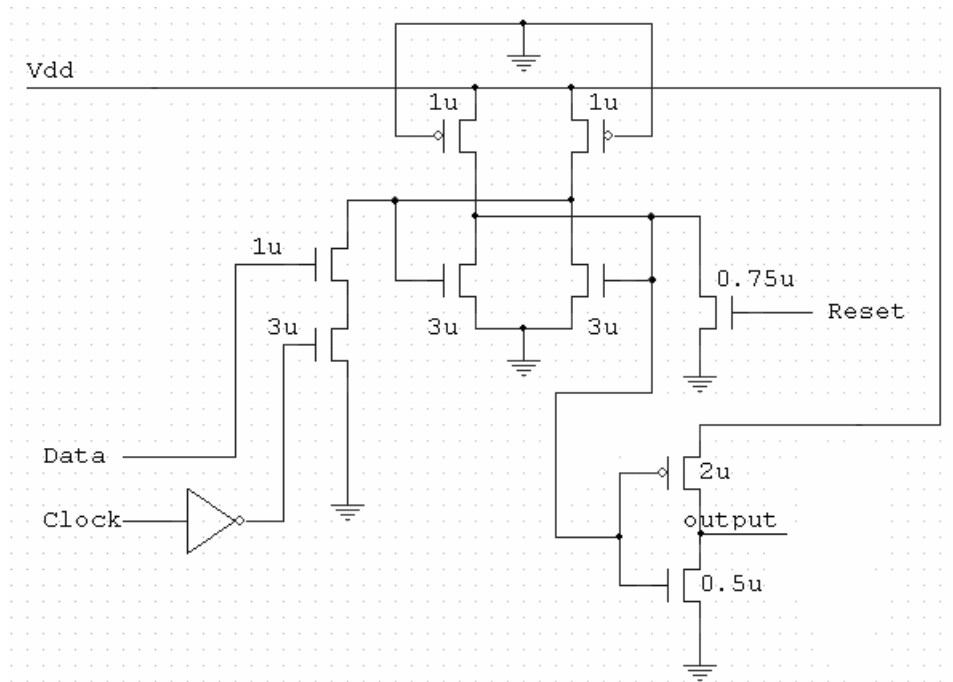


Figure 3.8 Modified Jamb latch

In this circuit the feedback p-type transistors are held on continuously rather than cross coupled as in the original Jamb latch. This allows the circuit to operate with a lower V_{dd} because the V_{dd} does not need to exceed the sum of the p-type and n-type threshold voltages. It only needs to be higher than the n-type threshold voltage, so the circuit continues to operate down to 0.6V even at low temperature. The capacitance on the two latch nodes is also reduced because the gates of the p-type transistors are connected to ground. In addition, the p-type transistors can be smaller than the n-type transistors because they conduct more current with a gate voltage of V_{dd} rather than the metastable level. Consequently the set/reset transistors can be smaller giving lower capacitance. Furthermore it is only the 3μ wide n-type transistors which now contribute to gain of the inverters. However, because the capacitance is significantly reduced, overall the modified Jamb latch is slightly

faster than the original Jamb latch at a V_{dd} of 1.8V. More importantly, this modification makes τ much less sensitive to V_{dd} , V_{th} and temperature variations than the conventional Jamb latch as shown in Figure 3.9.

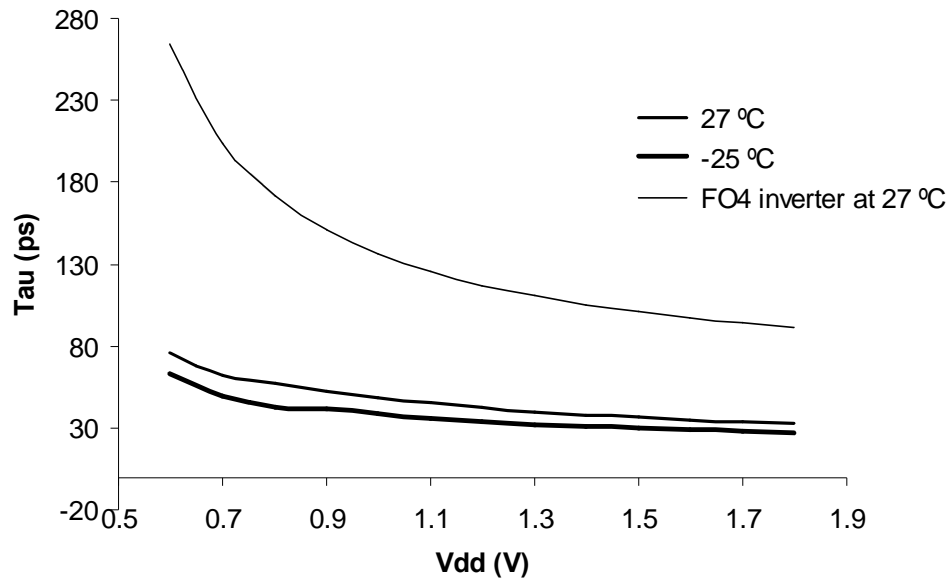


Figure 3.9 Plot of τ vs V_{dd} for modified Jamb latch

By comparing Figure 3.9 with Figure 3.5, it can be seen that the modified Jamb latch is not only faster but much less sensitive to V_{dd} variation than the conventional Jamb latch as τ rises to only 52ps at 0.9V, rather than 79ps, and rises to only 62ps at 0.7V, rather than 253ps.

The disadvantage of the modified Jamb latch is that its power, which includes both transient power and static power, is greater than the conventional Jamb latch because the p-type transistors are on all the time. For example, for a clock frequency of 500MHz, the energy consumed by the modified Jamb latch in a switching period is 0.88pj while it is only 0.14pj for the conventional Jamb latch.

3.3 Improved Synchronizer (Robust Synchronizer)

In order to reduce the power consumption it is necessary to turn the p-type loads off when the circuit is out of metastability; an improved synchronizer circuit which does this is shown in Figure 3.10.

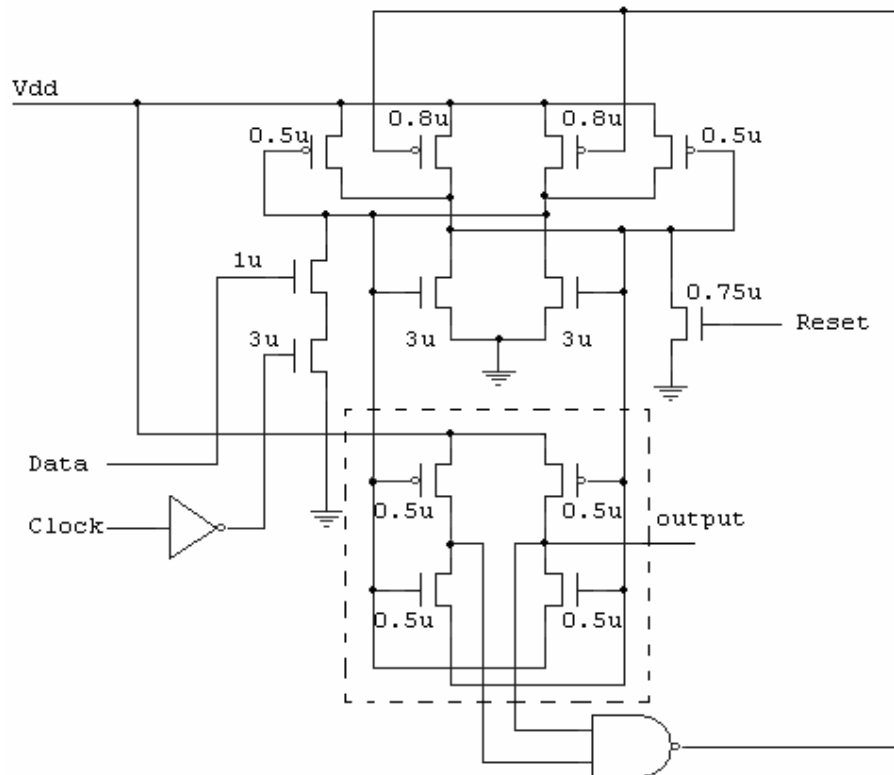


Figure 3.10 Improved synchronizer (robust synchronizer)

Two additional feedback p-type transistors (0.5μ in Figure 3.10) are added to the modified Jamb Latch in order to maintain the state of the latch when the main p-type transistors (0.8μ in Figure 3.10) are off. By introducing the additional feedback p-type transistors, the main p-type transistors need only to be switched on during metastability. A similar circuit is described in [35], but in our implementation a metastability filter [36] is used to produce the synchronizer output signal from the

nodes A and B, which only goes low if the two nodes have a significantly different voltage. The filter implementation is necessary to remove anomalous output voltages from the latch because both nodes A and B are pulled down to below 300mV during set/reset operation, and only return to the 700mV metastable level after some time. The outputs from the metastability filter are both high immediately after the circuit enters metastability, and are then fed into a NAND gate to turn on the two main p-type transistors. In this circuit, the two main p-type transistors are off when the circuit is not in metastability, operating like a conventional Jamb latch; When the circuit enters metastability the p-types are turned on to allow fast resolution of the metastability. The main output is taken from the metastability filter, again to avoid any metastable levels being presented to following circuits. There is no need for the feedback p-type transistors to be large, consequently the set and reset transistors can be small. The optimum transistor sizes for the improved synchronizer are shown in Figure 3.10, and the resultant τ at V_{dd} of 1.8v is as low as 27ps because the main transconductance is provided by large n-type transistors and also there are two additional p-type transistors contributing to the gain.

The relationship between τ and V_{dd} for the improved synchronizer is shown in Figure 3.11. Similar to the modified Jamb latch, τ is much less sensitive to V_{dd} , V_{th} and temperature variations than in the conventional Jamb latch and tracks logic gates delay quite well. At the same time as maintaining a low value for τ , the ratio between τ and FO4 is much more constant at around 1:4 over a wide range of V_{dd} and temperature values than the conventional Jamb latch.

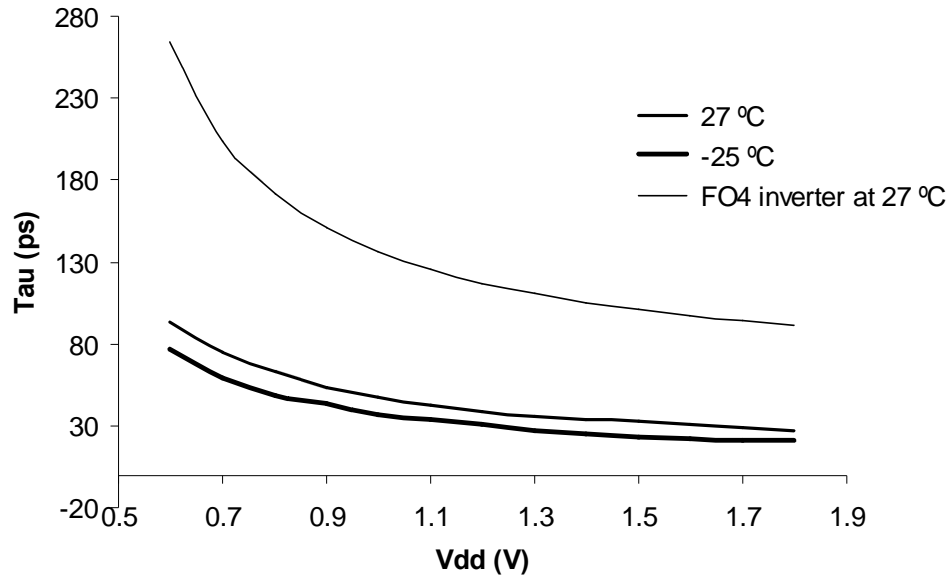


Figure 3.11 Plot of τ vs V_{dd} for improved synchronizer

The energy consumed for this circuit is much less than the modified Jamb Latch because the main p-type transistors are on only during metastability. For a clock of 500MHz, the energy consumed by the improved synchronizer in a switching period is 0.18pj, which is much less than the modified Jamb Latch and similar to the conventional Jamb latch.

The main advantage of a low value of τ is that the same reliability can be achieved with a shorter resolution time, thus reducing the latency of the synchronizer. Figure 3.12 and Figure 3.13 show the input time plotted against the output time for the conventional Jamb latch and the improved synchronizer. The curves shown are produced from detailed SPICE simulations down to an input time of 10^{-4} ns and using the long term value of τ to project below this point.

The disadvantage of the improved synchronizer is that it has a longer normal propagation delay because of the weaker set and reset transistors. This can be

observed from Figure 3.12 and Figure 3.13, but it only has a small effect on T_w , and the lower value of τ , particularly at 0.9V allows the circuit to show a smaller output time at the very small input time differences that determine the metastability resolution time in a synchronizer.

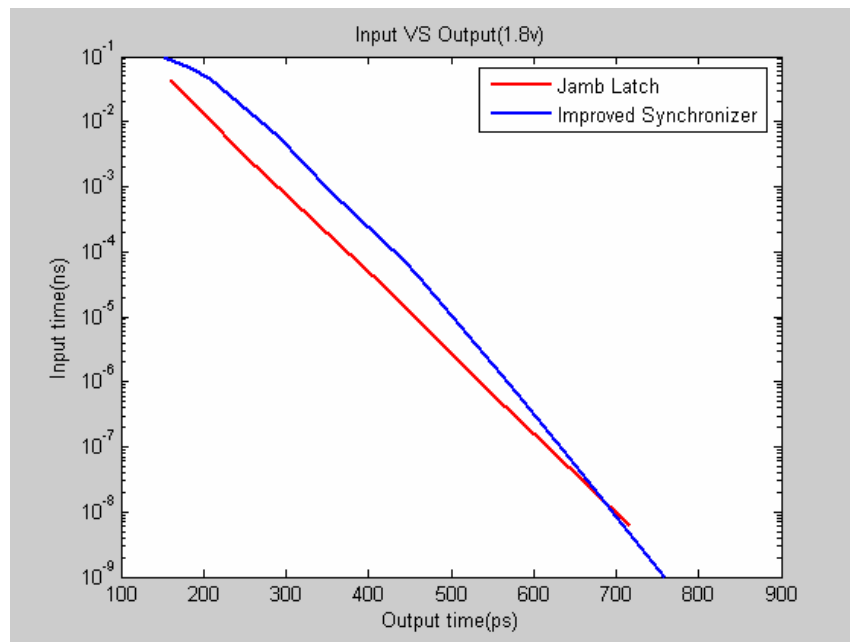


Figure 3.12 Improved synchronizer, input vs output time at 1.8v

The implication of this, is that for events with input time differences less than 10^{-17} seconds (10^{-8} ns) at 1.8V, and less than 10^{-15} seconds (10^{-6} ns) at 0.9V the new circuit is always faster than the Jamb latch. Typically it would be expected that a system with a 500MHz clock and 200 MHz data rate would give an metastable event that corresponds to the input time of 10^{-24} seconds or approximately once every $1/(10^{-24} * 500\text{MHz} * 200\text{MHz}) = 10^7$ seconds or about 4 months, thus at 0.9V, a Jamb latch synchronizer with better than 4 months MTBF might require 2700ps resolution time but the improved synchronizer would only need 2200ps.

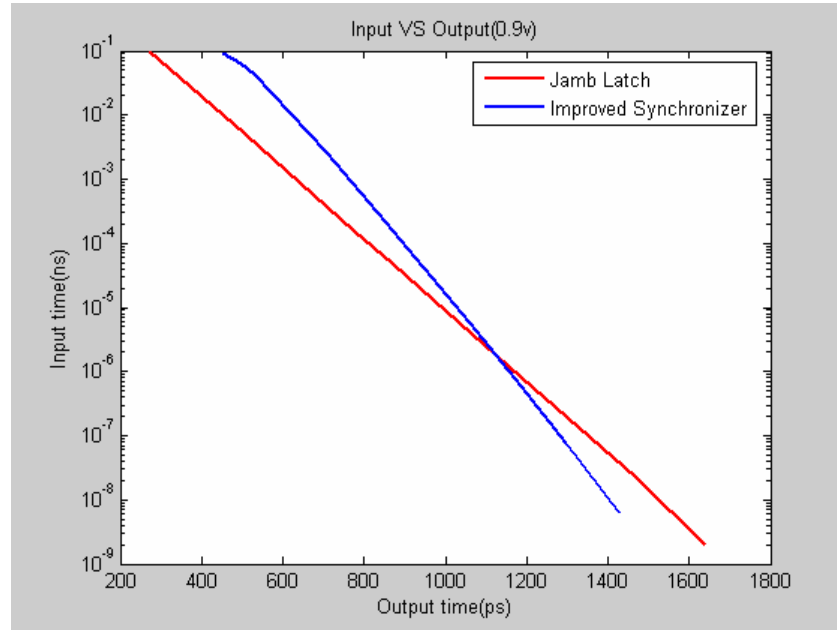


Figure 3.13 Improved synchronizer, input time vs output time at 0.9V

3.4 Summary

Synchronization can be a problem in networks on chip as it adds directly to the data transmission time between subsystems. The performance of synchronizers is heavily affected by variations in power supply voltage, transistor threshold voltage and temperature since the synchronizer τ depends on the small signal parameters in metastability rather than large signal switching times, and a 50% reduction in power supply voltage may result in over 100% increase in τ . This is due to many synchronizer circuits having metastable levels that can cause both p and n type transistors to have low transconductance, particularly at low voltages and low temperatures where V_{th} is high. As V_{dd} reduces in submicron processes, and V_{th} increases, the problem of increased τ and therefore greatly increased synchronization time becomes worse. In this chapter it is shown how the commonly used Jamb latch synchronizer can be made less sensitive to variations in power supply voltage,

transistor threshold voltage and temperature, and can be made to track variations in the FO4 value better. By removing the feedback from the p-type devices the node capacitance is reduced and the device transconductances are increased, and hence the synchronization time constant τ is improved. This modification enables the circuit to work at lower V_{dd} and make it robust to V_{dd} , V_{th} and temperature variations. The penalty, however, is greatly increased power dissipation.

To avoid this problem it has been shown that the p-type devices can be switched on only during metastability and switched off after metastability by using the outputs of a metastability filter to control their gates, so that the higher power dissipation is only present during metastability. In the improved synchronizer, the switching energy is only slightly greater than the Jamb latch, but it is much faster when work at low V_{dd} and much less sensitive to the V_{dd} , V_{th} and temperature variations than the conventional Jamb latch.

Chapter 4

On-chip Measurement of Deep Metastability in Synchronizers

As mentioned in previous chapters, in future systems on chip there are likely to be many synchronizers whose reliability is crucial to the integrity of the entire system. Synchronizer outputs are assumed to be stable after a fixed time interval, usually a clock cycle, therefore to know how reliable a synchronizer circuit actually is, it is necessary to measure how often the output changes after the clock cycle time. This is difficult because the MTBF being investigated may be as long as several months or years, therefore the MTBF is usually projected from simulation results for the value of τ or measurements that only measure failures over a few hours. Normally an input time and output time relationship is determined first and then the corresponding MTBF can be computed. Simulators such as SPICE [24] and MATLAB [37] have been used to estimate the MTBF of synchronizers, but they are not sufficiently accurate for long time metastability prediction because some devices exhibit variations in τ with output time. Traditional measurement methods [24][28][29][30] do not allow MTBF to be measured beyond the point where any initial switching transient has died away sufficiently to make accurate projections for long term reliability; this is what is called the deep metastability region.

To overcome the drawbacks of simulation and traditional measurement methods, a new measurement method has been proposed [38] which enables the

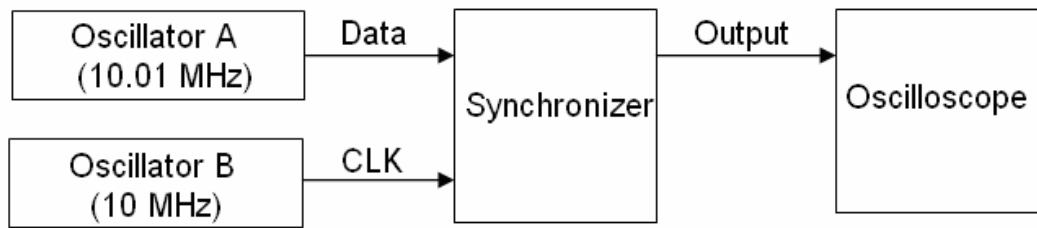
measurements to be carried out further into the deep metastability region. However, the previous work [38] was implemented using off-chip analog variable delay lines and an operational amplifier RC integrator as components in a delay locked loop. Due to the instability of the off-chip analog components, it is difficult to control the operation of the delay lines or to characterise the actual synchronizer input stimuli time distribution. An on-chip implementation of deep metastability measurement using digital variable delay lines and digital integrating counters would allow integration of both the synchronizer circuits and the measurement method, eliminating high speed off chip paths which are a source of inaccuracy. It also makes control at the picosecond level easier because of the inherent stability of digital integrating counters and digital delay lines.

This chapter describes the on-chip measurement of deep metastability in synchronizers [39]. In Section 4.1 the traditional measurement methods are reviewed and the principle of on-chip deep metastability measurement is described. Thereafter in Section 4.2, the implementation of the on-chip measurement circuit is described. Next, the measurement results are shown and comparison is made with the simulation results in Section 4.3, demonstrating that the on-chip measurement circuit works as expected. Finally the work outlined in this chapter and the results obtained are summarized in Section 4.4.

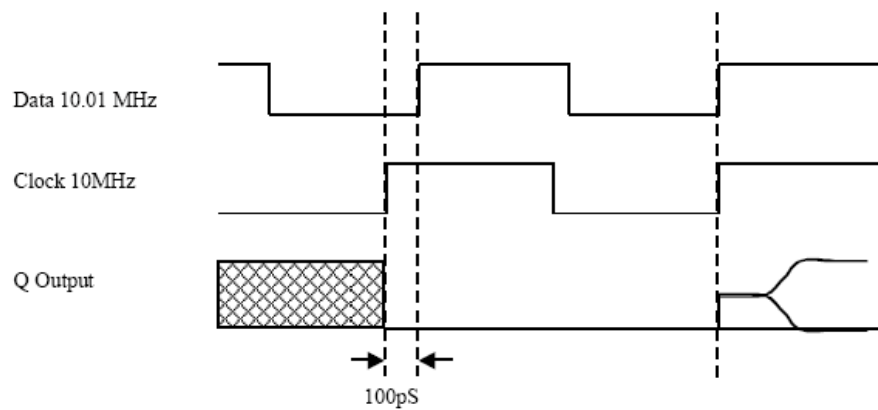
4.1 Measurement of Metastability in Synchronizers

In this section the traditional and deep metastability measurement methods are reviewed.

4.1.1 Traditional Measurement Methods



(a)



(b) [38]

Figure 4.1 Traditional measurement method using two oscillators

As shown in Figure 4.1 (a), traditionally metastability measurements are conducted by using two asynchronous oscillators with a similar frequency to provide data and clock for the synchronizer. The clock rising edge produces a change in the output of the synchronizer only if the data input is different on successive clock edges as shown in Figure 4.1 (b). In this example, the data oscillator has a frequency of 10.01 MHz and the clock 10 MHz, so the output changes only when the clock and data overlap is less than 100 ps, which is the difference between the two oscillator

periods (100 ns – 99.9ns), and even then, only if it changes very close to the second clock edge, causing metastability to occur.

If the data and clock oscillators are not locked together, all overlap times between data and clock should be generated with equal probabilities. To observe the delay in the output of synchronizer due to metastability, the output changes are used to trigger the recording of corresponding clock rising edge and generate an event histogram. Figure 4.2 shows a typical event histogram, where the X-axis represents time from a changing output back to the clock rising edge and the Y-axis represents the number of events recorded.

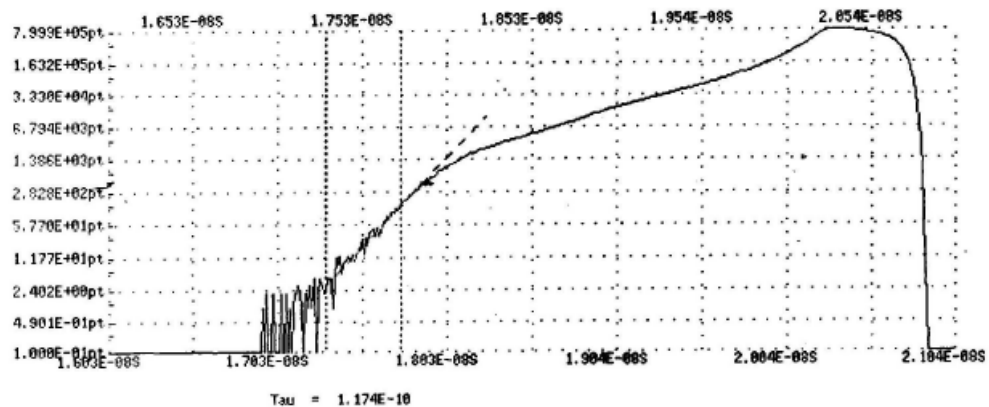


Figure 4.2 Typical event histogram [38]

The drawback of this method is that very few deep metastability events occur as these events are produced by very small overlap times which have a very small probability of occurrence. This makes it difficult to measure τ in the deep metastability region. Measurements or simulation of the early deterministic region can give a falsely optimistic result [24][38].

4.1.2 On-chip Deep Metastability Measurement

To overcome the problem of traditional measurement methods, an on-chip measurement circuit measuring deep metastability in synchronizers has been designed and implemented [39].

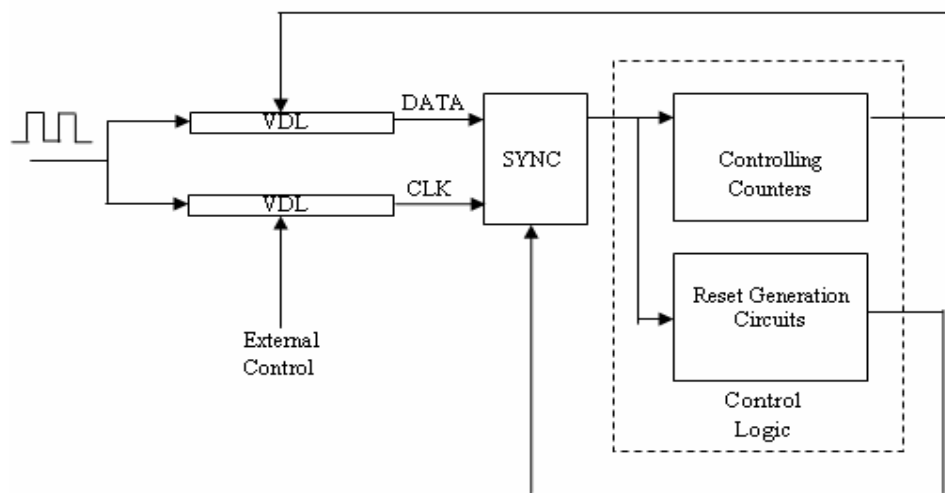


Figure 4.3 Deep metastability measurement

As shown in Figure 4.3, the on-chip deep metastability measurement uses only one oscillator and two variable delay lines to provide data and clock for the synchronizer. One variable delay line is controlled on chip and the other one is a fixed delay line which is controlled externally when setting up the chip. The output of the synchronizer is used to control one of the variable delay lines so that the loop settles at the balance point where the number of high output events is the same as the number of low output events. When the loop has settled the distribution of data input times is small and close to a normal distribution. In this way the synchronizer is forced into metastability on almost every clock cycle and many more deep metastability events can be observed than by the traditional measurement method.

The measurement can then be conducted in the deep metastability region, giving a more reliable result for the synchronizer performance. The measurement is made by comparing the distribution of input events with the distribution of output events [38]. As shown in Figure 2.23, the number of input events is counted where the data is ahead of the balance point by a time period between 0 and t_{in} and thereafter the number of output events between t_{out} and infinity. A problem is that the oscilloscope is unable to record the distribution of input and output events at the same time, so they need to be recorded separately and normalized in order to build a relationship between the input time and output time. Then value of t_{out} that gives the same output count as the input count given by t_{in} establishes the correspondence between t_{in} and t_{out} . The method allows the construction of the input time against output time from the input time and output time distributions recorded by the oscilloscope. One problem which is encountered is that the input time distribution is obscured by measurement noise. However, in Chapter 2 it was shown how this noise can be removed by adjusting the ratio of high output events and low output events. This can be done much more accurately with the on-chip measurement circuit using digital counters and digital variable delay lines than with the previous off-chip analogue measurement circuit.

4.2 Implementation of On-chip Deep Metastability

Measurement

As shown in Figure 4.3, the on-chip measurement circuit is composed of three blocks, namely, Variable Delay Lines, Devices Under Test (synchronizers) and Control Logic. Together they form a DLL to force the input time of the synchronizer

to stay around the balance point. The details of these blocks are described separately below.

4.2.1 Variable Delay Lines

There are two VDLs in the on-chip measurement circuit. One is used to vary the delay in the DATA path and the other is used to vary the delay in the CLK path. The VDL in the DATA path is controlled by a 16-bit on-chip counter. The VDL in the CLK path has a fixed delay and is controlled externally. Figure 4.5 shows the architecture of the VDL, which was proposed by Maymandi-Nejad and Sachdev [40] and is based on a current mirror structure. Compared with traditional VDLs, its advantage is that the delay behaviour is monotonic.

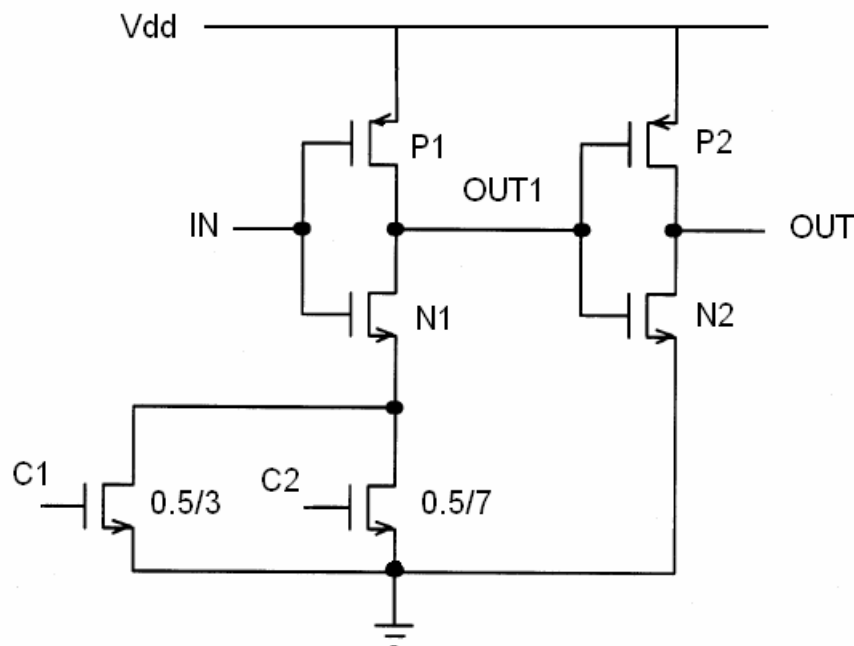


Figure 4.4 Traditional VDL

For traditional VDLs, the controlling transistors are usually placed below the N-type transistor as shown in Figure 4.4, and the transistor length L , instead of

transistor width, W , is usually used to control the W/L ratio because otherwise a small W/L ratio cannot be realized. Normally, the delay depends on the effective resistance of the controlling transistors ($C1$ and $C2$ in the figure). Turning on both $C1$ and $C2$ would give less resistance and thus a shorter delay than only turning one of them. Also, only turning on $C1$ would give shorter delay than only turning on $C2$ since $C1$ has a larger W/L and thus offers less resistance. In this way, the delay behaviour should be monotonic. However, the delay is also affected by the charge sharing effect. As $N1$ turns on, the charge at node $OUT1$ is immediately shared with the effective capacitance at the source of $N1$, which causes a sudden fall in the voltage at node $OUT1$ and decreases the delay. The subsequent fall in the voltage is controlled by the effective resistance of the controlling transistors. The amount of the voltage drop due to charge sharing depends on the effective capacitance at the source of $N1$. When only $C2$ is on, the effective capacitance seen by the source of $N1$ is $C_{total} = C1_{off} + C2_{linear}$, where $C1_{off}$ is the capacitance between the drain of $C1$ and the ground when $C1$ is off, and $C2_{linear}$ is the capacitance between the drain of $C2$ and the ground when $C2$ is in the linear region. When only $C2$ is on, C_{total} is larger compared to the case when only $C1$ is on since $C2$ has a larger size. Thus, the amount of voltage drop is greater and hence the delay is less, which is just the opposite of the normal situation where only turning on $C2$ (smaller W/L) should have longer delay than only turning on $C1$ (larger W/L). Therefore, the actual delay behaviour of the VDL is non-monotonic. Increasing the number of controlling transistors increases the difficulty of achieving a monotonic delay.

To solve this problem, the VDL proposed in [40] adopts a current mirror structure. As shown in Figure 4.5, a current starved buffer, $M0$ - $M5$, is the main

element of the VDL. The current through this buffer is controlled by a current mirror circuit composed of transistors M2 and M11.

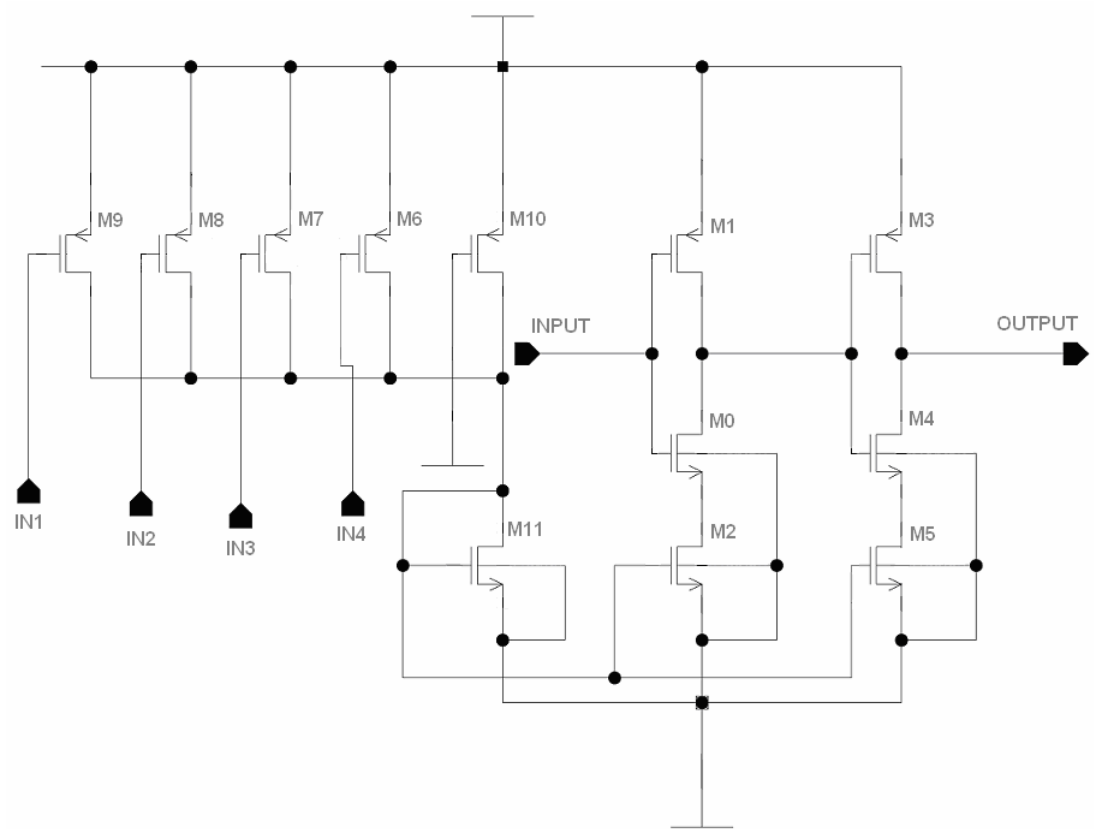


Figure 4.5 Improved VDL

The current mirror structure is such that, the controlling transistors do not have to be placed below the main N-type transistor, so the charge sharing effect is reduced and the delay behaviour of the VDL is monotonic. The appropriate current through M11 can be adjusted by turning on the controlling transistors M6-M9, while transistor M10 is always on as a base transistor. Here the W/L ratio of the controlling transistors M6-M9 are arranged in a binary fashion so that the number of controlling transistors can be minimized. In order to obtain a small incremental delay and also a large delay range, the VDL includes 4 cascaded stages similar to

Figure 4.5. The maximum delay of each stage is different and is designed to achieve an incremental delay of 0.1ps and a delay range of 0-500ps.

4.2.2 Devices Under Test (synchronizers)

Three different synchronizers have been incorporated on a chip for measurement and comparison. They are Jamb latch A, Jamb latch B and the improved synchronizer mentioned in Chapter 3. The Jamb latch A and Jamb latch B have the same structure but different output configurations. They have been reported to have different characteristics in the deterministic region [27]. Each synchronizer is made up of two latches similar to Figure 3.1 and Figure 3.10 in master-slave configuration. As shown in Figure 4.6, all the synchronizers share the same DATA, CLK and RESET signal. There is a multiplexer to select different synchronizers on the chip for measurement. When one of the synchronizers is selected, its output goes through the multiplexer to control the DLL and generate the RESET signal for all the tested synchronizers. The multiplexer is used to ensure the testing circuitry is identical for all the synchronizers, however it can introduce a relatively large delay. In order to obtain an accurate output time, measurement points are placed before the multiplexer.

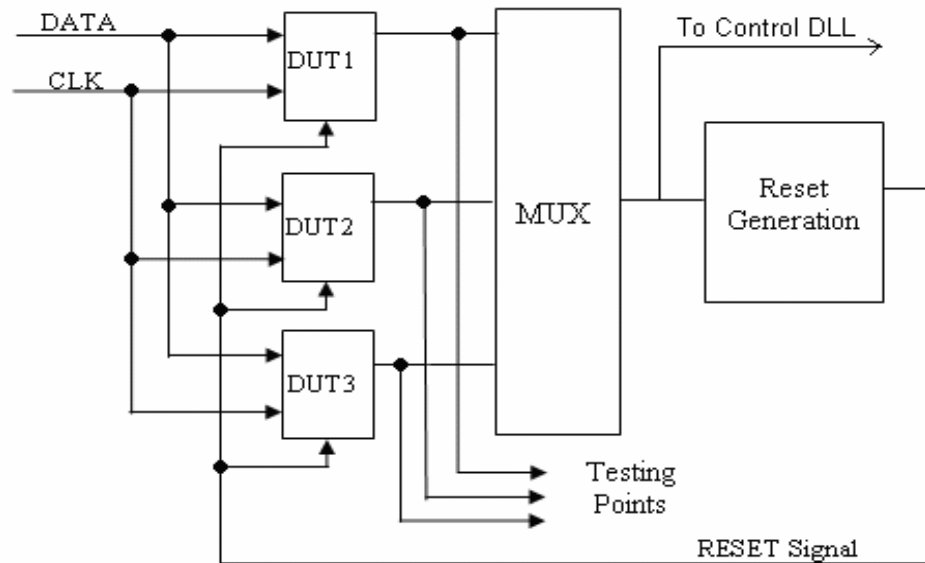


Figure 4.6 Multiplexer circuit for DUTs

4.2.3 Control Logic

The control logic consists of two parts, namely the controlling counters and reset generation circuits.

As shown in Figure 4.7, there are three controlling counters. The output of the main 16-bit counter is used to adjust the VDL in the DATA path. The outputs from the two 8-bit ratio controlling counters are used to control the ratio of the high to low output events.

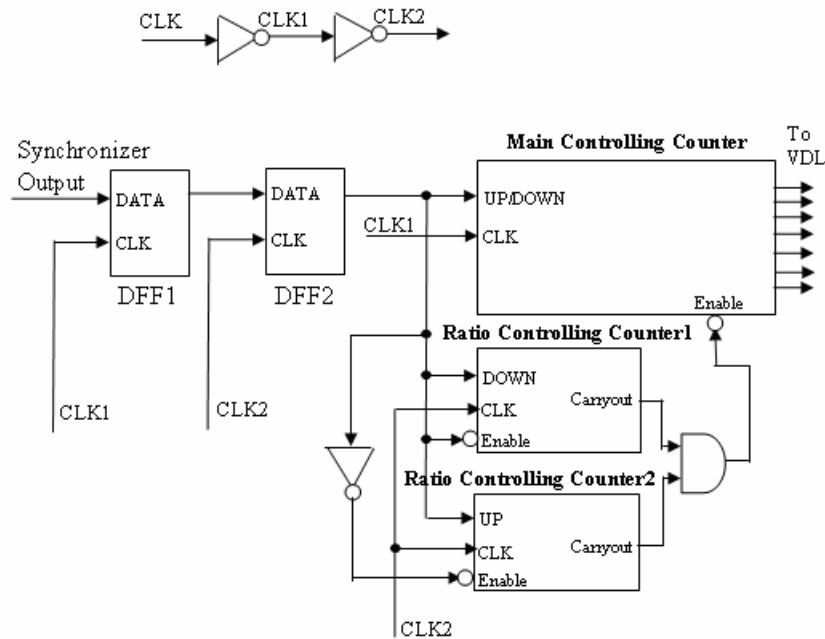


Figure 4.7 Controlling counters

Two D flip-flops as shown in Figure 4.7 are used to detect output events from the synchronizer. The ratio controlling counter 1 decrements only when there is a low output event from the synchronizer. The ratio controlling counter 2 increments only when there is high output event from the synchronizer. The main counter increments/decrements only when there is a carryout from either of the ratio controlling counters; it increments for carryout from counter 1 or decrements for counter 2, depending on the output event detected.

All the controlling counters must be loaded with initial values at the beginning of test. Due to the limitation of the number of pins, a multiplexer arrangement is used to load values into the different controlling counters. Figure 4.8 shows the architecture of the multiplexer circuit.

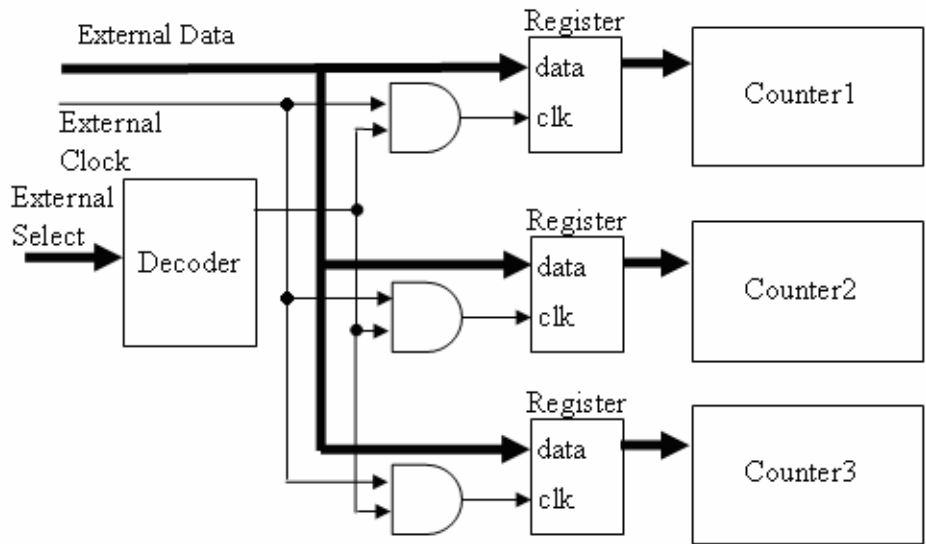
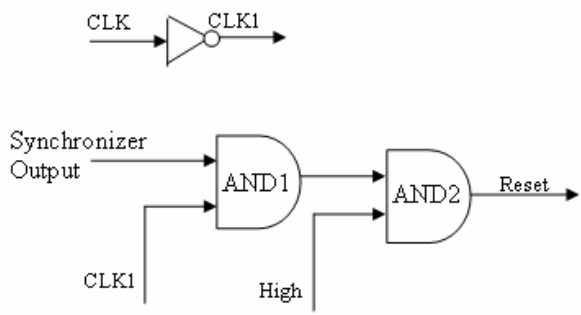
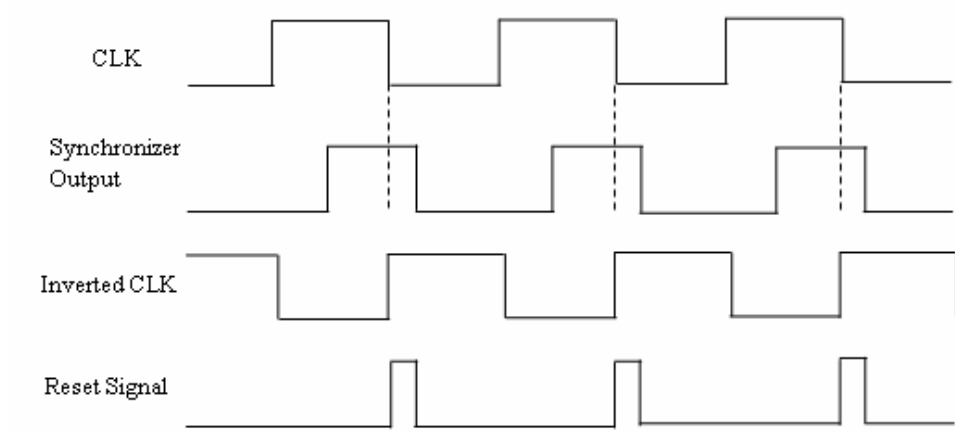


Figure 4.8 Loading circuit for controlling counters

As shown in Figure 4.8, some registers are used to hold the loaded values for different controlling counters. The clock signals for the registers are generated by ANDing the external clock and the outputs of a decoder which is controlled by an external select signal. If one controlling counter is selected, the corresponding output of the decoder goes high and thus the external clock can go through the AND gate to latch the data into the registers of the counter. In this figure the clock signals for the counters are not shown.



(a)



(b)

Figure 4.9 Generation of RESET signal

To ensure that the measurements are made consistent, the tested synchronizers are always reset before the data changes. Figure 4.9 (a) shows the RESET generation circuits. The RESET signal is generated by ANDing the synchronizer output and the back edge of the clock. In order to hold the RESET signal for some time another AND gate is used to add a delay to it. Figure 4.9 (b) shows the generation of the RESET signal.

4.2.4 Layout of On-chip Measurement Circuit

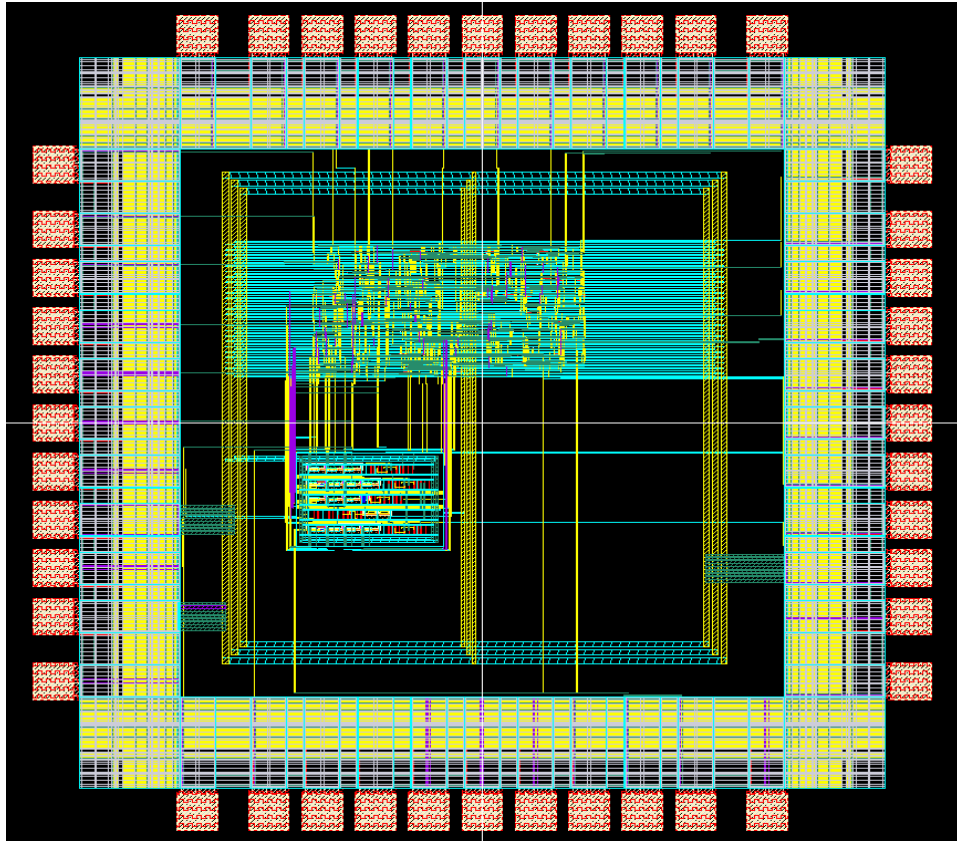


Figure 4.10 Layout of on-chip measurement circuit

The on-chip measurement circuit has been fabricated using UMC 0.18 μm technology and its layout is shown in Figure 4.10. The control circuits are designed using standard cells and occupy the larger block in Figure 4.10. The variable delay lines and the devices under test are full custom designs and are in the smaller block. The power supply to the devices under test can be varied separately from all other power supplies to the chip.

4.3 Measurement Results

4.3.1 Input Histogram

Figure 4.11 shows the input histogram for the Jamb Latch A synchronizer at a Vdd of 1.8 V.

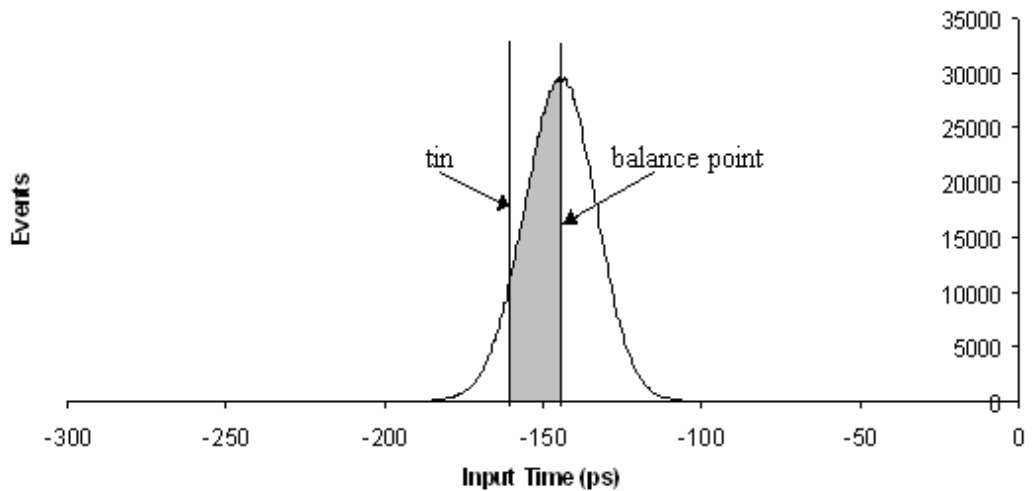


Figure 4.11 Input histogram

The clock is used as trigger to observe the data. As shown in Figure 4.11, the data time is held within a very small range around the balance point of the synchronizer demonstrating that the delay locked loop is stable. The standard deviation of the time distribution of the data change including oscilloscope measurement noise is about 11ps.

4.3.2 Output Histogram

Figure 4.12 shows the output histogram of Jamb Latch A at a Vdd of 1.8 V. Again, the clock is used as trigger to observe the output of the synchronizer. For this

experiment, a ratio of 1:1 is used between high and low outputs. To achieve this, the values of the two ratio controlling counters were both set to 1. By using a digital histogramming oscilloscope the total number of high output events and low output events can be recorded and displayed. The output events were recorded over a period of time and the total number of high output events were plotted against that of low output events as shown in Figure 4.13, where it can be seen that the ratio of high to low output events is always close to 1:1, which demonstrates that the ratio is held very constant over the time of the measurement.

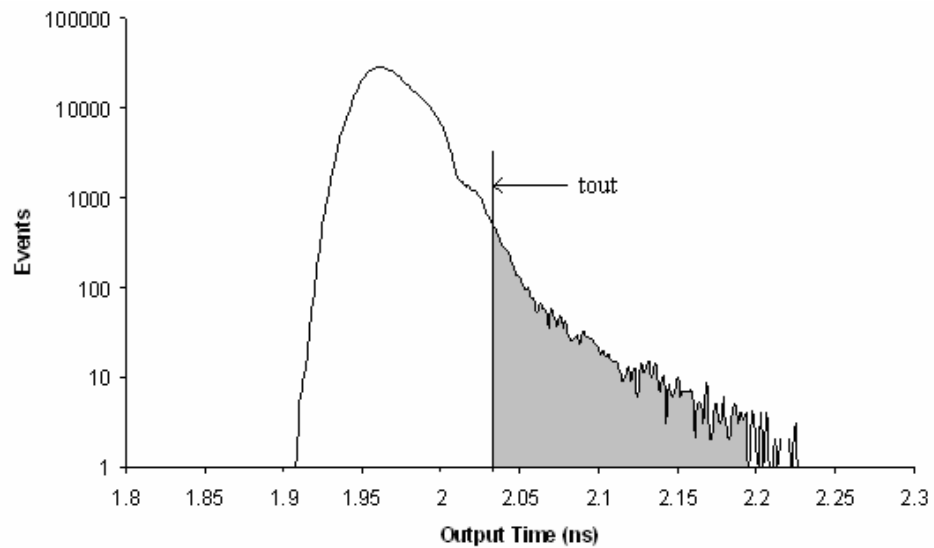


Figure 4.12 Output histogram

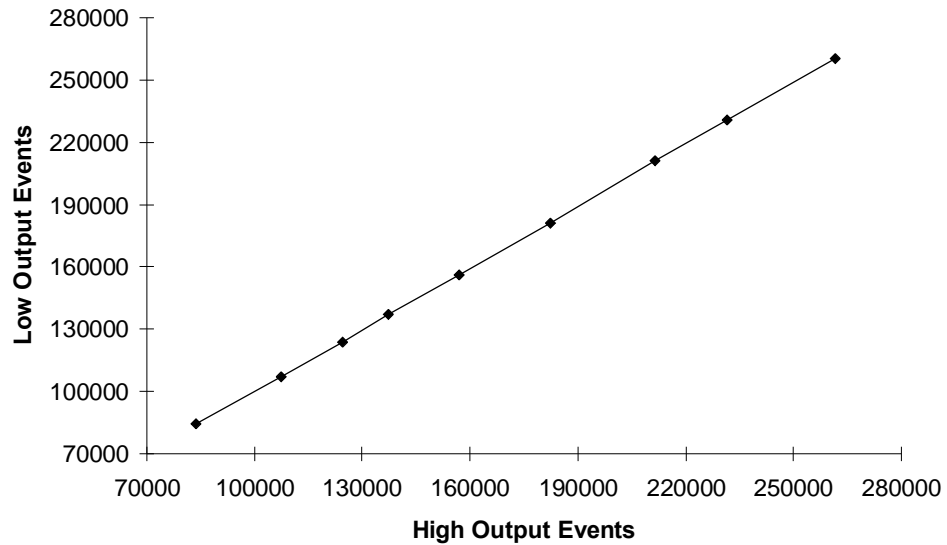


Figure 4.13 High output events vs low output events

By setting different values for the two ratio controlling counters the proportion of high to low output events can be changed and the median value of the input time distribution can be shifted. The relationship between the shift and the percentage of high output events are plotted as shown in Figure 4.14, which also demonstrates that the measurement of input events can be made to an accuracy of around 1ps.

Finally, the output histogram in Figure 4.12 is very similar to the one in Figure 6 in [24], where the output histogram of Jamb latch synchronizer has been measured using the traditional two-oscillator method, which demonstrates that the on-chip measurement is in good correlation to the previously published results [24].

4.3.3 Corrected Input Histogram

The input histogram recorded on the oscilloscope also contains the measurement noise from the oscilloscope itself which is typically 9.2 ps according to its specification. Due to this relatively large measurement noise component Figure 4.11

cannot be reliably used to assign input times to output times. To eliminate the measurement noise and find the real density of inputs around the balance point the ratio of high to low outcomes is altered, hence shifting the balance point. By measuring the time shift and knowing the average number of trajectories that have changed from high to low, then the number of inputs within the time represented by the shift can be determined despite any oscilloscope noise. In this way the actual average number of trajectories can be plotted against time. The correction of the input histogram can be done by adjusting the values of the two ratio controlling counters to produce different proportions of high and low outputs from the synchronizer. This causes the balance point, which is the peak of the input histogram, to shift in order to achieve the proportions set by the ratio controlling counters, and the proportion of high outputs can be plotted against the shift as in the method described in [38]. The shifts required to give different probabilities of high outputs are plotted in Figure 4.15.

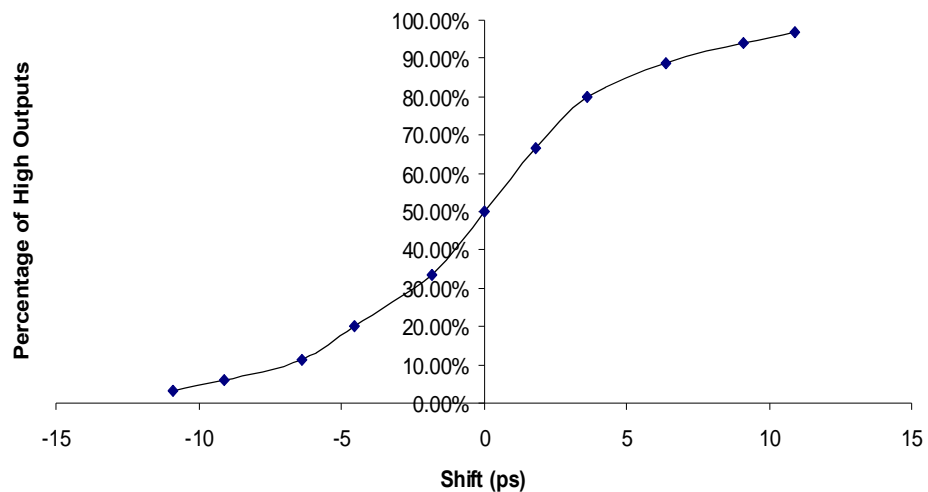


Figure 4.14 Measurement of actual input time distribution

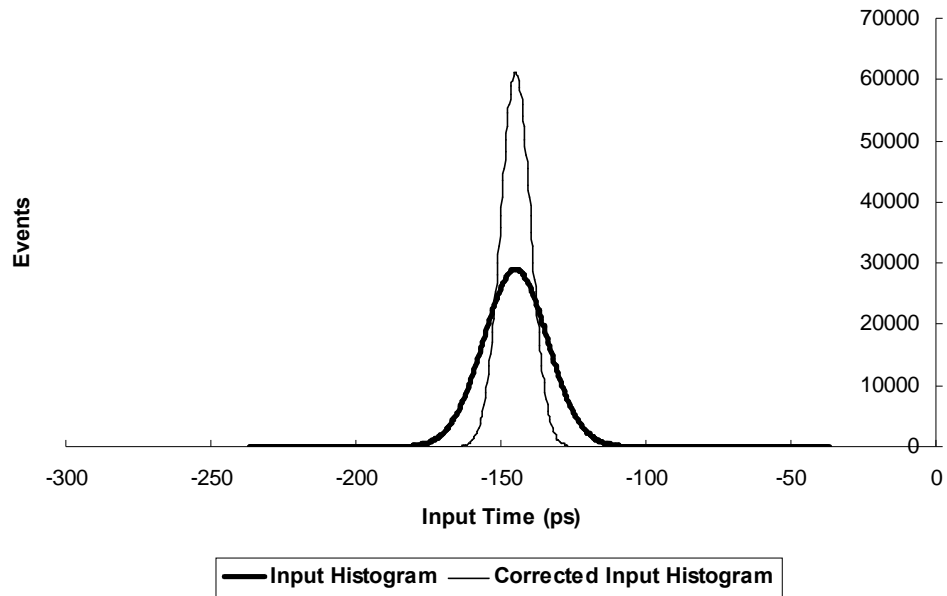


Figure 4.15 Corrected input histogram

If it is assumed that the time of input events follows a normal distribution, these shifts can be compared with distributions having different values of standard deviation, σ . The line with the closest fit to the points on Figure 4.14 represents the cumulative probability of a high output for a random input time deviation of 5.2 ps, so it can be concluded that the actual distribution has a deviation of this value. Furthermore, the observed input deviation of 11ps is close to the square root of the sum of the squares of 9.2ps (the measurement noise from the oscilloscope according to its specification) and 5.2ps. The corrected input histogram is shown in Figure 4.15.

As can be seen from Figure 4.15, the corrected input histogram has a standard deviation of about 5.2ps. This result demonstrates that the DLL holds the delay difference between data and the balance point to within very close limits, and that the distribution of the delay difference is nearly random.

4.3.4 Input Time vs Output Time

After creating the input and output histogram of the synchronizer, the input time and output time relationship can be plotted using the mapping method described in [38]. The basic principle of this method is to plot the total number of input events after a particular input time and before the balance point (the shadow area shown in Figure 4.11), and scale it from 0 to 1. Thereafter, plot the total number of output events occurring after a particular output time (the shadow area shown in Figure 4.12), and scale it from 0 to 1. After that the input time can be mapped to the output time which corresponds to the same normalized number of events. A significant advantage of this technique is that it allows the results to be presented in an easily understood standardized form, independent of oscillator frequency or number of events. With a knowledge of the clock and data frequencies, the input time and output time relationship can be easily converted to give the mean time between failures, since a single input will give an overlap less than Δt , in any particular clock cycle with a probability of $\Delta t \cdot f_c$, and over a time T , there will be $T \cdot f_d$ inputs. It follows that the $MTBF = \frac{1}{\Delta t \cdot f_c f_d}$ and given the values of f_c and f_d in a system, the scale can easily be converted from Δt to MTBF.

Figure 4.16 shows the measured input time vs output time for Jamb A, Jamb B and the robust synchronizer with a supply voltage of 1.8V. In order to avoid the problem of long interconnections on the chip and to compare the metastability characteristics of the three synchronizers, for all measurements, output times are computed relative to the time when the largest number of events (normal propagation delay) is recorded. The reciprocal of the slope of the curves in Figure

4.16 represents the synchronization time constant τ . As can be seen from the figure outputs with input time down to 10^{-17} s can be plotted within an experimental time of 10 minutes, which corresponds to an MTBF of 100 seconds given that both the clock frequency and data rates are 30MHz, enabling τ to be measured in the deep metastability region. In a future version of this chip, by filtering out early responses and extending the measurement time, a MTBF of 10^6 seconds or approximately 12 days could be measured.

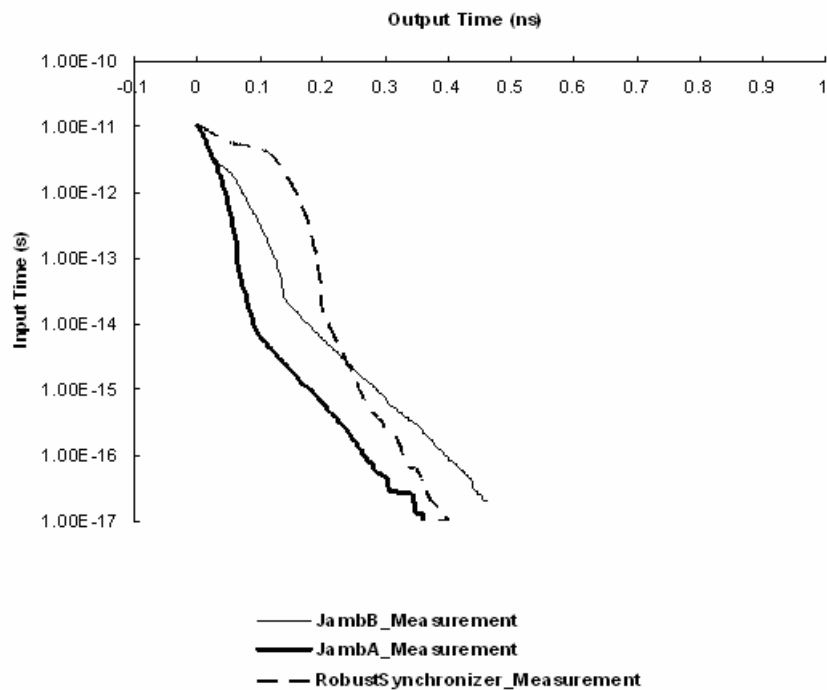


Figure 4.16 Measured Input time (s) vs output time (ns)

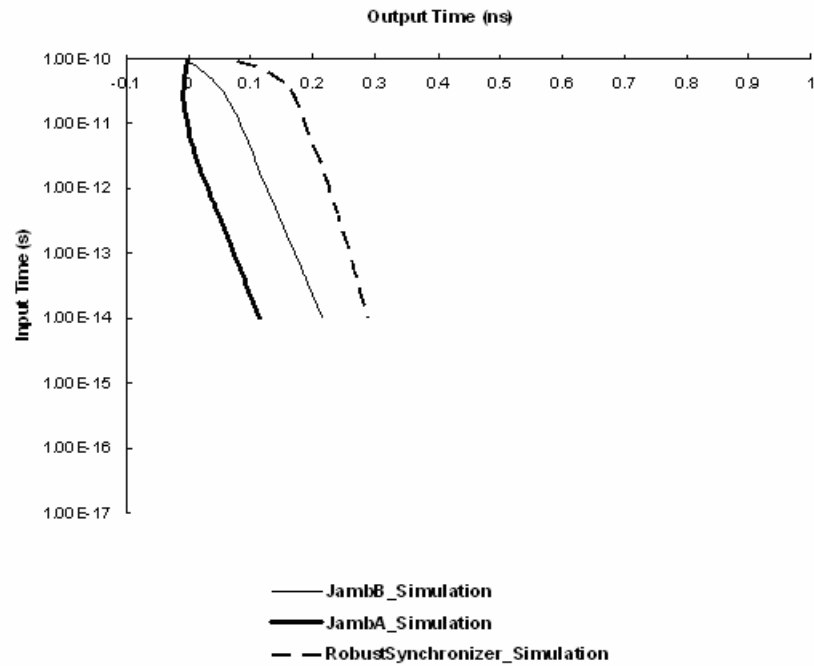


Figure 4.17 Simulated input time (s) vs output time (ns)

Figure 4.17 shows the simulation results of input time vs output time for the three tested synchronizers. Again the output times are made start from zero where the normal propagation delay is. By comparing Figure 4.16 and Figure 4.17 it can be seen that the slope of the curves between 10^{-11} s and 10^{-14} s in both figures are similar. In the simulation results only the input time down to 10^{-14} s are plotted because the minimum simulation step used is 10^{-14} s. Below this value the accuracy of the simulation results is not reliable. Figure 4.16 and Figure 4.17 also show that the robust synchronizer can be more reliable than both Jamb latch A and B, that is, it has a smaller τ , which leads to faster resolution of metastability and thus fewer very long output times. This is due to the latch current, which determines the speed of metastability resolution, being greater in the robust synchronizer than in the Jamb latch during metastability. This makes the robust synchronizer much less sensitive to V_{dd} , V_{th} and temperature variation as discussed in Chapter 3. Figure 4.16 and Figure

4.17 also show that the three tested synchronizers are slower in the deep metastability region than they are in the deterministic region, which indicates that the prediction of the MTBF based on simulation of the early deterministic region can lead to falsely optimistic results.

4.3.5 Tau vs Vdd

In order to compare the sensitivity of the Jamb latch and the robust synchronizer to Vdd variation, the value of τ for different values of Vdd was measured. Table 4.1 shows the measurement results. Here the simulation results are also shown for comparison.

Vdd (v)	Measurement Results(ps)				Simulation Results(ps)	
	Jamb Latch B		Robust Synchronizer		Jamb Latch B	Robust Synchronizer
	$>10^{-14}$	$<10^{-14}$	$>10^{-14}$	$<10^{-14}$		
1.8	19.44	35.55	15.27	34.92	18.99	14.69
1.7	21.75	37.29	16.53	35.76	20.36	15.36
1.6	25.64	40.93	19.38	38.25	22.24	16.19
1.5	28.77	52.36	20.29	43.07	24.99	17.23
1.4	36.22	66.17	23.75	50.36	29.31	18.59
1.35	45.43	75.35	28.51	58.19	36.85	20.39

Table 4.1 Tau vs Vdd for Jamb B and Robust Synchronizer

Table 4.1 shows that for both synchronizers, τ increases with V_{dd} decreasing. This is because the latch current which determines the resolution speed of metastability decreases with V_{dd} decreasing. Furthermore, the robust synchronizer

circuit performed at least as well as the Jamb Latch at all values of V_{dd} , and was more than 20% faster when V_{dd} was reduced by 25% (shaded row in Table 4.1).

Table 4.1 also shows that the values of τ match the simulation results well when the input time is above 10^{-14} s which is the minimum simulation step used. Below 10^{-14} s the simulation results are not reliable. Table 4.1 also shows that the measured value of τ below 10^{-14} s is greater than that above 10^{-14} s, which means that the tested devices are slower in the deep metastability region than they are in the deterministic region. For this reason, simulation of the early deterministic region cannot be relied upon to predict MTBF at realistic synchronization times, and it is necessary to check the value of τ in deep metastability region with accurate measurement.

4.4 Summary

An on-chip measurement circuit of synchronizer using deep metastability measurement method has been designed and implemented with UMC 0.18 μ m technology. Compared with the previous off-chip implementation using analog circuits, the on-chip implementation using digital circuits allows integration of both the synchronizer circuits and the measurement method, and eliminates high speed off-chip paths which are a source of inaccuracy. It also makes the control at the picosecond level easier because of the inherent stability of digital integrating counters and digital delay lines.

The results show that the measurement method is stable and reliable. The digital delay line was controllable to an increment of 0.1ps, and the input time distribution was 5.2ps compared with 7.6ps for the analog version. Through the use of high and low counters the actual input time distribution could be measured to within better

than 1ps. τ was measured down to 10^{-17} s within an experimental time of 10 minutes, corresponding to an MTBF of 100 seconds. In a future version of this chip by filtering out early responses and extending the measurement time, this could be extended to a MTBF of 10^6 seconds or approximately 12 days. The responses from the tested devices were shown to correspond with the simulation results down to 10^{-14} s, however values of τ for input times below that reachable by measurement were shown to be greater than simulation, which means that tested device is slower in the deep metastability region than it is in the deterministic region. For this reason simulation of the early deterministic region cannot be relied on to predict MTBF at realistic synchronization times, and it is necessary to check the value of τ in deep metastability with accurate measurement. A comparison was also made between the Jamb latch and the robust synchronizer at different values of supply voltage, showing that the robust synchronizer circuit performed at least as well as the Jamb latch at all values of Vdd, and was more than 20% faster when Vdd was reduced by 25%.

Chapter 5

Adapting Synchronizers to the Effects of On-chip Variability

Process, voltage, and temperature variations in nanometer technologies can be an important limit on the performance of systems on silicon. Components such as logic circuits, memories on chip are all affected, but the performance of synchronizers which are used to synchronize data passing between different clock regions in future SoCs may affect the system performance to a greater extent than other components for three reasons:

1. V_{th} is a major source of on-chip variability, and synchronizers are usually more strongly affected by V_{th} variation than logic circuits.
2. Synchronization time is usually one or more clock cycles in duration, and is directly affected by the synchronization time constant, whereas there are many logic gate delays in a clock cycle, allowing random variations in each gate within a critical path of gates to be subject to averaging.
3. In future SoCs, communication is likely to affect the system performance more than processing [18], and synchronization is a large overhead in a communication link.

A future multi-core system can incorporate hundreds of synchronizers on a single chip. As a critical part of on-chip communication network, the synchronizers'

performance is crucial to the system performance. The impact of process variation on circuit performance has been discussed in [41][42][1]. At 180nm, it can be expected that the standard deviation (σ) of the synchronization time constant τ , which determines the resolution time of metastability in synchronizers, to be about 5% [41]. So one synchronizer out of 1000 may have a 15% worse value of τ . τ was measured in a batch of synchronizers chips fabricated on the UMC 180nm process and found to have a variability consistent with the results given in [41]. At 90nm σ is about 8% [41], hence it can be expected that one synchronizer out of the 1000 will have a 24% worse value of τ . As the technology continues advancing, the effects of process variation on circuit performance becomes more and more significant. According to ITRS 2006 [1], at 45nm the circuit performance variability reaches 50%. In addition to process variations, power supplies and temperature variations disproportionately affect the synchronization time constant τ , since τ depends on the small signal parameters in metastability rather than large signal switching times [27]. As a result a 50% reduction in power supply voltage may result in over 100% increase in τ [23]. Additionally, for a synchronizer, the average data rate between different clock regions in a system on chip may vary over time. Hence the MTBF of the synchronizer which is determined by the data rate [27] may vary over time.

Recently, adaptive circuits have been used to mitigate the effect of process variation in microprocessor designs [43]. In this chapter two adaptation schemes proposed to reduce the effects of process, voltage, temperature and data rate variations on synchronizers on chip are described [44]. One scheme is aimed at improving synchronizer performance subject to process variation. Current practice to reduce the effects of process variation is to make the transistors in the synchronizer wider than normal so that the deviation is reduced. The main

disadvantage of this technique is that it uses a significant proportion of the system power budget because the current is also increased. An alternative is to make a number of identical synchronizers, measure their τ on chip and then select the best one. After selection, all the others are powered down, together with the selection circuitry. Power dissipation during normal operation is therefore the same as for a single synchronizer, and the performance can be improved.

The other scheme is to improve the system performance by adjusting the synchronization time according to the actual process, voltage, temperature and data rate variations on the condition that the required MTBF is met. This is targeted at oversized synchronization times due to synchronizer performance variability. For example, for a synchronizer in a multi-core system, due to the variations discussed before, extra synchronization time is required to ensure that the synchronizer works in the worst case. The multi-core system may incorporate a lot of synchronizers. Since it is unknown which synchronizer will operate in the worst case all the synchronizer times on the chip need to be extended. However, the actual amount of the variations for some of the synchronizers may not be as great as the worst case. With the synchronization time adjustment scheme, the synchronization time of each synchronizer on the chip can be adjusted according to the actual process, voltage, temperature and data rate variations to improve the performance of the system on the condition that the required MTBF is still met.

Both adaptation schemes proposed rely on the on-chip measurement of failure rates in individual synchronizers, followed in the first case by the selection of the best synchronizer to reduce the effect of the process variation on synchronizer performance, and in the second case by adjustment of the synchronization time

according to the actual variations to improve the system performance. The rest of the chapter is organized as follows. In Section 5.1 the on-chip measurement of failure rates is described, followed in Section 5.2 with an explanation of how τ and MTBF are calculated from the failure rates. In Section 5.3 the two proposed adaptation schemes are described, followed by the implementation details of the two adaptation schemes in Section 5.4. Section 5.5 discusses the applications of the two adaptation schemes. The test results are presented in Section 5.6 with an overall summary of the work in Section 5.7.

5.1 On-chip Measurement of Failure Rates

Figure 5.1 shows the on-chip measurement of failure rates. Here FF1 and FF2 sample the output of the synchronizer at two different times $SCLK+T1$ and $SCLK+T2$ ($T1 < T2$). Their outputs are XORed with the output of FF3 which sample the output of the synchronizer at the falling edge of SCLK. Assuming that there is a very high probability that metastability resolves before the falling edge of SCLK, if the output of synchronizer is in metastability at the sampling time $SCLK+T1$ or $SCLK+T2$, the output of FF1 or FF2 will have different value to the output of FF3, so the output of XOR will go high. This high output will then be clocked into FF5 or FF6 at the next $SCLK+T1$ time, indicating that a failure has been detected. Counter1 and Counter2 are used to count the number of failures at the two sampling times; Counter3 is used to count the number of clock cycles. When Counter1 reaches a preset value (say 200) all three counters will be halted.

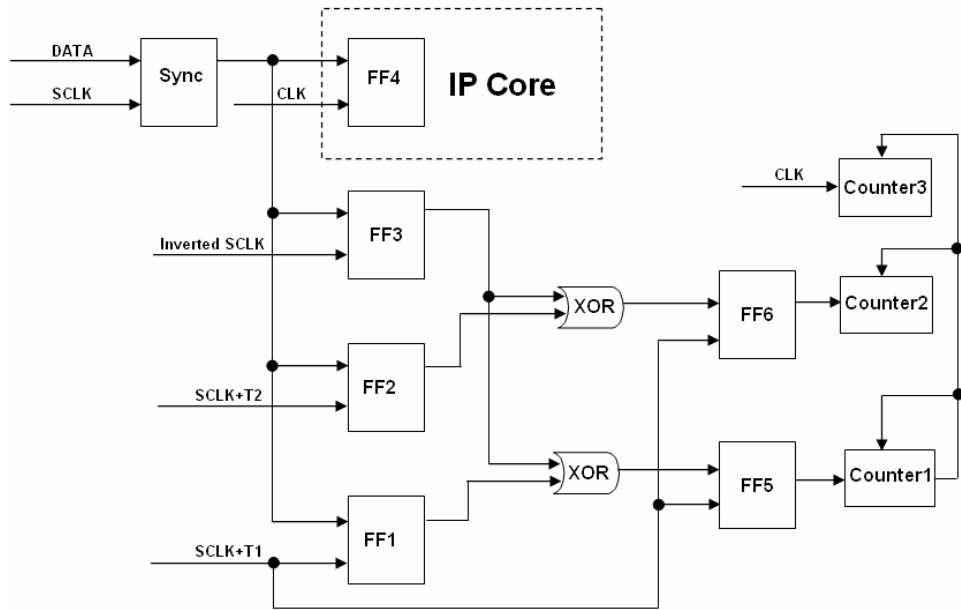


Figure 5.1 On-chip measurement of failure rates

5.2 Calculation of τ and MTBF

In order to ensure that the value of τ measured by this technique is the same as the long term τ , the sampling times must be taken where any initial transients leading to variation in τ have died away (usually 30τ to 40τ). From the measured failure rates, τ and MTBF can be calculated.

5.2.1 Calculate τ from Measured Failure Rates

The parameter τ is the synchronization time constant which determines the resolution time of metastability. It can be calculated from the measured failure rates using the formula below, where t is the synchronization time, T_w is the metastability window, f_c is the clock frequency and fd is the data rate. $MTBF1$ and $MTBF2$ are obtained by substituting t with the sampling times $T1$ and $T2$ (shown in Figure 5.1) respectively in the formula of MTBF, and $Count1$ and $Count2$ are the number of

failures counted by Counter1 and Counter2 at $T1$ and $T2$. $Count3$ is the number of clock cycles counted by Counter3.

$$\begin{aligned} \therefore MTBF &= \frac{e^{\frac{t}{\tau}}}{T_w f_c f_d} \\ \therefore \frac{MTBF2}{MTBF1} &= e^{\frac{T2-T1}{\tau}} \\ \therefore \frac{Count1}{Count2} &= e^{\frac{T2-T1}{\tau}} \\ \therefore \tau &= \frac{T2-T1}{\ln \frac{Count1}{Count2}} \end{aligned}$$

5.2.2 Calculate MTBF from Measured Failure Rates

After the calculation of τ , the long term MTBF corresponding to the currently given synchronization time can be calculated using Equation (5.1), where $T3$ is the current synchronization time and $T1$ is the earlier of the two sampling times.

$$MTBF3 = MTBF1 * e^{\frac{T3-T1}{\tau}} \quad (5.1)$$

However, $MTBF3$ is usually very large compared to $MTBF1$ (say 10^{10} times larger), and the calculation would require floating point hardware. To reduce the hardware overhead for estimating $MTBF3$ conversion to a simpler fixed point calculation is necessary.

$$\begin{aligned}
\therefore MTBF3 &= MTBF1 * e^{\frac{T3-T1}{\tau}} \\
\therefore MTBF3 &= \frac{Count3 * Clock_period}{Count1} * e^{\frac{T3-T1}{\tau}} \\
\therefore \frac{Count1 * MTBF3}{Clock_period} &= Count3 * e^{\frac{T3-T1}{\tau}} \\
\text{Let } X &= \ln \frac{Count1 * MTBF3}{Clock_period}, \quad Y = \ln(Count3) \\
\therefore e^X &= e^Y * e^{\frac{T3-T1}{\tau}} \\
\therefore X &= Y + \frac{T3-T1}{\tau}
\end{aligned}$$

Now it is only necessary to calculate X instead of the real MTBF, and the required MTBF can also be converted to required X in the same way for later comparison.

5.3. Two Proposed Adaptation Schemes

Based on the on-chip measurement of failure rates, two adaptation schemes used to mitigate the effects of on-chip variability on synchronizers have been proposed and are presented in this section.

5.3.1 Synchronizer Selection Scheme

A synchronizer selection scheme is used to reduce the effects of process variation by selecting the synchronizer with the best performance from a number of redundant synchronizers. In the future a multi-core design can incorporate hundreds of synchronizers on the same chip. Their performance is critical to the system performance. Assuming that a synchronizer has a τ of 11 ps, and a standard deviation, σ , of 8% on 90nm technology. Assuming that the variability is

completely random, then in the worst case a 3.09σ must be allowed to ensure that the probability of a synchronizer having a τ worse than this is 0.001. This means that the synchronization time must be set to allow for a τ of $11+11\times 0.08\times 3.09=13.72$ ps. The usual solution to this is to make the width of all transistors in the synchronizer N times larger (say $N=4$). Assuming that this will reduce the standard deviation to $\sigma = \frac{8\%}{\sqrt{4}} = 4\%$, now the worst case of τ is 12.36 ps, but the power is increased by four times.

An alternative approach is to make N identical synchronizers, measure their τ on chip, and select the best one. After the selection process, all the others are powered down, together with the measurement circuitry. Power dissipation during normal operation is therefore the same as for a single synchronizer, but the performance is improved. The probability of one synchronizer having a τ worse than 11.81 ps is 17.8%, but the probability of all four synchronizers having τ worse than this is 0.178^4 , which is around 0.001. In this way a small worst case improvement has been achieved from 12.36 ps to 11.81 ps for τ , together with a significant power saving. A synchronization time of 40τ could be required to give a MTBF of 4 months, so the improvement in synchronization time in this case is about 22 ps.

The above analysis assumes that the variability over the four synchronizers is completely random. This is unlikely to be the case. There will be some correlation between circuits, but note that this correlation will be greater for the transistors in the large synchronizer, because the increase in size is located within a small area, so the selection technique will always give at least as good a result as the simple method of increasing transistor size. In addition, enlarging the synchronizer size

cannot reduce all kinds of process variations. For example, it has no effect on the variation in gate insulator thickness. Therefore the actual deviation after increasing the transistor size is more than 4% for the example discussed, and thus the improvement is less than expected. On the other hand, the selection technique is used to deal with all kinds of process variations. Hence, it is a much better way to improve the synchronizer performance.

5.3.2 Synchronization Time Adjustment Scheme

The synchronization time adjustment scheme is used to improve the performance of the system by adjusting the synchronization time according to the actual process, voltage, temperature and data rate variations on the condition that the required MTBF is met. Table 5.1 shows the variation of the synchronization time constant τ with Vdd and temperature variations for a Jamb latch realized in a 90nm technology. The results are obtained by extensive SPICE simulation using UMC 90nm technology.

Vdd(v)	τ (ps) at 27 °C	τ (ps) at -25 °C
1.2	11.47	9.23
1.1	12.19	10.24
1.0	13.67	12.06
0.9	15.46	14.28
0.8	19.64	18.66
0.7	30.71	36.33
0.6	60.55	97.81
0.5	159.45	338.43
0.4	525.82	1403.76
0.3	2742.56	8151.86

Table 5.1 Jamb latch τ vs V_{dd} at 90nm

It can be seen from Table 5.1 that τ increases rapidly with V_{dd} decreasing. The value of τ is more than doubled at a V_{dd} of 0.7V, and more than an order of magnitude greater at 0.5V. Below 0.5V, τ increases more rapidly with a decreasing V_{dd} and lowering the temperature makes this situation worse because lower temperatures give higher threshold voltages. Variations in V_{dd} , V_{th} and temperature could make the synchronizer unviable, especially for deep submicron processes.

In addition, the average data rate between different clock regions in a multi-clock system may vary over time. Hence the MTBF of the synchronizer which is determined by the data rate may also vary over time.

Due to the variations discussed above, extra synchronization time is required to ensure that the system works in the worst case. For example, at 45nm, in a multi-clock SoC which incorporates hundreds of synchronizers, if τ can increase by 25% because of V_{dd} and temperature variation and a further 25% because of process variation, the worst case synchronizer will have an over 50% worse value of τ . In order to achieve the required MTBF it is necessary to extend the synchronization time of the synchronizer to over 1.5 times its original value, and because it is unknown which synchronizer will give the worst case all the synchronizer times on the chip need to be extended to over 1.5 times their original values. However, the actual amount of the variations for some of the synchronizers may be less than the worst case. With a synchronization time adjustment scheme, the synchronization time of each synchronizer can be adjusted according to the actual process, voltage, temperature and data rate variations to improve the performance of the system on the condition that the required MTBF is still met. For example, in the above case, for the

synchronizers which have nominal values of τ , the synchronization time can be reduced by 33%. As a result the system performance is greatly improved.

Note that the Jamb latch is not necessarily the best synchronizer as shown in Chapter 3. Developing transistor level design techniques for a more robust synchronizer [23] can also be a way to improve the synchronizer's performance as well as reducing its sensitivity to Vdd and temperature variations, but all synchronizers exhibit variability, and the synchronizer's performance can be further enhanced by adaptability.

5.4 Implementation

To assess their feasibility, the two proposed adaptation schemes have been implemented using a Xilinx's 90nm Spartan 3 FPGA.

5.4.1 Architecture of Synchronizer Selection Scheme

The synchronizer selection scheme is based on comparison of τ . In Figure 5.1 counter1 is used to count the number of failures at the earlier sampling time T1. When it reaches a preset value (say 200) all the three counters will be halted. Given that τ is expressed by Equation (5.2), and because T2-T1 and Failure_rate1 are constants, instead of comparing τ , the selection can be done by directly comparing Failure_rate2 of different synchronizers. The smaller the Failure_rate2, the smaller the value of τ . In this way division and log calculations can be avoided greatly simplifying the hardware implementation.

$$\tau = \frac{T2 - T1}{\ln \frac{Failure_Rate1}{Failure_Rate2}} \quad (5.2)$$

Figure 5.2 shows the architecture of the synchronizer selection scheme. It consists of an on-chip part and an off-chip part. The on-chip part is per synchronizer. It includes N redundant synchronizers and the failure detector. The failure detector is used to detect failures and has to be placed on chip alongside the synchronizers to ensure that the measurement is accurate. Each failure detector is shared by the N redundant synchronizers from which the best synchronizer is to be selected. The off-chip part is shared by all the synchronizers on the chip. It can be put off chip because the selection scheme is used to deal with process variation and only needs to operate once when setting up the chip. In this way the on-chip overhead is reduced. The off-chip part includes the failure counters, storage registers and comparator. The failure counters are used to count the number of the failures at different sampling times. After that the values from counter2 are stored in the storage registers for comparison and then the best synchronizer is selected. Thereafter all the other synchronizers plus the selection circuitry are powered down as is selection circuitry so the power consumption is the same as for a single synchronizer.

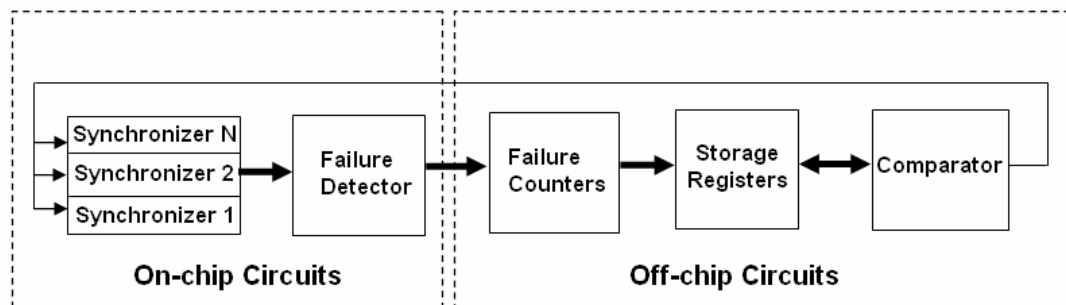


Figure 5.2 Architecture of Synchronizer Selection Scheme

In the FPGA implementation of the synchronizer selection scheme, the on-chip overhead per synchronizer is equivalent to 9 flip-flops and 6 gates. The total off-chip

overhead is equivalent to 34 flip-flops and 110 gates. It is possible to put this scheme entirely on chip since the off-chip overhead is not large.

5.4.2 Architecture of Synchronization Time Adjustment Scheme

The synchronization time adjustment scheme is based on a calculation of the MTBF. As shown in Figure 5.3, it also consists of an on-chip part and an off-chip part. The on-chip part includes the VDL, registers and failure detector. The VDL is used to control the synchronization time of the synchronizer and the registers are used to hold the delay setting of the VDL. Again, the on-chip part is per synchronizer and the off-chip part can be shared by all the synchronizers on the chip. This way the on-chip overhead is reduced. From the failure rates τ and MTBF are calculated. After that the calculated MTBF is compared with the user-required MTBF and then the synchronization time is adjusted to give the required value. After some iteration, the MTBF of the synchronizer will stabilize close to the user-required MTBF. The memory is used to store the calculation results for later use and user-inputted data such as clock frequencies for calculation.

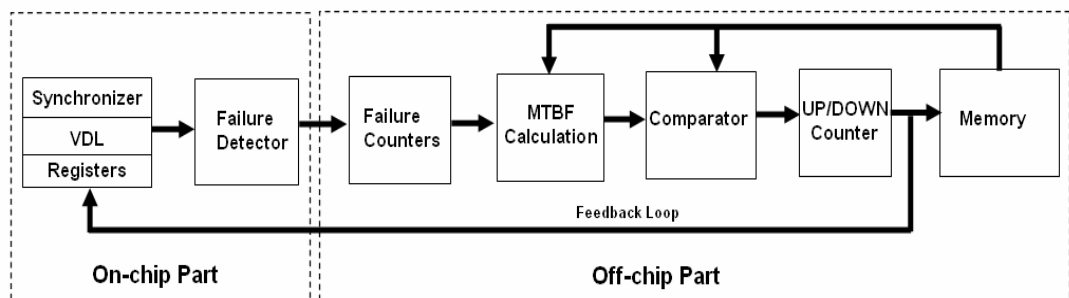


Figure 5.3 Architecture of Synchronization Time Adjustment Scheme

In the FPGA implementation of the synchronization time adjustment scheme, the on-chip overhead per synchronizer is equivalent to 33 flip-flops and 104 gates. The total off-chip overhead is equivalent to 436 flip-flops and 732 gates. The on-chip overhead of this scheme is larger than that of the synchronizer selection scheme. However, 80% of the on-chip overhead in this instance is caused by implementing the variable delay line on an FPGA. When implemented on chip using transistors it will consume much less hardware. For example, an FPGA based variable delay line consisting 20 four-input lookup tables or 40 equivalent gates would need only 12 transistors or 3 equivalent gates when implemented on chip. The on-chip overhead can be reduced by 50% when implemented full custom on chip. The off-chip overhead can also be reduced by making a trade off between the calculation accuracy and the hardware complexity. This is discussed in Section 5.8.

The synchronization time adjustment scheme can work in two modes.

a) Self-adjusting Mode: in this mode the user needs to input the required MTBF. The adjusting circuits will measure the failure rates and calculate the MTBF that would be given by the current synchronization time. This estimated MTBF is then compared with the user-required MTBF and the synchronization time is automatically adjusted to give the required value. After some iteration, the MTBF of the synchronizer will stabilize close to the user-required value.

b) User Mode: in this mode the adjusting circuits will measure failure rates, calculate the MTBF corresponding to the current synchronization time, and output the estimated MTBF for the user to make any adjustment needed such as changing Vdd or clock frequency to meet the required MTBF. This mode is mainly used as a

means for the user to monitor the MTBF of the system and make any adjustment needed themselves.

In both modes the user needs to input the clock frequency used for the calculation of the MTBF.

5.4.3 Failure Detector

The failure detector is used to detect the failure at two different sampling times of the output of the synchronizer. The detector has to be placed close to the synchronizer to ensure that the measurement is accurate. As shown in Figure 5.1, the synchronizer is clocked by the signal SCLK which is generated from the local clock signal CLK. The synchronization time here is the time from the rising edge of SCLK to the rising edge of CLK and is controlled by the variable delay line. FF1 and FF2 sample the output of the synchronizer at two different times. Their outputs are XORed with the output of FF3 which samples the output of synchronizer at the falling edge of SCLK as described in Section 5.1. In the FPGA implementation the time between T1 and T2 is 100 ps which is achieved by using the interconnection delay difference.

5.4.4. Failure Counters

The failure counters count the number of failures detected at different sampling times. As shown in Figure 5.4, it consists of three counters. Counter1 and Counter2 are used to count the number of failures at the sampling times $SCLK+T1$ and $SCLK+T2$ ($T1 < T2$). Counter3 is used to count the number of clock cycles. When Counter1 reaches a preset value it will send a stop signal to the control logic and then all the three counters will be halted. Thereafter the values stored in the counters

will be used for the calculation of τ and MTBF. Note that for the synchronizer selection scheme counter3 is not needed so the hardware overhead can be further reduced.

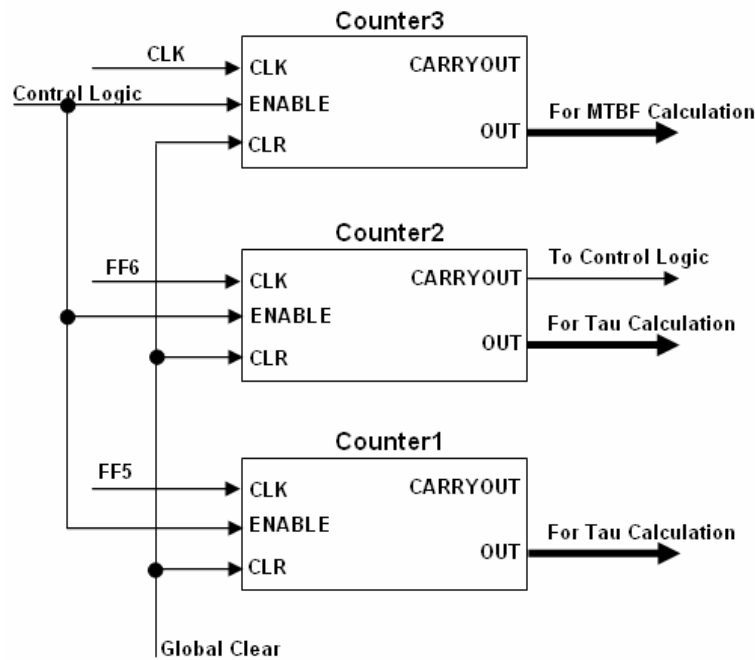


Figure 5.4 Failure counters

5.4.5 Synchronizer Selection Circuit

Figure 5.5 shows the synchronizer selection circuit (note that this circuit was not implemented on FPGA but estimated by using SPICE simulation for future on-chip implementation because FPGA does not support transistor-level design). Four P-type transistors are used to switch the power for the four synchronizers. After the best synchronizer is selected, the other three synchronizers are powered down together with the selection circuitry so the power consumption is the same as for a single synchronizer. An OR gate is used to produce the output signal since all the powered down synchronizers have low outputs. Simulation using 90nm technology shows that the delay of the OR gate is about 18 ps. Considering that the

improvement in synchronization time is 22 ps as mentioned in Section 3.1, the synchronizer selection scheme is at least as good as the synchronizer size enlargement scheme, and will probably be better than it for smaller geometries because the standard deviation is larger and the delay of the OR gate is less for smaller geometries. More importantly, the power consumption is much less than the synchronizer size enlargement scheme.

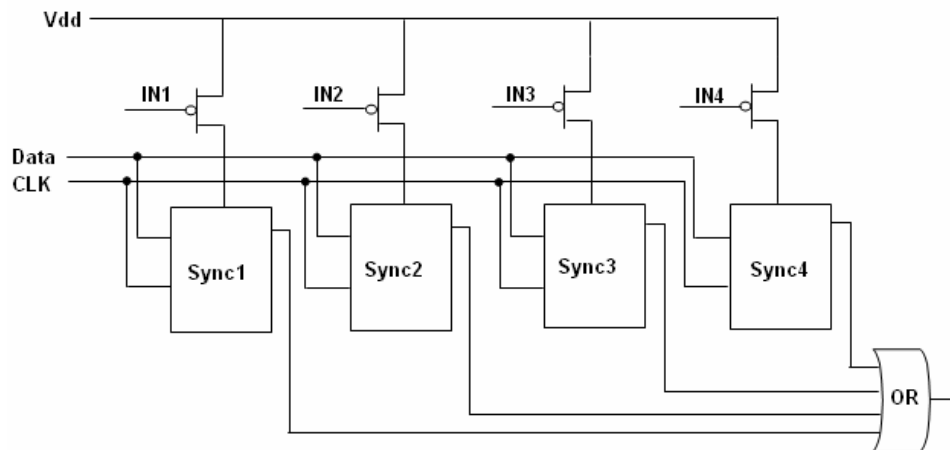


Figure 5.5 Synchronizer Selection Circuit

5.4.6 Variable Delay Line

Variable delay lines are usually implemented using transistor level circuits. However, in FPGAs they can only be implemented as inverter chains. Another problem is that in FPGAs inverters are implemented by using lookup tables [45]. In the device used (Xilinx Spartan 3) the delay of the lookup table plus wire delay is greater than 1 ns, which is too large for the incremental delay considering that the synchronization time constant τ of a synchronizer has a typical value of 11 ps on a 90nm technology. However, a smaller incremental delay can be achieved by using the interconnection delay difference in FPGAs. As shown in Figure 5.6, by carefully

placing the internal XOR gates in the FPGA an incremental delay can be achieved which is the delay difference between the two neighbouring interconnections down to 100 ps. Note that an FPGA is simply used to demonstrate the feasibility of the proposed schemes; The eventual aim is to implement the schemes on chip. Using a variable delay line implemented on chip an incremental delay of 1 ps can be easily achieved.

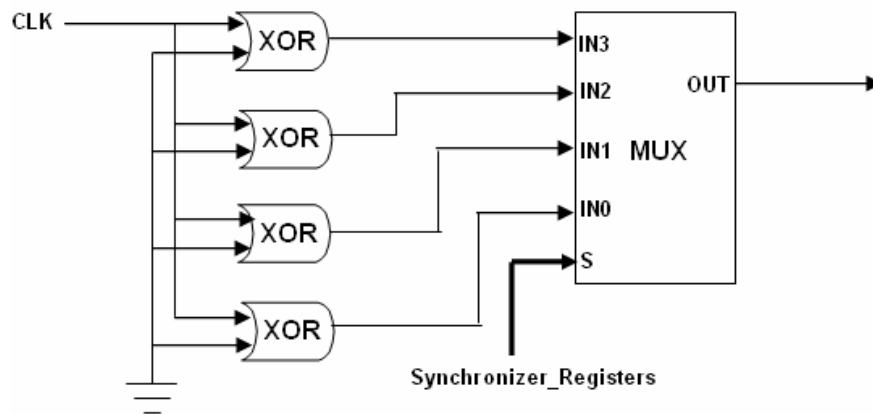


Figure 5.6 Variable delay line

5.4.7 Implementation of τ and MTBF Calculation

In this section the calculation flow is described and the implementation details of the division operation and log calculation are presented.

5.4.7.1 Calculation Flow

As developed in Section 5.2.1 and 5.2.2, the measured MTBF

$$X = \ln(\text{Count3}) + \frac{T3 - T1}{\tau}, \text{ where } \tau = \frac{T2 - T1}{\ln \frac{\text{MTBF2}}{\text{MTBF1}}}$$

MTBF calculation flow, where A=MTBF2, B=MTBF1, E=T2-T1, G=T3-T1 and I=Count3.

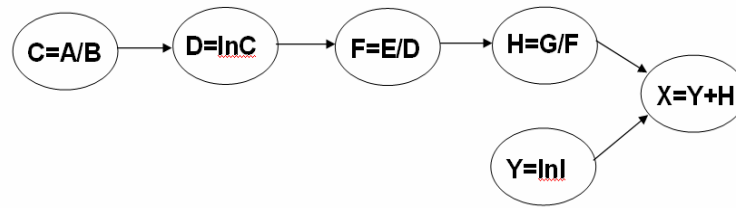


Figure 5.7 Calculation flow

5.4.7.2 Implementation of Division Operation

As can be seen in Figure 5.7, the algorithm for calculating X contains three divisions. The divider required can be reused by multiplexing its inputs. Figure 5.8 shows the implementation details of the divider. A pipelined divider is used to achieve high performance and low area. The divisor and dividend inputs are multiplexed to make it reusable. A counter is employed to count the number of clock cycles used to carry out the division. When the counter reaches a preset value, it will send a completion signal to the control logic and then the divider will be disabled; the calculation flow will then move on to the next step. The output of the divider is stored in a register as it will be used in later steps.

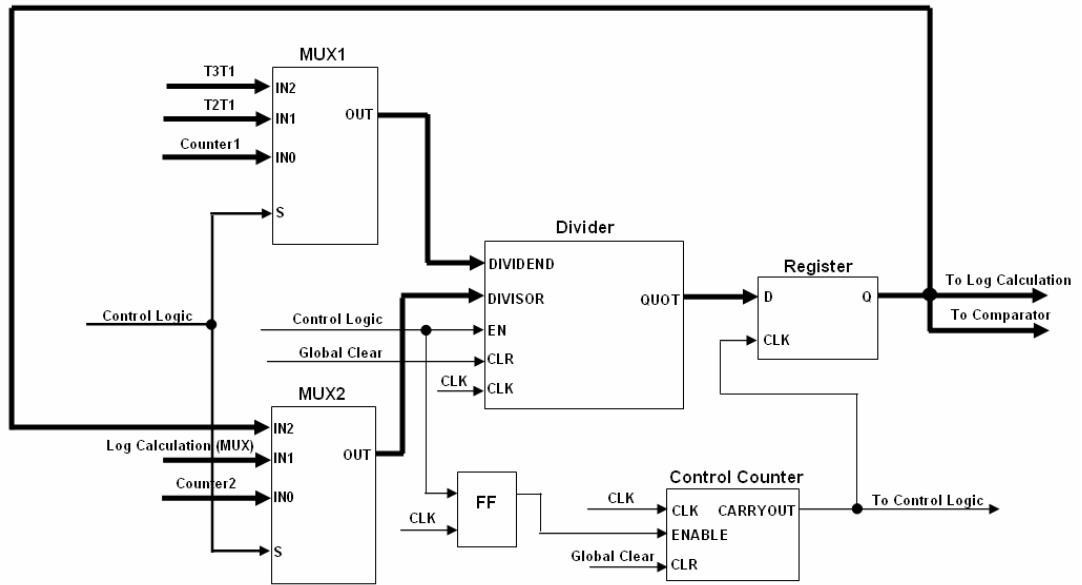


Figure 5.8 Divider

5.4.7.3 Implementation of Log Calculation

To calculate X the log calculation needs to be done twice. In a similar way to the divider circuitry, the log calculation circuit can be reused by multiplexing its inputs. As shown in Figure 5.9, the log calculation is done by using lookup tables. Since the value that needs to be calculated can be very large (up to 10^{10} , which is from the output of counter3), it is impossible to build a full log lookup table. However, considering that the log curve is non-linear, different resolutions can be used for calculating different values (high resolution for small values and low resolution for large values). Consequently three lookup tables with different resolution are used to provide an accuracy of two decimal places, which leads to an error of 1% in the calculated MTBF. For example, if the calculated MTBF is 10 years, the calculation error is only about 1 month. The memory used to implement the lookup tables is 250K Bytes, which can be reduced to less than 25K by increasing the calculation error to 10% which is still acceptable in the calculation of MTBF.

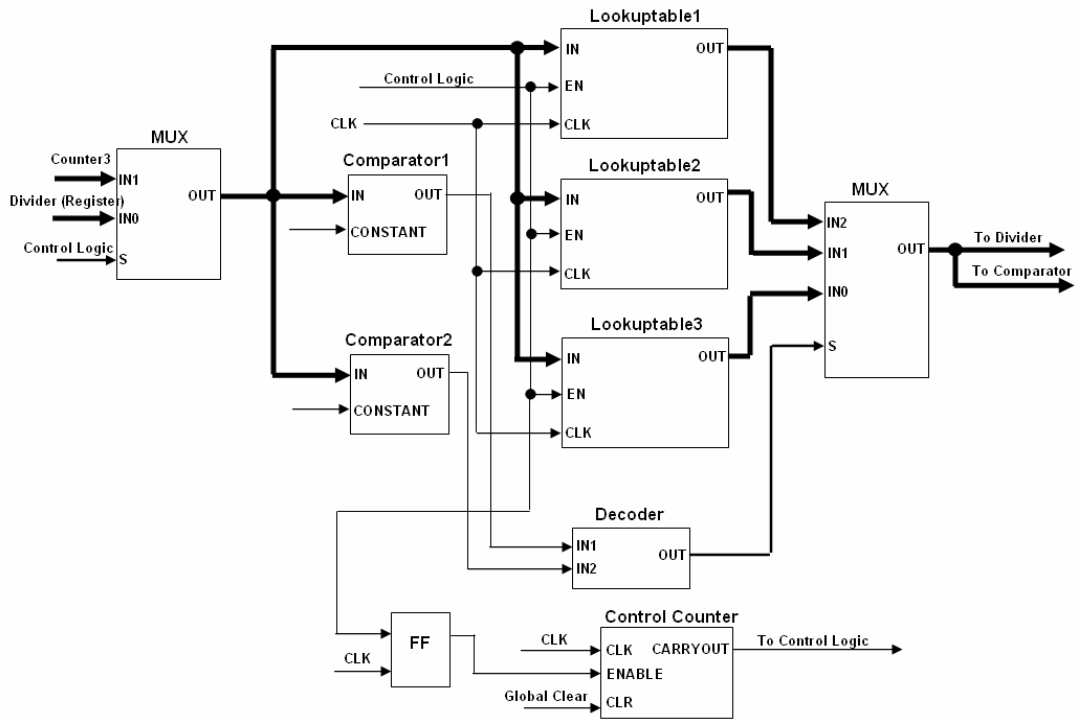


Figure 5.9 Log calculation circuit

5.4.8 Hardware Saving

Compared to the synchronizer selection scheme, the synchronization time adjustment scheme consumes relatively large amount of hardware. However, 80% of the on-chip overhead is caused by implementing the variable delay line on the FPGA. When implemented on chip using transistor level circuits it will consume much less hardware and it is expected that the on-chip overhead will be reduced by 50%. The off-chip part of the synchronization time adjustment scheme which is used to calculate τ and the MTBF can be also reduced by reducing the calculation accuracy such as using only the most significant bit of the count values to do the divisions. In addition, the memory used to implement the log calculation can be reduced from 250KB to 25KB by increasing the calculation error from 1% to 10% which is still acceptable in the calculation of MTBF. A trade off can thus be made between the calculation accuracy and the hardware complexity.

5.5 Applications of Two Schemes

The synchronizer selection scheme is aimed at improving synchronizer performance subject to process variation. It only needs to operate once when setting up the chip since the process variation is fixed when the chip is fabricated. After the best synchronizer is selected out all the other redundant synchronizers plus selection circuitry are powered down so the power consumption is the same as for a single synchronizer. This scheme has small off-chip overhead and consequently can be entirely put on chip.

The synchronization time adjustment scheme is used to deal with the process, voltage, temperature and data rate variations. It consumes relatively large amount of power and hardware. However, when used to deal with the process variation or infrequent V_{dd} variations such as IR drop it only needs to operate once when setting up the chip like the synchronizer selection scheme. After that all the adjusting circuits can be powered down to reduce the power consumption. Also, without the need to track frequent variations, most of the adjusting circuits can be placed off chip to reduce the on-chip overhead. When used to deal with frequent V_{dd} variation or data rate variation, the scheme needs to be put entirely on chip and operate frequently. It is possible, however, to reduce the power consumption by making the adjustment relatively rare and reduce the hardware complexity by using the methods discussed in Section 5.4.8.

5.6 Test Results

a) Calculated MTBF vs Data Rate

Figure 5.10 shows the calculated MTBF against the data rate with synchronization time fixed at 3.5 ns. Here the measurement of failure rates and calculation of long term MTBF are carried out on the FPGA, and the data and clock are provided by two external oscillators. The calculated MTBF decreases with the data rate increasing as expected, showing that the synchronization time could be reduced for data rates below 4MHz which corresponds to a MTBF of 5 months.

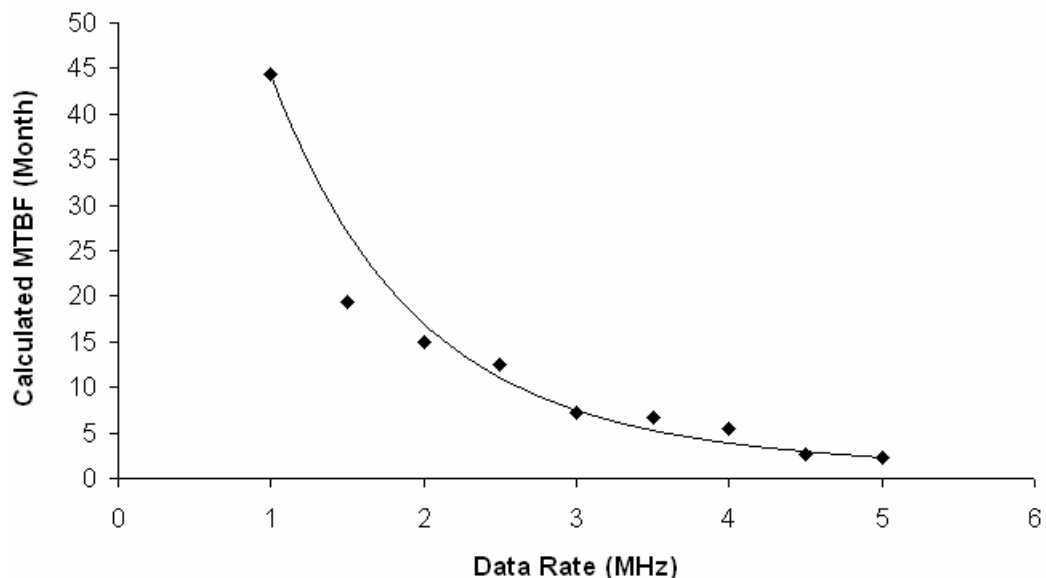


**Figure 5.10 Calculated MTBF vs Data Rate (Synchronization Time=3.5ns,
Clock Frequency=10MHz)**

b) Calculated MTBF vs Synchronization Time

Figure 5.11 shows the calculated MTBF against the synchronization time with data rate fixed at 5 MHz. The calculated MTBF increases as expected with the synchronization time increasing.

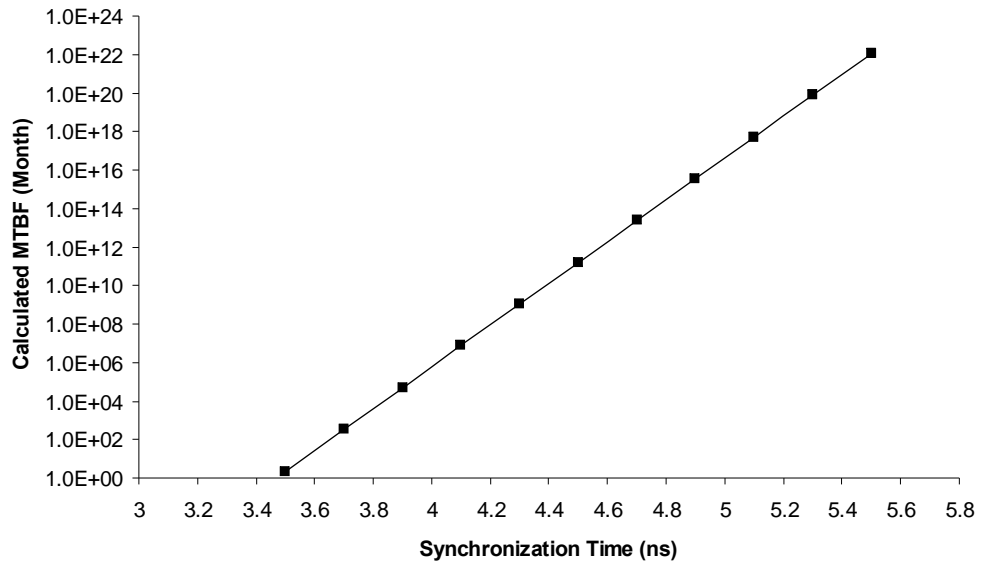


Figure 5.11 Calculated MTBF vs Synchronization Time (Data Rate=5MHz, Clock Frequency=10MHz)

c) Calculated Tau vs Vdd

Figure 5.12 shows the calculated Tau against Vdd. The calculated Tau increases with Vdd decreasing as expected.

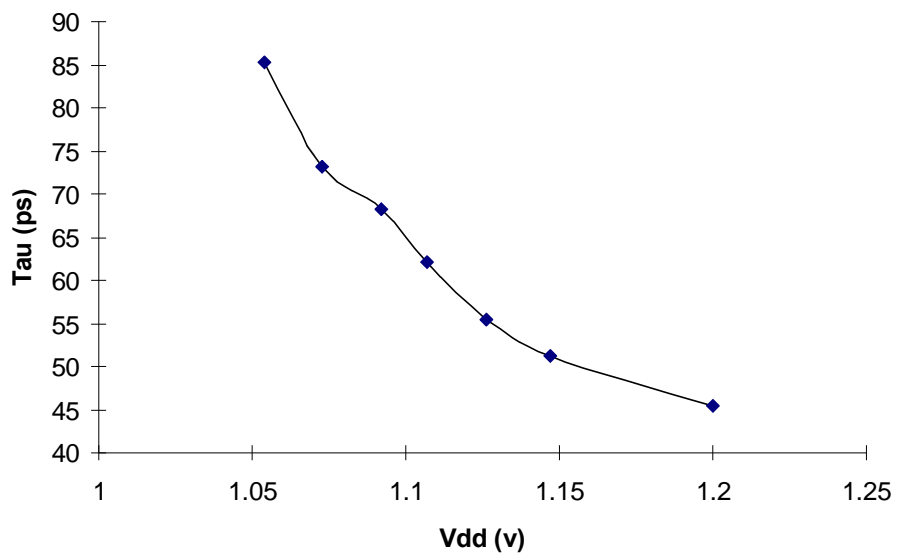


Figure 5.12 Tau vs Vdd

5.7 Summary

Two adaptation schemes based on the on-chip measurement of failure rates have been proposed to reduce the effects of process, voltage, temperature and data rate variations in on-chip synchronizers. The first scheme attempts to improve the synchronizer performance subject to process variation by selecting the best synchronizer out of a number of synchronizers to use. Compared to simply increasing the transistor size in the synchronizer, this scheme can further reduce the effects of process variation and significantly reduce the power consumption.

The Second scheme is targeted at over designed synchronization times due to synchronizer performance variability caused by on-chip variability. It is used to improve the system performance by adjusting the synchronization time according to the actual process, voltage, temperature and data rate variations on the condition that the required MTBF is met. Assuming that the synchronization time constant τ which determines the resolution speed of metastability in synchronizers can increase by 25% due to process variation and a further 25% due to Vdd and temperature variations, this scheme can improve the performance of the system by 33%.

To assess the feasibility of the synchronizer selection and synchronization time adjustment schemes they have been implemented on a Xilinx's 90nm Spartan 3 FPGA. The synchronizer selection scheme is simple and consumes small amount of hardware (9 flip-flops and 6 gates per synchronizer for the on-chip part, and 34 flip-flops and 110 gates for the off-chip part). This scheme can be entirely put on chip since the off-chip overhead is not large. The synchronizer selection scheme is used to deal with the process variation, consequently it only needs to operate once when

setting up the chip. After the best synchronizer is selected all the other redundant synchronizers together with the selection circuitry are powered down so the power consumption is the same as for a single synchronizer.

The synchronization time adjustment scheme consumes a relatively large amount of power and hardware (33 flip-flops and 104 gates per synchronizer for the on-chip part, and 436 flip-flops and 732 gates for the off-chip part). However, when used to deal with the process variation or infrequent V_{dd} variation such as IR drop it only needs to operate once when setting up the chip similar to the synchronizer selection scheme. After that all the adjusting circuits can be powered down to reduce the power consumption. Also, without the need to track frequent variations, most of the adjusting circuits can be put off chip to reduce the on-chip overhead. Only when used to deal with frequent V_{dd} variation or data rate variation, the scheme needs to be put entirely on chip and operate frequently. It is possible, however, to reduce the power consumption by making relatively rare adjustment and reducing the hardware complexity by sacrificing a little calculation accuracy.

Chapter 6

Conclusions and Future Work

6.1 Conclusions

Future SoCs are likely to consist of many independent or semi-independent clock regions because it has become difficult or impossible to distribute a single global clock across the entire system. This is the result of the increased complexity of SoCs in terms of the number of IP cores on a single chip and the dramatic shrinkage in device dimensions. Consequently there will be many synchronizers which are used to retime data passing between different clock regions as part of on-chip communications. In future SoCs, the on chip-communication is likely to affect the system performance more than processing, because the long wires needed for global interconnect become slower, causing unpredictable delays, propagation and synchronization errors, high power consumption, etc. As a critical part of on-chip communication network, the performance of the synchronizers on chip is therefore crucial to the performance of the entire system.

There are several issues related to synchronizer design and measurement that have not been investigated or have not been satisfactorily addressed in the past.

- a) **Synchronizer Robustness:** The synchronizer performance degrades rapidly with V_{dd} decreasing or V_{th} increasing because the synchronization time constant τ is determined by the transconductance of the bistable element in

the synchronizer. As power saving techniques such as DVFS are widely used and the process technology advances, V_{dd} will become lower and lower to the extent where synchronizer circuits may fail to operate. In addition, increasing variations in V_{dd} , V_{th} and temperature could significantly degrade the synchronizer performance. It is therefore necessary to design more synchronizers which are able to work at low V_{dd} and are robust to the V_{dd} , V_{th} and temperature variations.

- b) **Synchronizer Measurement:** Simulation methods are not sufficiently accurate to estimate synchronizer performance in the deep metastability region, which is the region for long metastability events that correspond to very small input time differences between clock and data and is used to predict long term MTBF, because the resolution of simulators is limited and some devices exhibit variations in τ in the deep metastability region. Another disadvantage of simulation methods is that noise may be important for the nondeterministic part of the synchronizer response, and so the result of a deterministic simulation may or may not be a true representation of the results in practice. The traditional two-oscillator measurement method is not good enough either, for measuring deep metastability in synchronizers because different input times are generated at equal probabilities leading to very few deep metastability events and making it difficult to measure τ in the deep metastability region. To estimate the synchronizer performance and MTBF accurately, the measurement of synchronizers needs to be extended into the deep metastability region and carried out on chip.
- c) **On-chip Variability:** As the process technology continues advancing, the on-chip variability is becoming a major issue in circuit design as well as

manufacture. The main factors of on-chip variability include process, voltage and temperature variations. Components such as logic circuits, memories on chip are all affected, but the synchronizer performance subject to the on-chip variability may affect the system performance to a greater extent than other components, because the synchronization time constant τ depends on small rather than large signal behavior and thus synchronizers are more sensitive to the V_{dd} , V_{th} and temperature variations than logic circuits. Another reason is that in future systems on chip, the on-chip communication is likely to affect the system performance more than processing, and synchronization is a critical part of on-chip communication. Therefore, the effects of on-chip variability on the synchronizers will have a great impact on the system performance. As the on-chip variations grow and the size of systems on chip increases, this problem needs to be resolved. Developing transistor level techniques for more robust synchronizer may be a solution to this problem, but all synchronizers exhibit variability, and the synchronizer's performance needs to be further enhanced on the system level.

To address the above issues, the following work has been done and presented in this thesis:

- a) The basic theories of metastability and synchronization have been reviewed. Some of the existing synchronizers have been investigated and the common problems in synchronizer design have been discussed. The main synchronizer simulation and measurement methods have been studied and their disadvantages have been discussed. The main factors of the on-chip

variability have been studied and their effects on synchronizer performance have been analyzed.

- b) Based on the commonly used Jamb latch synchronizer, modifications have been done and an improved synchronizer which is able to work at very low V_{dd} and is robust to the V_{dd} , V_{th} and temperature variations has been proposed. By removing the feedback from the p-type devices the node capacitance is reduced and the device transconductances are increased, and hence the synchronization time constant τ is improved. A disadvantage of this modification is that the power is significantly increased. To avoid this problem it has been shown that the p-type devices can be switched on only during metastability and switched off after metastability by using the outputs of a metastability filter to control their gates, so that higher power dissipation is only present during metastability. The simulation results in Section 3.3 show that, for the improved synchronizer, the switching energy required is only a little higher than the Jamb latch, but it is much faster when working at low V_{dd} and much more robust than the Jamb latch to the V_{dd} , V_{th} and temperature variations. When the power supply voltage is reduced to 0.9V, with τ being 53.1ps compared with 78.5ps in the conventional Jamb latch, and low temperatures emphasize this advantage. T_w is also affected by the modifications, so that the output time for a metastable event is not faster than the Jamb latch for input event time differences longer than 10^{-15} seconds. Nevertheless, for the much shorter input time differences that create long output resolution times there is an improvement in the low V_{dd} resolution time of more than 500ps.

c) An on-chip measurement circuit of synchronizer using deep metastability measurement method has been designed and implemented using UMC 0.18 μm technology along with the tested synchronizers. Compared with the previous off-chip implementation using analog circuits, the on-chip implementation using digital circuits allows integration of both the synchronizer circuits and the measurement method, and eliminates high speed off-chip paths which are a source of inaccuracy. It also makes control at the picosecond level easier because of the inherent stability of digital integrating counters and digital delay lines. The results in Section 4.3 show that the measurement method is stable and reliable. The digital delay line was controllable to an increment of 0.1ps, and the input time distribution was 5.2ps compared with 7.6ps for the analog version. Through the use of high and low counters the actual input time distribution could be measured to within better than 1ps. τ was measured down to 10^{-17} s within an experimental time of 10 minutes, corresponding to an MTBF of 100 seconds. By extending the measurement time and filtering early responses in a future version of this chip, this could be extended to 1,000,000 seconds or approximately 10 days MTBF. The responses from the tested devices were shown to correspond with simulation down to 10^{-14} s, but values of τ for input times below that reachable by measurement were shown to be greater than simulation, which means that the tested devices are slower in the deep metastability region than it is in the deterministic region. For this reason the early simulation cannot be relied on to predict MTBF at realistic synchronization times, and it is necessary to check the value of τ in deep metastability with accurate measurement. A comparison was also made

between the Jamb latch and the robust synchronizer at different V_{dd} , the results show that the robust synchronizer circuit performed at least as well as the Jamb latch at all values of V_{dd} , and was more than 20% faster when V_{dd} was reduced by 25%.

- d) Two schemes used to mitigate the effects of on-chip variability on synchronizer performance have been proposed and their feasibility has been demonstrated using FPGA. The first scheme, namely **Synchronizer Selection Scheme**, is to improve the synchronizer performance subject to process variation by selecting the best synchronizer out of a number of synchronizers to use. Compared to simply increasing the transistor size in the synchronizer, this scheme can further reduce the effects of process variation and significantly reduce the power consumption. The second scheme, namely **Synchronization Time Adjustment Scheme**, is targeted at overdesigned synchronization times due to synchronizer performance variability caused by on-chip variability. It is used to improve the system performance by adjusting the synchronization time according to the actual process, voltage, temperature and data rate variations on the condition that the required MTBF is met. Assuming that the synchronization time constant τ which determines the resolution speed of metastability in synchronizers can increase by 25% due to process variation and a further 25% due to V_{dd} and temperature variations, this scheme can improve the performance of the system by 33%. To assess their feasibility, the two schemes have been implemented using a Xilinx's 90nm FPGA Spartan 3. The synchronizer selection scheme is simple and consumes small amount of hardware (9 flip-flops and 6 gates per synchronizer for the on-chip part, and 34 flip-flops and

110 gates for the off-chip part). This scheme can be entirely put on chip since overall overhead is not big. Because the synchronizer selection scheme is used to deal with the process variation, it only needs to operate once when setting up the chip. After the best synchronizer is selected all the other redundant synchronizers are powered down as is measurement and selection circuitry so the power consumption is the same as for a single synchronizer. The synchronization time adjustment scheme consumes relatively large amount of power and hardware (33 flip-flops and 104 gates per synchronizer for the on-chip part, and 436 flip-flops and 732 gates for the off-chip part). However, when used to deal with the process variation or fixed Vdd variation it only needs to operate once when setting up the chip like the synchronizer selection scheme. After that all the adjusting circuits can be powered down to reduce the power consumption. Also, without the need to track frequent variations, most of the adjusting circuits can be put off chip to reduce the on-chip overhead. Only when used to deal with frequent Vdd variation or data rate variation, the scheme needs to be put entirely on chip and operate frequently. It is possible, however, to reduce the power consumption by making the adjustment relatively rare and reduce the hardware complexity by sacrificing a little calculation accuracy.

The proposed techniques have given solutions to the issues discussed before in synchronizer design, measurement and performance variability, and will show greater advantages in future process technologies where these issues are likely to become worse.

6.2 Future Work

The work in this thesis has shown that how synchronizer can be made more robust to V_{dd} , V_{th} and temperature variations, how synchronizer measurement can be carried out on chip into the deep metastability region and how the effects of on-chip variability on synchronizers can be mitigated by using adaptive circuit. However, there are some issues that have not been investigated in the work, but need to be considered in the future work.

- 1) In synchronizer design, the synchronizer performance has been greatly improved by developing circuit level design techniques. However, the synchronizer performance on system level has not been investigated in the work. For example, the architecture of synchronizer-based communication system and the handshake protocol can be optimized to reduce the synchronization latency and improve throughput on the system level. Another thing is that the synchronizer modelling based on small signal behaviour is only applicable to the simplest synchronizers, but may not hold for more complex synchronizers made from gates with more than one time constant in the feedback loop. This is worth investigating in order to build more accurate synchronizer model to support synchronizer design. In addition, the techniques used in the robust synchronizer may also be applied to MUTEX circuits which are used to arbitrate between multiple requests in asynchronous designs and have similar structure to synchronizer circuits since their performance are also subject to V_{dd} , V_{th} and temperature variations.

- 2) In synchronizer measurement, the proposed on-chip measurement technique is able to generate much more deep metastability events so the measurement of τ can be carried out in the deep metastability region. However, due to the limited response speed of oscilloscopes, the number of the recorded deep metastability events is still much less than that of generated. It is possible to increase the number of recorded deep metastability events by filtering out the events with normal propagation delay.
- 3) The feasibility of the two proposed adaption schemes has been demonstrated using FPGA, but the final aim is to implement them on chip to mitigate the effects of on-chip variability on synchronizer performance. In the on-chip implementation, it is possible to reduce the on-chip overhead by using full custom design for the variable delay lines and simplifying the arithmetic units by trading off the calculation accuracy. An alternative may be to find a direct mapping relationship between measured failure rates and long term MTBF and then the arithmetic units can be replaced by a lookup table to calculate MTBF. Moreover, the adaptation schemes based on on-chip measurement of circuit parameters may be applied to other circuits to deal with process variation.

Appendix A

TSMC 0.18 μ m SPICE Parameters from MOSIS (TSMC

CL018/CR018_Mixed-Mode_1.8V/3.3V_1P6M_NON-

EPI) [46]

```
.MODEL CMOSN NMOS (                LEVEL = 49
+VERSION = 3.1          TNOM  = 27          TOX   = 4.2E-9
+XJ   = 1E-7           NCH   = 2.3549E17    VTH0  = 0.3729345
+K1   = 0.5911591     K2    = 3.007223E-3   K3    = 1E-3
+K3B  = 2.3393631     W0    = 1E-7         NLX   = 1.742723E-7
+DVT0W = 0            DVT1W = 0            DVT2W = 0
+DVT0  = 1.5143867    DVT1  = 0.4394265    DVT2  = 0.0461099
+U0   = 256.2652827   UA    = -1.528208E-9   UB    = 2.382175E-18
+UC   = 4.869842E-11 VSAT  = 1.048225E5    A0    = 1.9933604
+AGS  = 0.4270688    B0    = 3.490909E-7    B1    = 5E-6
+KETA  = -0.0131087   A1    = 0              A2    = 0.9073425
+RDSW  = 137.1370976 PRWG  = 0.3389529    PRWB  = -0.2
+WR   = 1            WINT  = 1.948048E-10   LINT  = 1.447793E-8
+XL   = 0            XW    = -1E-8         DWG   = -4.571064E-9
+DWB  = 9.725675E-9  VOFF  = -0.0920056    NFACTOR = 2.4661822
+CIT  = 0            CDSC  = 2.4E-4        CDSCD = 0
+CDSCB = 0           ETA0  = 2.799633E-3    ETAB  = 9.440921E-6
+DSUB  = 0.0163514   PCLM  = 0.7476704    PDIBLC1 = 0.1642233
+PDIBLC2 = 2.170537E-3 PDIBLCB = -0.1        DROUT  = 0.6895268
+PSCBE1 = 8E10       PSCBE2 = 1.714915E-9    PVAG  = 1.745429E-3
+DELTA = 0.01        RSH   = 6.7          MOBMOD = 1
+PRT   = 0           UTE   = -1.5         KT1   = -0.11
+KT1L  = 0           KT2   = 0.022        UA1   = 4.31E-9
+UB1   = -7.61E-18   UC1   = -5.6E-11    AT    = 3.3E4
+WL   = 0           WLN   = 1           WW   = 0
+WWN  = 1           WWL   = 0           LL   = 0
+LLN  = 1           LW    = 0           LWN  = 1
+LWL  = 0           CAPMOD = 2          XPART = 0.5
+CGDO  = 8.02E-10    CGSO  = 8.02E-10    CGBO  = 1E-12
+CJ   = 9.50106E-4   PB    = 0.8         MJ    = 0.3783704
+CJSW  = 2.429356E-10 PBSW  = 0.8         MJSW  = 0.1155199
+CJSWG = 3.3E-10    PBSWG  = 0.8         MJSWG = 0.1155199
+CF   = 0           PVTH0 = -9.861363E-4    PRDSW = -3.1061658
+PK2  = 8.347166E-4  WKETA  = 2.838389E-4   LKETA  = -7.160166E-3
+PU0  = 4.1578782   PUA    = -1.64205E-13  PUB    = 0
+PVSAT = 1.305917E3  PETA0  = 6.567234E-5   PKETA  = -8.535331E-4 )
*
```

```

.MODEL CMOS PMOS (
LEVEL = 49
+VERSION = 3.1 TNOM = 27 TOX = 4.2E-9
+XJ = 1E-7 NCH = 4.1589E17 VTH0 = -0.4075115
+K1 = 0.5857189 K2 = 0.0331921 K3 = 0
+K3B = 12.2405601 W0 = 1E-6 NLX = 8.34956E-8
+DVT0W = 0 DVT1W = 0 DVT2W = 0
+DVT0 = 0.540657 DVT1 = 0.3618395 DVT2 = 0.1
+U0 = 114.351172 UA = 1.500235E-9 UB = 1E-21
+UC = -7.63355E-11 VSAT = 2E5 A0 = 1.8616494
+AGS = 0.4071023 B0 = 5.347155E-7 B1 = 1.719601E-6
+KETA = 0.0184405 A1 = 0.5644893 A2 = 0.3
+RDSW = 247.8365148 PRWG = 0.5 PRWB = -0.0937912
+WR = 1 WINT = 0 LINT = 2.540644E-8
+XL = 0 XW = -1E-8 DWG = -3.336159E-8
+DWB = 9.779975E-9 VOFF = -0.0923541 NFACTOR = 1.8856469
+CIT = 0 CDSC = 2.4E-4 CDSCD = 0
+CDSCB = 0 ETA0 = 0.0558438 ETAB = -0.0374936
+DSUB = 0.8784624 PCLM = 2.9106088 PDIBLC1 = 1.331262E-4
+PDIBLC2 = 0.0333116 PDIBLCB = -1E-3 DROUT = 9.970234E-4
+PSCBE1 = 3.204313E9 PSCBE2 = 9.273321E-10 PVAG = 15
+DELTA = 0.01 RSH = 7.7 MOBMOD = 1
+PRT = 0 UTE = -1.5 KT1 = -0.11
+KT1L = 0 KT2 = 0.022 UA1 = 4.31E-9
+UB1 = -7.61E-18 UC1 = -5.6E-11 AT = 3.3E4
+WL = 0 WLN = 1 WW = 0
+WWN = 1 WWL = 0 LL = 0
+LLN = 1 LW = 0 LWN = 1
+LWL = 0 CAPMOD = 2 XPART = 0.5
+CGDO = 6.58E-10 CGSO = 6.58E-10 CGBO = 1E-12
+CJ = 1.16195E-3 PB = 0.8347189 MJ = 0.4033366
+CJSW = 2.053873E-10 PBSW = 0.8582178 MJSW = 0.3123837
+CJSWG = 4.22E-10 PBSWG = 0.8582178 MJSWG = 0.3123837
+CF = 0 PVTH0 = 1.204949E-3 PRDSW = 2.1519589
+PK2 = 1.902399E-3 WKETA = 0.0277547 LKETA = -3.019454E-3
+PU0 = -0.8585387 PUA = -4.63302E-11 PUB = 1E-21
+PVSAT = -50 PETA0 = -2.003159E-4 PKETA = -3.997451E-3 )
*

```

Appendix B

UMC 0.18 μ m SPICE Parameters from Europractice

(UMCL180_Mixed-Mode_1.8V/3.3V_1P6M) [47]

		Process Name		
		L180		
		Logic GI I		MixedMode/RF
Process technology specifications	units	Std Logic + MMC	Low Leakage	
Substrate Type		P-substrate		P-substrate
Nwell - Sal (Poly[n][p] / Active[n][p]) Unsalicided (Poly[n][p] / Active[n][p])	Ohm/sq	415 - ([8] [8] / [8] [8]) ([80] [158] / [126] [360])		415 - ([8] [8] / [8] / [8]) ([80] [158] / [113] [352])
Wafer size (6) / available die thicknesses		8 Inch / 29 Mils - 11 Mils		8 Inch / 29 Mils - 11 Mils
High Ohmic Resistor (HR)	Ohm/sq	-	-	1039
Metal Metal Cap (MiM cap)	fF/ μ m ²	1	-	1
Low Vt / Zero VT implant		-		Y / Y
Twin well / Triple well / Thick gate for 3.3V		Y / - /Y		Y / Y /Y
Number of Poly/Metal Layers	#	1P 6M		1P 6M
Metal1/2/3/4/5 /6 /7/8 Pitch	μ m	0.48/0.56/0.56/0.56/0.56/0.88		0.48/0.56/0.56/0.56/0.56/0.88
Min drawn MOS Length (regular/3.3V)	μ m	0.18 / 0.34		0.18 / 0.34
Min diffusion width for MOS	μ m	0.24		0.24
Operating Voltage	V	1.8 / 3.3		1.8 / 3.3
Vton(N / P)	V	0.5 / -0.5	0.61 / -0.6	0.51 / -0.5
Ioff(N / P) core transistor (VD = VDD, Vg = 0V)	pA/ μ m	15 / -10	2 / -2	7.6 / -8
Number of Masks (all options included)	#	27	28	35
Ring Oscillator stage delay (2 conditions)	pSec/stage	27 (@1.8V) 55 (@3.3V)	36 (@1.8V) 55 (@3.3V)	27 (@1.8V) 55 (@3.3V)
RF Top Level Metal Pitch	μ m	-		2.2
RF Top Level Thickness	kA	-		20
Ft	GHz	-		49GHz @ 300 μ A/ μ m Vg/Vd=1.2V/1.8V
Fmax	GHz	-		34GHz @ 300 μ A/ μ m Vg/Vd=1.2V/1.8
Cadence Design Kit		(1)	(1)	MixedMode + RF

UMC 90nm SPICE Parameters from Europractice

(UMCL90N_ Mixed-Mode_1.0V/2.5V_1P9M) [48]

UMC L90N 1P9M 1.0V/2.5V lowK Logic/MixedMode							
Process technology specifications	units	Standard Performance (SP)			Low Leakage (LL)		
Application		ASIC - Consumer - Network			Portable - Wireless		
		LVT	RVT	HVT	LVT	RVT	HVT
Substrate Type		P-substrate					
Nwell - Non salicide (N+ P+ N+Poly P+Poly)	Ohm/sq	370 - 82 95 100 240					
Wafer size (6) - available die thicknesses		12 Inch - 29 Mils or 11 Mils					
Core devices		SP_Lvt (1.0V)	SP_Rvt (1.0V)	SP_Hvt (1.0V)	LL_Lvt (1.2V)	LL_Rvt (1.2V)	LL_Hvt (1.2V)
Core devices Tox - Min gate length	Å - μm	15.5 - 0.08	15.5 - 0.08	15.5 - 0.08	22 - 0.09	22 - 0.09	22 - 0.09
Core devices Ioff	Amp/um	50n	10n	400p	400p	30p	10p
Core devices Delay	ps/stage	9.8	10.6	16.1	15.5	20.5	21.3
Core devices VtON N/P	V	0.26/-0.22	0.33/-0.277	0.457/-0.39	0.49/-0.394	0.562/-0.502	0.648/-0.54
Core device overdrive (OD) feasibility	V	1.2V	1.2V	1.2V	-	-	-
Core device overdrive (OD) Ioff	Amp/um N/P	60n/100n	5n/12n	400p/600p	-	-	-
Core device overdrive (OD) Delay	ps/stage	7.7	8.6	11.9	-	-	-
Core device overdrive (OD) VtSAT N/P	V	0.137/-0.09	0.227/-0.167	0.362/-0.287	-	-	-
IO devices	V	1.8V 2.5V(default) 3.3V					
IO devices Tox_g1 (VG=-2V, VB=0V) - Min gate length	Å - μm	31 - 0.18 52 - 0.24 65 - 0.34					
IO devices Ioff	Amp/um N/P	10p/400p 15p/15p 10p/10p					
IO devices Delay	ps/stage	26 24.7 39.4					
IO devices VtON N/P	V	0.527/-0.413 0.548/-0.5 0.57/-0.566					
IO device underdrive (UD) feasibility		1.8V at Gox52 Ioff N/P 8p/8p delay 34.5 ps/stage Vtsat N/P 0.462/-0.432 min gate length 0.4μ					
IO device overdrive (OD) feasibility		3.3V at Gox52 Ioff N/P 15p/52p delay 70 ps/stage Vtsat N/P 0.45/-0.436 min gate length 0.7μ					
High Ohmic Resistor (HR)	Ohm/sq	1012					
Metal Metal Cap (MiM cap)	fF/μm ²	1.544					
NCAP	fF/μm ²	15.3 @ 1.0V thin oxide - 11.7 @1.2V medium oxide - 8.9 @1.8V thick oxide - 5.8 @2.5V thick oxide - 4.8 @3.3V thick oxide					
Native threshold voltage NFET		SP_NVT 1.0_1.2V OD LL_NVT 1.2V NVT 1.8V NVT 2.5V NVT 3.3V					
Number of Poly/Metal Layers	#	1 Poly - 9 Metals : M1 M2->M6(1X) - M7->M8(2X) - M9(4X)					
Metal pitch	μm	M1(0.12) M2->M6(0.14) - M7->M8(0.28) - M9(0.56)					
Metal Resistivity	mOhm/sq	M1(115) M2->M6(105) - M7->M8(44) - M9(27)					
Cadence Design Kit		Yes					

References

- [1] International Technology Roadmap for Semiconductors (ITRS), 2007 update.
- [2] N. A Kurd, J.S. Barkatullah, R.O.Dizon, T.D.Fletcher, and P.D.Madland, "Multi-GHz Clocking Schemes for Intel Pentium 4 Microprocessors", Proc. ISSCC 2001, pp. 404-405, 2001.
- [3] S Tam, S Rusu, U. N. Desai, R Kim, J. Zhang, and I Young, "Clock Generation and Distribution for the first IA-64 Microprocessor", IEEE JSSC Vol. 35 No.11, pp. 1545-1552, 2000.
- [4] E. Beigne, F. Clermidy, S. Miermont, P. Vivet, "Dynamic Voltage and Frequency Scaling Architecture for Units Integration within a GALS NoC," Networks-on-Chip, 2008. NoCS 2008. Second ACM/IEEE International Symposium on , vol., no., pp.129-138, 7-10 April 2008.
- [5] K. Y. Yun, and A. E. Dooply, "Pausible clocking based heterogeneous systems", IEEE trans, VLSI systems, Vol.7, No. 4, pp. 482-487, 1996.
- [6] Simon Moore, George Taylor, Robert Mullins, Peter Robinson, "Point to Point GALS Interconnect", Proc. Of ASYNC'02, Manchester, UK, April 2002.
- [7] Stephan Oetiker, Frank K. Gürkaynak, Thomas Villiger, Hubert Kaeslin, Norbert Felber, Wolfgang Fichtner, "Design Flow for a 3-Million Transistor GALS Test Chip," Integrated Systems Laboratory, ETH Zurich, ACiD 27, 2003.
- [8] Thomas Villiger, Hubert Kaeslin, Frank K. Gürkaynak, Stephan Oetiker, Wolfgang Fichtner, "Self-Timed Ring for Globally-Asynchronous Locally-Synchronous Systems," Proceedings of the Ninth International Symposium on Asynchronous Circuits and Systems (ASYNC'03), pp. 141-150.
- [9] Jens Mutersbach, Thomas Villiger, and Wolfgang Fichtner, "Practical Design of Globally-Asynchronous Locally-Synchronous Systems," 6th International Symposium on Advanced Research in Asynchronous Circuits and Systems, Eilat, Israel, April 2000, pp. 52-61.
- [10] W.J. Dally and J.W. Poulton, "Digital Systems Engineering", Cambridge University Press, 1998.

- [11] T. J. Chaney and C. E. Molnar, "Anomalous behavior of synchronizer and arbiter circuits", *IEEE Trans. Comput.*, vol. C-22, pp. 421-422, Apr. 1973.
- [12] S. H. Unger, "Asynchronous sequential switching circuits with unrestricted input changes", *IEEE Trans. Comput.*, vol. C-20, pp. 1437-1444, Dec. 1971.
- [13] M. Pechoucek, "Anomalous response times of input synchronizers", *IEEE Trans. Comput.*, vol. C-25, pp. 133-139, Feb. 1976.
- [14] L. R. Marine, "The effect of asynchronous inputs on sequential network reliability", *IEEE Trans. Comput.*, vol. C-26, pp. 1082-1090, Nov. 1977.
- [15] G. R. Couranz and D. F. Warm, "Theoretical and experimental behavior of synchronizers operating in the metastable region", *IEEE Trans. Comput.*, vol. C-24, pp. 604-616, June 1975.
- [16] E. G. Friedman, "Clock Distribution Networks in Synchronous Digital Integrated Circuits," *Proc. of the IEEE*, vol. 89, pp. 665-692, 2001.
- [17] A. Chakraborty, and M. Greenstreet, "Efficient Self-Timed Interfaces for crossing Clock Domains". *Proceedings ASYNC2003, Vancouver*, pp. 78-88, 2003.
- [18] Umit Y. Ogras, Jingcao Hu, Radu Marculescu, "Communication-Centric SoC Design for Nanoscale Domain", *ASAP 2005*, pp. 73-78, 2005.
- [19] D. J. Kinniment, *Synchronization and arbitration in digital systems*, Wiley, 2007, p.20.
- [20] D. J. Kinniment and J.V. Woods, "Synchronization and arbitration circuits in digital systems", *Proc. IEE* vol. 123, No. 10, 1976.
- [21] H. J. M. Veendrick, "The behavior of flip-flops used as synchronizers and prediction of their failure rate", *IEEE Journal of Solid-State Circuits*, SC-15, (2), pp. 169-176, 1980.
- [22] K. O. Jeppson "Comments on the Metastable Behavior of Mismatched CMOS Latches" *IEEE Journal of Solid State Circuits* Vol. 31 No. 2 pp. 275-277, 1996.
- [23] J. Zhou, D. J. Kinniment, G. Russell, and A. Yakovlev, "A Robust Synchronizer Circuit", *IEEE Computer Society Annual Symposium on VLSI*, pp. 442-443, 2006.
- [24] C. Dike and E. Burton. "Miller and Noise Effects in a Synchronizing Flip-Flop". *IEEE Journal of Solid State Circuits* Vol. 34 No. 6, pp. 849-855, 1999.

- [25] S. T. Flannagan, "Synchronization reliability in CMOS technology," IEEE. J. Solid-State Circuits, vol. SC-20, pp. 880–882, Aug. 1985.
- [26] L. Kim and R. W. Dutton, "Metastability of CMOS latch/flip-flop," IEEE. J. Solid-State Circuits, vol. 25, pp. 942–950, Aug. 1990.
- [27] D. J. Kinniment, A. Bystrov, A.V. Yakovlev, "Synchronization Circuit Performance", IEEE Journal of Solid-State Circuits, 37(2), pp. 202-209, 2002.
- [28] J. Jex and C. Dike, "A fast resolving BiNMOS synchronizer for parallel processor interconnect," IEEE Journal of Solid-State circuits, 30(2), pp. 133-139, 1995.
- [29] C. Foley, "Characterizing metastability," Proc. 2nd IEEE Symp. Adv. Res. Asynchronous Circuits and Systems, pp. 175-184, 1996.
- [30] Yaron Semiat , Ran Ginosar, "Timing Measurements of Synchronization Circuits", Proceedings of the 9th International Symposium on Asynchronous Circuits and Systems, p. 68, May 12-15, 2003.
- [31] R. Ginosar "Fourteen ways to fool your synchronizer" Proc. ASYNC2003, Vancouver, pp. 89-196, 2003.
- [32] Charles Dike, "BackGate Biased Synchronizing Latch," United State Patents No. 6,512,406 January 2003.
- [33] Guy Tamir, "Synchronizers Metastability", Research thesis M.Sc., Electrical Engineering Faculty, Technion, 2003.
- [34] A El-Amawy, M. Naraghi-pour, and M. Hegde. "Noise modeling effects in redundant synchronizers", IEEE Trans on Computers Vol 42, No.12, pp. 1487-1494, 1993.
- [35] R. L. Cline. "Method and circuit for improving metastable resolving time in low-power multi-state devices" US patent 5,789,945, February 27, 1996.
- [36] C. L. Seitz, Ideas about arbiters. Lambda, 1 (1,First Quarter): 1980.
- [37] S Yang and M Greenstreet, "Computing Synchronizer Failure Probabilities", Proc. DATE'07, 2007.
- [38] D. Kinniment, K. Heron, and G. Russell, "Measuring Deep Metastability", Proc. ASYNC'06, pp. 2-11, 2006.
- [39] J. Zhou, D. J. Kinniment, G. Russell, and A. Yakovlev, "On-Chip Measurement of Deep Metastability in Synchronizers", IEEE Journal of Solid-State Circuits, Vol. 43, No. 2, pp. 550-557, 2008.

- [40] M. Maymandi-Nejad and M. Sachdev, "A digitally programmable delay element: Design and analysis", IEEE Transactions on Very Large Scale Integration (VLSI) Systems, vol.12 no.10, pp.1126-1126, 2004.
- [41] M. Garg, A. Kumar, J. van Wingerden, L. Le Cam, "Litho-driven layouts for reducing performance variability", ISCAS 2005, pp. 3551-3554, 2005.
- [42] K. A. Bowman, X. Tang, J. C. Eble, and J. D. Meindl, "Impact of extrinsic and intrinsic parameter fluctuations on CMOS circuit performance", IEEE J. Solid-State Circuits, vol. 35, pp. 1186-1193, 2000.
- [43] Eric S. Fetzer, "Using Adaptive Circuits to Mitigate Process Variations in a Microprocessor Design," IEEE Design and Test of Computers, vol. 23, no. 6, pp. 476-483, Nov/Dec, 2006.
- [44] J. Zhou, D. J. Kinniment, G. Russell, and A. Yakovlev, "Adapting Synchronizers to the Effects of On Chip Variability", 14th IEEE International Symposium on Asynchronous Circuits and Systems, pp. 39-47, 2008.
- [45] Nikolaos Minas, David Kinniment, Keith Heron and Gordon Russell, "A High Resolution Flash Time-to-Digital Converter Utilizing Process Variability", ASYNC 2007, pp. 163-172, 2007.
- [46] <http://www.mosis.com/products/fab/vendors/tsmc/tsmc018/>
- [47] http://www.euopractice-ic.com/technologies_UMC.php?tech_id=018um
- [48] http://www.euopractice-ic.com/technologies_UMC.php?tech_id=90nm